

APPLICATION OF
PC BASED SUTRA MODEL



आये क्षि प्त मयोभुमः

NATIONAL INSTITUTE OF HYDROLOGY
JAL VIGYAN BHAWAN
ROORKEE - 247 667 (U.P.)
INDIA

1993-94

PREFACE

Ground water quality modelling is relatively a new area and as such there is still much research to be undertaken before an optimal approach to environmentally sound water management can be defined. Numerical models yield information with the level of confidence dependent on the availability and quality of field data and the skillful interrelation of the results by an experienced modeler with a strong background in ground water analysis.

The transport of solutes in groundwater flow has been studied in most parts of the world with increasing intensity in the last three decades as a result of growing concern about water quality and pollution but hardly any literature support is available which signifies the same trend in India. On the other hand intensification of groundwater exploitation, increase in solute concentration in aquifers due to saltwater intrusion, leaking repositories, use of fertilizers, etc. have made this a subject of immediate and wide interest.

Need of the hour has been initiated by introducing the concepts of an highly and widely used algorithm SUTRA generated by Voss Clifford I. of United States Geological Survey, Washington, through actual phase of development on personnel computers. The code is ready for use in the wide range of practical field problems related to ground water contamination. Subject to the storage allocation needed, this can be executed straightaway on PCs or can be transferred to bigger system.

Present study and its documentation is carried out by Shri P.K. Majumdar, Scientist C', RCNIH, Belgaum; Dr. Rama Mehta, SRA, NIH, Roorkee; and Dr. B.K. Purandara, SRA, RCNIH, Belgaum under the guidance of Dr. P.V. Seethapathi, Scientist 'F', NIH, Roorkee.


DIRECTOR

CONTENTS

CHAPTER	SUBJECT	PAGE
	LIST OF FIGURES	i-ii
	LIST OF TABLES	ii
	LIST OF NOTATIONS	iii-v
	ABSTRACT	vi
I	1.0 INTRODUCTION	001
	1.1 SOME REVIEWS	002
	1.2 PURPOSE & SCOPE	005
	1.3 APPLICATION	006
	1.4 RARE LIMITATIONS	006
	1.5 OBJECTIVES	007
II	2.0 PHYSICAL-MATHEMATICAL CONCEPTS	009
	2.1 SATURATED UNSATURATED GROUND WATER FLOW	012
	2.2 ENERGY TRANSPORT IN GROUND WATER	018
	2.3 SOLUTE TRANSPORT IN GROUND WATER	020
	2.4 DESCRIPTION OF DISPERSION	027
III	3.0 PROGRAM ALGORITHMS	035
	3.1 SOLUTION SEQUENCING	039
	3.2 SPECIFICATION OF BOUNDARY CONDITIONS	039
IV	4.0 DEVELOPMENT AND APPLICATION OF THE MODEL	041
	4.1 PROGRAM COMPILATION	041
	4.2 TEST RUN	041
	4.3 NUMERICAL SIMULATION	044
V	5.0 RECOMMENDATION	095
	5.1 CONCLUSION	097
	Bibliography	099

LIST OF FIGURES

SR. NO.	FIG. NO.	PARTICULARS	PAGE NO.
1	1	DEFINITION OF ANISOTROPIC PERMEABILITY AND EFFECTIVE PERMEABILITY.	031
2	2	DEFINITION OF FLOW-DIRECTION-DEPENDENT LONGITUDINAL DISPERSIVITY.	032
3	3	SUTRA LOGIC FLOW.	036
4	4	SCHEMATIC REPRESENTATION OF SPECIFIED HEAD BOUNDARY CONDITION.	040
5	5	RADIAL FINITE-ELEMENT MESH FOR CONSTANT DENSITY SOLUTE AND ENERGY TRANSPORT EXAMPLE.	040
6	6	COMPARISON OF SUTRA SOLUTION WITH ANALYTICAL SOLUTION IN TIME STEP 15.	046
7	7	COMPARISON OF SUTRA SOLUTION WITH ANALYTICAL SOLUTION IN TIME STEP 30.	047
8	8	COMPARISON OF SUTRA SOLUTION WITH ANALYTICAL SOLUTION IN TIME STEP 45.	048
9	9a	LOCATION MAP OF THE STUDY AREA.	049
10	9b	INDUSTRY LOCATION MAP.	049
11	10	OBSERVED WELL HYDROGRAPH AND TDS VARIATION IN VANIYAMBADI.	051
12	11	OBSERVED WELL HYDROGRAPH AND TDS VARIATION IN MINNUR.	051
13	12	DESCRETIZED MESH OF STUDY AREA.	055
14	13	ALLOCATION OF SOURCES AND BOUNDARY FLUXES IN EQUAL-SIZED ELEMENTS.	056
15	14a	PRESSURE VS POROSITY IN NODE 5.	060
16	14b	PRESSURE VS POROSITY IN NODE 77.	060
17	14c	PRESSURE VS POROSITY IN NODE 150.	061
18	15a	CONCENTRATION VS POROSITY IN NODE 5.	061
19	15b	CONCENTRATION VS POROSITY IN NODE 77.	062
20	15c	CONCENTRATION VS POROSITY IN NODE 150.	062
21	16a	PRESSURE VS PERMEABILITY IN NODE 5.	063
22	16b	PRESSURE VS PERMEABILITY IN NODE 77.	063
23	16c	PRESSURE VS PERMEABILITY IN NODE 150.	064
24	17a	CONCENTRATION VS PERMEABILITY IN NODE 5.	064
25	17b	CONCENTRATION VS PERMEABILITY IN NODE 77.	065
26	17c	CONCENTRATION VS PERMEABILITY IN NODE 150.	065
27	18a	PRESSURE VS STORATIVITY IN NODE 5.	066
28	18b	PRESSURE VS STORATIVITY IN NODE 77.	066
29	18c	PRESSURE VS STORATIVITY IN NODE 150.	067
30	19a	CONCENTRATION VS STORATIVITY IN NODE 5.	067
31	19b	CONCENTRATION VS STORATIVITY IN NODE 77.	068
32	19c	CONCENTRATION VS STORATIVITY IN NODE 150.	068
33	20a	CONCENTRATION VS DISPERSIVITY IN NODE 5.	070
34	20b	CONCENTRATION VS DISPERSIVITY IN NODE 77.	071
35	20c	CONCENTRATION VS DISPERSIVITY IN NODE 150.	072
36	21	ARIAL STEADY STATE PRESSURE DISTRIBUTION.	073
37	22	TEMPORAL CONCENTRATION VARIATION IN STEADY STATE CONDITION.	075

38	23	ARIAL VARIATION OF CONCENTRATION IN STEADY STATE CONDITION.	Ø76
39	24	TEMPORAL PRESSURE VARIATION IN TRANSIENT CONDITION.	Ø78
40	25	TEMPORAL CONCENTRATION VARIATION IN TRANSIENT CONDITION.	Ø79
41	26	ARIAL VARIATION OF CONCENTRATION IN TRANSIENT CONDITION.	Ø80
42	27	TEMPORAL CONCENTRATION VARIATION IN CASE 1	Ø81
43	28a	ARIAL VARIATION OF CONCENTRATION FOR CASE1 TIME STEP 31.	Ø82
44	28b	ARIAL VARIATION OF CONCENTRATION FOR CASE1 TIME STEP 61.	Ø83
45	29	TEMPORAL CONCENTRATION VARIATION IN CASE 2	Ø84
46	30a	ARIAL VARIATION OF CONCENTRATION FOR CASE2 TIME STEP 31.	Ø85
47	30b	ARIAL VARIATION OF CONCENTRATION FOR CASE2 TIME STEP 61.	Ø86
48	31	TEMPORAL CONCENTRATION VARIATION IN CASE 3	Ø87
49	32a	ARIAL VARIATION OF CONCENTRATION FOR CASE3 TIME STEP 31.	Ø89
50	32b	ARIAL VARIATION OF CONCENTRATION FOR CASE3 TIME STEP 61.	Ø90
51	33	TEMPORAL CONCENTRATION VARIATION IN CASE 4	Ø91
52	34a	ARIAL VARIATION OF CONCENTRATION FOR CASE4 TIME STEP 31.	Ø92
53	34b	ARIAL VARIATION OF CONCENTRATION FOR CASE4 TIME STEP 61.	Ø94
54	35	OBSERVATION NETWORK FOR FUTURE SIMULATION IN PALAR RIVER BASIN.	Ø98

LIST OF TABLES

SR.NO.	TABLE NO.	PARTICULARS	PAGE NO.
1	1	STEADY STATE PRESSURE RESULTS OF ENERGY TRANSPORT EXAMPLE.	Ø45
2	2	PUMP TEST DATA	Ø77

List of Notations

Mesh and coordinate data

ρ_x	$[L/\sigma^2]$	GRAVX	x-component of gravity vector
ρ_y	$[L/\sigma^2]$	GRAVY	y-component of gravity vector
x_i	[L]	X(I)	x coordinate of node i, for all nodes in mesh
y_i	[L]	Y(I)	y coordinate of node i, for all nodes in mesh
NN		NN	total number of nodes in mesh
		IIN(1-4)	counter-clockwise nodal incidence list in each element
		IEDGE(1-4)	ordered list of pinch nodes in each element according to Figure 5.5
NE		NE	total number of elements in mesh
		NPINCH	total number of pinch nodes in mesh
		NDI	full band-width of global banded matrix

Flow parameters

β	$[\beta/(L \cdot \sigma^2)]^{-1}$	COMPFL	fluid compressibility
α	$[\alpha/(L \cdot \sigma^2)]^{-1}$	COMPMA	solid matrix compressibility
ϵ_i	[1]	POR(I)	volumetric porosity of solid matrix at each node
$k_{max,i}$	$[L^2]$	PMAX(L)	maximum component of permeability in each element
$k_{min,i}$	$[L^2]$	PMIN(L)	minimum component of permeability in each element
θ_i	[°]	ANGLEX(L)	angle between k_{max} and +x-axis in each element
ρ_0	$[M/L^3]$	RHOWO	fluid base density

$\frac{\partial \rho}{\partial H}$	{	[M/L ³ ·°C]	DRWDU	for energy transport: coefficient of fluid density change with temperature
		or		
		{ [M ² /L ³ ·M _g]	DRWDU	for solute transport: coefficient of fluid density change with concentration
U_0	{	[°C]	URHOWO	for energy transport: base temperature for density calculation
		or		
		{ [M _g /M]	URHOWO	for solute transport: base concentration for density calculation

Transport parameters

α_{LmaxL}	[L]	ALMAX (L)	value of longitudinal dispersivity in direction of k_{max} in each element	
α_{LminL}	[L]	ALMIN (L)	value of longitudinal dispersivity in direction of k_{min} in each element	
α_{Tf}	[L]	ATAVG (L)	value of transverse dispersivity in each element	
σ_w	{	[E/(L·°C·s)]	SIGMAW	for energy transport: fluid thermal conductivity
		or		
		{ [m ² /s]	SIGMAW	for solute transport: molecular diffusivity of solute in fluid
σ_n	[E/(L·°C·s)]	SIGMAS	for energy transport: solid grain thermal conductivity (equals zero for solute transport)	
c_w	[E/(M·°C)]	CW	for energy transport: fluid specific heat capacity (equals one for solute transport)	
c_n	[E/(M·°C)]	CS	for energy transport: solid grain specific heat capacity (not specified in input data for solute transport)	
ρ_n	[M/L ³]	RHOS	density of a solid grain in the solid matrix	

Reaction and production parameters

Linear Sorption Isotherm

x_1 $[L_f^3/M_G]$ CHI1 linear distribution coefficient ~~CHI1~~
 (x_2 is zero for this isotherm)

Freundlich Sorption Isotherm

x_1 $[L_f^3/M_G]$ CHI1 Freundlich distribution coefficient
 x_2 [1] CHI2 Freundlich coefficient

Langmuir Sorption Isotherm

x_1 $[L_f^3/M_G]$ CHI1 Langmuir distribution coefficient
 x_2 $[L_f^3/M_n]$ CHI2 Langmuir coefficient

Production

γ_1^w $[s^{-1}]$ PRODF1 for solute transport: rate of first-order production of adsorbate mass in the fluid mass (equals zero for energy transport)

γ_1^v $[s^{-1}]$ PRODS1 for solute transport: rate of first order production of solute mass in the immobile phase (equals zero for energy transport)

γ_0^w $\left\{ \begin{array}{l} [(E/M)/n] \\ [(M_n/M)/s] \end{array} \right.$ PRODF0 for energy transport: zero-order rate of energy production in the fluid

γ_0^w $\left\{ \begin{array}{l} [(E/M)/n] \\ [(M_n/M)/s] \end{array} \right.$ PRODF0 for solute transport: zero-order rate of solute mass production in the fluid

γ_0^v $\left\{ \begin{array}{l} [(E/M_G)/n] \\ [(M_n/M_G)/n] \end{array} \right.$ PRODS0 for energy transport: zero-order rate of energy production in the immobile phase

γ_0^v $\left\{ \begin{array}{l} [(E/M_G)/n] \\ [(M_n/M_G)/n] \end{array} \right.$ PRODS0 for solute transport: zero-order rate of adsorbate mass production in the immobile phase

ABSTRACT

SUTRA, the Saturated-Unsaturated-Transport algorithm generated by Voss Clifford I. of United States Geological, Washington, has been recompiled on personnel computers after making needful modifications. The results of the test runs both for energy and solute transport has been checked through the appended output listing for the same problem in U.S. Geological Survey Water Resources Investigation Report B4-4369 and also verified with some analytical solutions.

A pilot simulation has been carried out for an hypothetical case based on the available field data of Vaniyambadi-Minnur river stretch of Palar river basin. Results of the simulation are encouraging. Conclusions are drawn in terms of fruitful recommendations for more realistic simulated aquifer response, which would represent a global scenario of the pollution problem and its management.

CHAPTER I

1.0 Introduction

In recent years there has been an explosive increase in the use of deterministic , distributed-parameter , ground water simulation models for analysing contaminant transport in ground-water systems and for predicting system responses to changes in stresses.

Analytical solutions are available to solve the solute transport equation . However , obtaining the exact analytical solution to the partial differential equation requires that the properties and boundaries of the flow system be highly and perhaps unrealistically idealised. For simulating most field problems , the mathematical benefits of obtaining an exact analytical solution are probably outweighed by the errors introduced by the simplifying approximations of the complex field environment that are required to apply the analytical approach.

Because of the difficulty in obtaining analytical solutions to groundwater flow problem , numerical solutions are widely in practice. With the formulation of governing equation and numerical methods, a specific computer code can be developed by constructing an algorithm , eliminating coding errors , running sample problems and producing a user's guide.

The solute transport equation is in general more difficult to solve numerically than the groundwater flow equation, largely because certain mathematical properties of the transport equation vary depending upon which terms in the equation are dominant in a particular situation. The numerical methods that work best for parabolic partial differential equations are not best for solving hyperbolic equations, and vice versa. Thus , no one numerical method or simulation model will be ideal for the entire spectrum of groundwater transport problems likely to be encountered in the field. Further compounding this difficulty is the fact that the groundwater flow velocity within a given multidimensional flow field will normally vary greatly, from near zero in low permeability zones or near stagnation points , to several feet or meters per day in high permeability areas or near stress points. Thus for a given single groundwater system , the mathematical characteristic of the transport process may vary between hyperbolic and parabolic , so that no one model may even be best over the entire domain of a single problem.

Three types of numerical methods are commonly used to solve the solute transport equation : finite difference methods, finite element methods, and the method of characteristics. Each has some advantages , disadvantages and special limitations for applications to field problems.

The method of characteristics was originally developed to solve hyperbolic equations. This approach will be useful if solute transport is dominated by convective transport, as is common in many field problems. Finite difference and finite element methods can accurately and efficiently solve the transport equation, particularly when dispersive transport is large compared to convective transport. However, problems of numerical dispersion and oscillations may induce significant errors for some problems.

1.1 Some Reviews

Peaceman and Rachford(1962) presented a centered in time and centered in distance equation combined with a 'transfer of overshoot' procedure which was demonstrated to work well in one dimension. Gardner, Peaceman and Pozzi (1964) used the method of characteristics to improve the numerical solution to the miscible flow problem, but did not consider the dispersion coefficient as a tensor. Shamir and Harleman(1966) used a very ingenious concept in their numerical technique. First they wrote the dispersion equation in terms of stream function and potential function and found it to be one dimensional in the convective term. They then used the Stone and Brian (1963) numerical technique for one dimensional flow and handled the lateral dispersion with an ADIP technique. If the major axis of the dispersion tensor coincides with the velocity vector, then Shamir and Harleman's technique will consider the dispersion coefficient as a tensor.

Nelson(1965) described a computer program for predicting waste transport in groundwater. The programme generated permeability information and stream functions using a potential map with a small amount of permeability information. He however neglected dispersion entirely. Reddell and Sunada (1970) developed a computer programme using a two dimensional finite equations and explicit scheme for the solution of dispersion.

Maddaus and Aarson (1972) used a computer based finite difference model of two dimensional aquifer flow to predict quality trends throughout a groundwater basin. Lyons and Stewart(1973) developed a distributed two dimensional finite difference model coupled with a storage effect for the unsaturated zone to predict TDS in a basin. Pinder(1973) used a finite element method to predict concentration distribution in an aquifer including the effects of hydrodynamic dispersion. A comprehensive review of solute transport models is presented by Anderson (1979). The model survey of Van der Heijde and others (1985) reviews a total of 84 numerical, mass transport models. Hamilton and others (1985) compare the application of three different transport models to a single field problem; they conclude that the Peclet number is a critical criterion to evaluate. Documented models based on variants of the method of characteristics approach include Konikow and Bredehoeft (1978) and Prickett and others (1981). Examples of recently documented three dimensional, transient, finite difference models that simultaneously solves the fluid pressure, energy transport, and solute transport equa-

tions for nonhomogeneous miscible fluids include Kipp (1987) and Reeves and others (1986). A two dimensional finite element transport model is documented by Voss(1984).

Anand and Pandit (1982) developed a two dimensional finite element model for coupled ground water flow and transient transport conditions, concluded that the refinement of the mesh as well as the appropriate region size required for the solution depend largely upon the magnitude of the field parameters and in particular the Peclet number. Frind (1982) used the principal direction technique based on Galerkin finite element to ground-water contaminant transport modelling more accurately and efficiently. Pandit and Anand (1984) conducted a detailed a parametric study to determine the influence of various nondimensional field parameters on salt water encroachment, considering coefficient of hydrodynamic diversion to be a function of soil dispersivity and interstitial pore velocity as proposed by Bear(1960). For the boundary conditions utilised by Henry, results of the study indicate that for this particular case the ratio of the principal hydraulic conductivity tensors K_{yy}/K_{xx} doesnot greatly affect the extent of salt water encroachment. Similarly, the ratio of the transverse to longitudinal dispersivity also does not exert a major influence on the encroachment.

R.W. Raige et al (1986), presented a computer programme for analysing groundwater flow and pollutant transport for sites where waste is to be buried in the ground at shallow depth. It is shown that ignoring non linear sorption mechanisms for pollutant transport, calculations may have a significant effect on the results. H.C. Ammentrop et al (1986) developed a tool for evaluations of irrigation schemes in areas with salinity problems in the form of a numerical model for solute transport in the unsaturated zone, based on the basic equation for soil water flow in one dimension and the general convection dispersion equation.

D.Tolikaaset et al (1986) presented a mathematical model for optimal groundwater quality management. Groundwater contamination is simulated by a two dimensional transport model which requires the numerical solution of the partial differential equation describing solute transport in one dimension only. R. Mockey et al (1986) developed a 2D finite element model incorporating all the major groundwater flow controls. The data assigned to the nodes of the model are generated using a linear interpolation technique known as Kriging.

Bear et al (1988) presented a model of heat and mass transfer in the unsaturated zone taking into account the effect of temperature gradient in the advective water flux and of enhanced thermal conduction by the processes of latent heat transfer with the vapour flow. Sorek (1988) used Eulerian -Lagrangian scheme to reformulate the equation of solute transport with groundwater in saturated soil. Simulation with coarse grid and high Peclet numbers yielded minute mass balance errors. Bobba and Joshi (1988) developed a finite element model for delineating radioactive contaminant plumes via groundwater.

Mathematical models of ground-water flow and salt transport were used by Zonooz and Duffy (1993) to identify the important mechanisms controlling the migration of dissolved salts in the sub surface return flows and to estimate the impact of changing irrigation practices on downstream salinity at the Miller creek field site. A Galerkin finite element method was used in conjunction with a triangular element discretization scheme to investigate flow and salt transport involving two spatial dimensions in the vertical plane. The parameters of the flow and salt transport models were adjusted by trial and error or using independent field information to estimate the impacts of water infiltrating from canals and irrigated fields and its salt content on the amounts, timing and chemical composition of the ground water.

Because none of the standard numerical methods are ideal for a wide range of transport problems, there is currently much research on mixed or adaptive methods that aim to minimize numerical errors and combine the best features of alternative standard numerical approaches. Examples include Carrera and Melloni (1987), Ewing, Russell, and Wheeler (1983), Fujinawa (1986), and Neuman (1984).

Due to the complexity of most groundwater systems the solution to the flow and transport problem is generally derived by numerical treatment of the equation. A variety of numerical schemes have been applied to the groundwater flow and transport problems using computers and a number of generalised computer codes are now available which can be used for the simulation of most aquifer systems. However, although simulation models can be very complex in their formulation, it must be remembered that they remain highly simplified representation of the aquifer system.

Organisations such as EPA, NRC, and DOE, among others have sponsored several surveys to review the capabilities of various codes. United States Geological Survey has developed number of generalised codes.

MOC, the USGS computer model of two dimensional solute transport and dispersion in Groundwater is developed by L.F. Konikow and J.D. Bredehoeft. Other important models developed at USGS are MOC DENSE, SUTRA, HST3D, FEMSEEP and AQUA.

MOC DENSE developed by W.E. Sanford and L.F. Konikow simulates solute transport and dispersion of either one or two constituents in groundwater where there is two-dimensional density dependent flow.

HST3D is developed by Kenneth L. Kipp, Jr. for simulation of Heat and solute transport in three dimensions. INTERTRANS is a three dimensional solute transport model which uses the particle tracking technique in simulating contaminant advection and dispersion.

FEMSEEP is a powerful groundwater flow and contaminant transport model based on the finite element method with particle tracking algorithm. It is capable of steady and non-steady groundwater flow and solute transport in a two dimensional horizontal plane , a vertical cross-section , or three dimensional axisymmetric systems.

AQUA is designed to solve problems like groundwater flow with inhomogeneous and anisotropic flow conditions , and steady state and transient transport of contaminants and heat with velocity dependent dispersion , convection , decay and adsorption.

SUTRA, A finite element simulation model for saturated - Unsaturated , fluid density -dependent groundwater flow with energy transport or chemically reactive single species solute transport is a versatile computer program by Clifford I.Voss of USGS. This model can be used for areal and cross sectional modelling of saturated flow systems, and for cross section of one dimensional vertical modelling of unsaturated zone flow.

It may be concluded from the above review that Finite Element Method is best and widely used as compared to the other methods specially when the contaminant transport is due to dispersion. Peclet number is the main criteria for simulation. In the present study , SUTRA model has been redeveloped and used for simulating groundwater flow and contamination due to its following salient features.

1.2 Purpose & Scope

SUTRA is based on a general physical , mathematical and numerical structure implemented in the computer code in a modular design. The model employs a two-dimensional hybrid finite element and integrated finite difference method to approximate the governing equations that describe the two interdependent processes that are simulated:

1) fluid density-dependent saturated or unsaturated groundwater flow,

and either

2) transport of a solute in the groundwater , in which solute may be subject to : equilibrium adsorption on the porous matrix, and both first-order and zero order production or decay,

or

3) transport of thermal energy in the groundwater and solid matrix of the aquifer.

SUTRA is a very convenient and a simple model which may be used for the evaluation of the time-dependent fluid pressure and either solute concentration or temperature. This model stresses general applicability, numerical robustness and accuracy, and clarity in coding. Generally aquifer and transport parameters may vary in value throughout the simulated region. Sources and boundary conditions of fluid, solute and energy may be specified to vary with time or may be constant. SUTRA also consider the diffusion and dispersion processes. Longitudinal and transverse dispersivity varies depending on the angle between the flow direction and the principal axis of aquifer permeability when permeability is anisotropic.

1.3 Application

Application of SUTRA model is manifold. It can be used for both one and two dimensional analyses. Simulation of flow may be either steady state or transient. SUTRA flow simulation may be employed for areal and cross-sectional modeling of saturated groundwater flow systems, and unsaturated zone flow. SUTRA solute transport simulation may be employed to model natural or man-induced chemical species transport including processes of solute sorption, production and decay. Such simulation may be used to analyse groundwater contaminant transport problems and aquifer restoration designs.

SUTRA solute transport simulation may be used for modeling of variable density leachate movement, and for cross-sectional modeling of salt-water intrusion in aquifers at both near-well or regional scales with either dispersed or relatively sharp transition zones between fresh and salt water. SUTRA energy transport simulation may be employed to model thermal regimes in aquifers, subsurface heat conduction, aquifer thermal energy systems, geothermal reservoirs, thermal pollution of aquifers, and natural hydrogeologic convection systems.

1.4 Rare limitations

SUTRA will provide clear, accurate answers only to well posed, well-defined, and well discretized simulation problems. In less-well-defined systems, SUTRA is not useful for making exact predictions of future responses of the typical hydrologic systems which are not well defined. Rather, SUTRA is useful for hypothesis testing and for helping to understand the physics of such a system. On the other hand, developing an understanding of a system based on simulation analysis can help make a set of worthwhile predictions which are predicted on uncertainty of both the physical model design and model parameter values. In particular, transport simulation which relies on large amounts of dispersion must be considered an uncertain basis for prediction, because of the highly idealised description inherent in the SUTRA dispersion process.

In some cases , the available real data on a system may be so poor that a simulation using SUTRA is so ambiguously defined that no prediction at all can be made. In this instance , the simulation may be used to point out the need for particular types of data collection . The model could be used to advantage in visualising possible regimes of system behaviour rather than to determine which is accurate.

In general, SUTRA is best suitable for the simulation of two dimensional flow and either solute or energy transport in saturated variable density systems. However, for the unsaturated problems it cannot be easily applied because numerical algorithms are not specialised for the non-linearities of unsaturated flow. Lacking these special methods, SUTRA requires fine spatial and temporal discretization for unsaturated flow , and is therefore not an economical tool for extensive unsaturated flow modeling. In the case of steady state solutions only single solution step is usually not appropriate for non-linear problems with variable density , saturation , viscosity and non linear sorption.

1.5 Objectives of the present study

Groundwater quality modelling as such is comparatively a new area of research and investigation. More over not much of work has been initiated in India using sophisticated model technology. This may be because of the fact that ready made numerical models are not so easy to apply to the field problems directly due to the complications in understanding both, the model configuration and physical site conditions. Also numerical models largely depended upon the sophisticated systems having huge quantity of storage facilities. In contrast to this ground water pollution problems has increased manifolds during last few decades. Therefore the objective of the present study is to:

- (1) To initiate an understanding of the numerical modelling of groundwater pollution through some existing model , preferably Sutra in the present study.
- (2) To redevelop the computer code from available source listing, with due modifications, which can be used on personal computers quite easily.
- (3) To apply the model to an hypothetical problem based upon the data base of an actual field problem to the extent it is available.
- (4) To recommend the observation network for simulating the field problem specified at point (3) successfully in future.

This report contains in all five chapters. First chapter which we are presently undergoing introduces with sutra model after some useful literature reviews. Second chapter includes an overview of the physical and mathematical background on which sutra simulation depends and physical parameter required as an input data. Programme algorithms are described in chapter three

along with some important information for the users regarding solution sequencing and boundary conditions. Chapter four deals with the development and application of the model which includes the modifications made in the source listing, test runs, comparison of model results with analytical solutions, and numerical simulation of an hypothetical case developed for the Palar River basin in Tamilnadu between Vaniyambadi and Minnur.

Conclusions and recommendations of the study are mentioned in chapter five alongwith a trial network of observations wells which can be utilised while simulating the flow and concentration in the region of Palar river basin in future.

CHAPTER II

2.0 Physical-Mathematical Concepts : A Review

SUTRA simulation combines two physical models, one to simulate the flow of ground water, and the second to simulate the movement of either thermal energy or a single solute in the ground water which has identical mathematical expressions. The primary variable upon which the flow model is based is fluid pressure, which may vary spatially in ground-water system, as well as with time. Variation in fluid density, aside from fluid pressure difference, may also drive flow. The effects of gravity acting on fluids with different density must therefore be accounted for in the flow field.

The flow of ground water, is a fundamental mechanism upon which the physical models of energy transport and solute transport are based. SUTRA allows only the transport of either thermal energy or a single solute to be modeled in a given simulation. Thus, when simulating energy transport, a constant value of solute concentration is assumed in the ground water. When simulating solute transport, a constant ground-water temperature is assumed.

SUTRA simulation is carried out in two space dimensions with parameters varying in these two directions. However, the region of space to be simulated may be defined as three dimensional, when the assumption is made that all SUTRA parameters and coefficients have a constant value in the third space direction. A SUTRA simulation may be carried out over a region defined over two space coordination (x,y) in which the thickness of the region measured in the third coordinate direction (z) varies depending on (x,y) position.

The ground-water fluid density and viscosity may vary depending on pressure, temperature and solute concentration. Total fluid density is the sum of pure water density, w , and solute volumetric concentration (Ms/L), c . The solute concentration refers to solute mass fraction (Ms/M), C and not c . Fluid density, while a weak function of pressure is primarily dependent upon fluid solute concentration and temperature. The approximate density models employed by SUTRA are first order Taylor expansions about a base (reference) density.

For energy transport:

$$\rho = \rho(T) = \rho_o + \frac{\delta\rho}{\delta T} (T - T_o) \text{-----(1)}$$

Where ρ_o is the base fluid density at a base (reference) temperature of T_o , and $\delta\rho/\delta T$ is a constant value of density change with temperature.

For solute transport:

$$\rho = \rho(C) = \rho_o + \frac{\delta\rho}{\delta C} (C - C_o) \text{-----(2)}$$

where ρ_o is the base fluid density at base concentration, C_o . The factor $\delta\rho/\delta C$ is a constant value of density change with concentration.

Fluid viscosity, is a weak function of pressure and of concentration, (for all except very high concentrations), and depends primarily on fluid temperature. For energy transport the viscosity of pure water is given in m-k-s units by:

$$\mu(T) = (239.4 \times 10^{-7} \cdot 248.37 / (T + 133.15)) \text{ [kg/(m.s)]-----(3)}$$

For solute transport, viscosity is taken to be constant. For example at 20°C , it is equal to 1.0×10^{-3} [Kg/M.S].

The total volume of a porous medium is composed of a matrix of solid grains, and of void space. The volume of void space may be fully or partly filled with gas or liquid, and is commonly referred to as the pore volume. Porosity is defined as a volume of voids in the soil matrix per total volume of voids plus matrix. SUTRA employs only one type of porosity, . In some instances there may be need to distinguish between a porosity for pores which take part in fluid flow, and pores which contain stagnant fluid. The fraction of total volume filled by the fluid is S_w , where, S_w is water saturation, when $S_w=1$, the void space is completely filled with fluid and is said to be saturated. When $S_w < 1$, the void space is only partly water filled and is referred to as being unsaturated.

When $S_w < 1$, water adheres to the surface of solid grains by surface tension effects, and the fluid pressure is less than

atmospheric. Fluid pressure, p , is measured with respect to background or atmospheric pressure. The negative pressure is defined as capillary pressure, which exists only for $p < 0$. In a saturated porous medium, as fluid (gauge) pressure drops below zero, air may not directly enter the void space, but may enter suddenly when a critical capillary pressure is reached. This pressure, P_{cent} , is the entry pressure (or bubble pressure). The relationship between fluid saturation and capillary pressure in a given medium is typically determined by laboratory experiment, and except for the portion near bubble pressure, tends to have an exponential character

Aquifer storativity under fully saturated conditions is related to the factor, $\delta(\epsilon\rho)/\delta p$, by definition, (Bear, 1979). The specific pressure storativity, S_{op} , is the volume of water released from saturated pore storage due to a unit drop in fluid pressure per total solid matrix plus pore volume. Note

-1

that the common specific storativity, S_o [L], which when multiplied by confined aquifer thickness gives the well known storage coefficient, $S[1]$, is related to S_{op} as, $S_o = \rho [g] S_{op}$, where $[g]$

2

[L/s] is the magnitude of the gravitational acceleration vector. The common specific storativity, S_o , is analogous to specific pressure storativity, S_{op} , used in SUTRA, except that S_o expresses the volume of water released from pore storage due to a unit drop in piezometric head.

SUTRA employs an expanded form of the specific pressure storativity based on fluid and bulk porous matrix compressibilities. The relationship is obtained as follows:

$$\rho S_{op} = \rho \frac{\delta \epsilon}{\delta p} + \epsilon \frac{\delta \rho}{\delta p} \quad \text{----- (4)}$$

The coefficient of compressibility of water is defined by

$$\beta = \frac{1}{\rho} \cdot \frac{\delta \rho}{\delta p} \quad \text{----- (5)}$$

and $\delta \epsilon / \delta p = (1 - \epsilon) \alpha$ where α is porous matrix compressibility.

which allows the last term of the previous equation, to be replaced by $\epsilon \beta \rho$. Thus the specific pressure storativity, S_{op} , is expanded as:

$$S_{op} = (1 - \epsilon)\alpha + \epsilon\beta$$

2.1 Description of Saturated-Unsaturated Ground-water Flow

2.1.1. Fluid flow and flow properties

Fluid movement in porous media where fluid density varies spatially may be driven by either differences in fluid pressure or by unstable variations in fluid density. Pressure-driven flows, for example, are directed from regions of higher than hydrostatic fluid pressure toward regions of lower than hydrostatic pressure. Density-driven flows occur when gravity forces act on denser regions of fluid causing them to flow downward relative to fluid regions which are less dense. A stable density configuration drives no flow, and is one in which fluid density remains constant or increases with depth.

The mechanisms of pressure and density driving forces for flow are expressed for SUTRA simulation by a general form of Darcy's law which is commonly used to describe flow in porous media:

$$\underline{y} = - \left(\frac{k k_r}{\epsilon S_w \mu} \right) \cdot (\nabla p - \rho \underline{g}) \quad \text{-----(7a)}$$

where:

$\underline{y}(x,y,t)$	[L/S] 2	average fluid velocity
$\underline{k}(x,y)$	[L]	solid matrix permeability (2 X 2 tensor of values)
k^r	[1]	relative permeability to fluid flow (assumed to be independent of direction.)
\underline{g}	[L/S] 2	gravitational acceleration (gravi ty vector) (1 X 2 vector of values)

The gravity vector is defined in relation to the direction in which vertical elevation is measured:

$$\underline{g} = -|\underline{g}| \nabla \cdot (\text{ELEVATION}) \quad \text{-----(7b)}$$

where $|g|$ is the magnitude of the gravitational acceleration vector. For example, if the y-space-coordinate is oriented directly upwards, then $\nabla(\text{ELEVATION})$ is a vector of valued (for x and y directions, respectively): $(0,1)$, and $g = (0,-|g|)$. If for example, ELEVATION increases in the x-y plane at a 60° angle to the x-axis, then $\nabla(\text{ELEVATION}) = ((1/2), (3^{1/2}/2))$ and $g = (-(1/2)|g|, -(3^{1/2}/2)|g|)$.

The average fluid velocity, \underline{v} , is the velocity of fluid with respect to the stationary solid matrix. The so-called Darcy velocity, q , for the sake of reference, is $q = \epsilon.S_w.\underline{v}$. This value is always less than the true average fluid velocity, \underline{v} , and thus, not being a true indicator of the speed of water movement, 'Darcy velocity', q , is not a useful concept in simulation of subsurface transport. The velocity is referred to as an 'average', because true velocities in a porous medium vary from point to point due to variations in the permeability and porosity of the medium at a spatial scale smaller than that at which measurements were made.

Fluid velocity, even for a given pressure and density distribution, may take on different values depending on how mobile the fluid is within the solid matrix. Fluid mobility depends on the combination of permeability, k , relative permeability, k_r , and viscosity, μ . Permeability is a measure of the ease of fluid movement through interconnected voids in the solid matrix when all voids are completely saturated. Relative permeability expresses what fraction of the total permeability remains when the void are only partly fluid-filled and only part of the total interconnected void space is, in fact, connected by continuous fluid channels. Viscosity directly expresses ease of fluid flow; a less viscous fluid flows more readily under a driving force.

As a point of reference, in order to relate the general form of Darcy's law, back to a better-known form dependent on hydraulic head, the dependence of flow on density and saturation must be ignored. When the solid matrix is fully saturated, $S_w = 1$, the relative permeability to flow is unity $k_r = 1$. When, in addition, fluid density is constant, the right side of (7a) expanded by (7b) may be multiplied and divided by $\rho|g|$. Putting

$$\underline{K}(x,y,t) = (\underline{k}_r \rho |g|) / \mu$$

which is nothing but hydraulic conductivity [L/S], and hydraulic head, $h(x,y,t) = \text{pressure head, } hp(x,y,t) + \text{Elevation, where } hp(x,y,t) = p/(\rho|g|)$,

$$\underline{v} = - \left(\frac{K}{\epsilon} \right) \cdot \underline{\nabla} h \quad \text{-----(8)}$$

which is Darcy's law written in terms of the hydraulic head. Even in this basic form of Darcy's law, flow may depend on solute concentration and temperature. The hydraulic conductivity, through viscosity, is highly dependent on temperature, and measurably, but considerably less on concentration. In cases where density or viscosity are not constant, therefore, hydraulic conductivity, \underline{K} , is not a fundamental parameter describing ease of flow through the solid matrix. Permeability, \underline{k} , is in most situations, essentially independent of pressure, temperature and concentration and therefore is the appropriate fundamental parameter describing ease of flow in the SUTRA model.

Permeability, \underline{k} , describes ease of fluid flow in a saturated solid matrix. When permeability to flow in a particular small volume of solid matrix differs depending upon in which direction the flow occurs, the permeability is said to be anisotropic. Direction-independent permeability is called isotropic. It is commonly assumed that permeability is the same for flow forward or backward along a particular line in space. When permeability is anisotropic, there is always one particular direction, \underline{X}_p , along which permeability has an absolute maximum value, k_{max}

[L]. Somewhere in the plane perpendicular to the 'maximum direction' there is a direction, \underline{X}_m , in which permeability has the

absolute minimum value, k_{min} [L] which exists for the particular volume of solid matrix. Thus, in two dimensions, there are two principal orthogonal directions of anisotropic permeability. Both principal directions, \underline{X}_p and \underline{X}_m , are assumed to be within the (x,y) plane of the two-dimensional model.

The permeability tensor, \underline{k} , of Darcy's law, equation(7) has four components in two dimensions. These tensorial components have values which depend on effective permeabilities in the x and y, coordinate directions which are not necessarily exactly aligned with the principal directions of permeability. The fact that maximum and principal permeability values may change in both value and direction from place to place in the modeled region makes the calculation of the permeability tensor, which is aligned in x and y, complex.

An anisotropic permeability field in two dimensions is completely described by the values k_{max} and k_{min} and the angle orienting the principal directions, X_p and X_m , to the x and y directions through the permeability ellipse shown in Figure 1. The semi-major and semi-minor axes of the ellipse are defined as

$k_{max}^{1/2}$, and $k_{min}^{1/2}$, respectively, and the length of any radius is $k^{1/2}$ where k is the effective permeability for flow along that direction. Only, k_{max} , k_{min} and O , the angle between the x -axis and the maximum direction X_p need be specified to define the permeability, k , in any direction, where:

$k_{max}(x,y)$	[L]	absolute maximum value of permeability
$k_{min}(x,y)$	[L]	absolute minimum value of permeability
$O(x,y)$	[]	angle from +x-coordinate axis to direction of maximum permeability, x_p

In the case of isotropic permeability, $k_{max} = k_{min}$, and O is arbitrary.

The discussion of isotropic and anisotropic permeability, k , applies as well to flow in an unsaturated solid matrix, $Sw < 1$, although unsaturated flow has additional unique properties which require definition. When fluid capillary pressure, P_c , is less than entry capillary pressure, P_{cent} , the void space is saturated $Sw = 1$, and local porous medium flow properties are not pressure dependent but depend only on void space geometry and connectivity. When $P_c > P_{cent}$, then air or another gas has entered the matrix and the void space is only partly fluid filled, $Sw < 1$. In this case, the ease with which fluid can pass through the remaining cross-section of well-connected fluid channels through the matrix, as well as on surface tension forces at fluid-gas, and fluid-solid interfaces. When saturation is so small such that no interconnected fluid channels exist and residual fluid is scattered about and tightly bound in the smallest void spaces by surface tension, flow ceases entirely. The relative permeability to flow, k_r , which is a measure of this behavior, varies from a value of zero or near-zero at the residual fluid saturation, Sw_{res} , to a value of one at saturation, $Sw = 1$. A relative permeability-saturation relationship is typically determined for a particular solid matrix material in the laboratory as is the relationship, $Sw(P_c)$. Relative permeability is assumed in SUTRA to be independent of direction in the porous media.

SUTRA allows any desired function to be specified which gives the relative permeability in terms of saturation or pressure.

Flow in the gaseous phases that fills the remaining void space not containing fluid when $S_w < 1$ is assumed not to contribute significantly to total solute or energy transport which is due primarily to fluid flow and other transport processes through both fluid and solid matrix. Furthermore it is assumed that pressure differences within the gas do not drive significant fluid flow. These assumptions are justified in most common situations when gas pressure is approximately constant throughout the solid matrix system. Should gas pressure vary appreciably in a field system, simulation with SUTRA, which is by definition a single phase flow and transport model, must be critically evaluated against the possible necessity of employing a multiphase fluid flow and transport model.

2.1.2 Fluid mass balance

The "so-called" flow simulation provided by SUTRA is in actuality a calculation of how the amount of fluid mass contained within the void spaces of the solid matrix changes with time. In a particular volume of solid matrix and void space, the total fluid mass $(\epsilon S_w \rho) VOL$, may change with time due to: ambient ground-water inflows or outflows, injection or withdrawal wells, changes in fluid density caused by changing temperature or concentration, or changes in saturation. SUTRA flow simulation is, in fact, a fluid mass balance which keeps track of the fluid mass contained at every point in the simulated ground-water system as it changes with time due to flows, wells, and saturation or density changes.

The fluid mass balance is expressed as the sum of pure water and pure solute mass balances for a solid matrix in which there is negligible net movement:

$$\frac{\delta(\epsilon \cdot S_w \rho)}{\delta t} = - \nabla \cdot (\epsilon \cdot S_w \cdot \rho \cdot \underline{v}) + Q_p + T \text{ ----- (9)}$$

where:

$Q_p(x,y,t)$ $[M/(L^3 \cdot s)]$ fluid mass source (including pure water mass plus solute mass dissolved in source water)
 $T(x,y,t)$ $[M/(L^3 \cdot s)]$ Solute mass source (e.g. dissolution of solid matrix or desorption)

The term on the left may be recognized as the total change in fluid mass contained in the void space with time. The term involving, ∇ , represents to local fluid mass change due to excess of fluid inflows over outflows at a point. The fluid mass source term, Q_p , accounts for external additions of fluid including pure water mass plus the mass of any solute dissolved in the source fluid. The pure solute mass source term, T , may account for external additions of pure solute mass not associated with a fluid source. In most cases, this contribution to the total mass compared to the total pure water mass contributed by fluid sources, Q_p . Pure solute sources, T , are therefore neglected in the fluid mass balance, but may be readily included in SUTRA for special situations. Note that solute mass sources are not neglected in the solute mass balance.

While (9) is the most fundamental form of the fluid mass balance, it is necessary to express each mechanism represented by a term of the equation, in terms of the primary variables, P , C , and T . As SUTRA allows variation in only one of C or T at a time, the letter U is employed to represent either of these quantities. For a time derivative, the above discussed equations may be expanded as:

$$\frac{\delta(\epsilon \cdot S_w \cdot \rho)}{\delta t} = \left(S_w \cdot \rho \cdot S_{op} + \epsilon \rho \frac{\delta S_w}{\delta p} \right) \frac{\delta p}{\delta t} + \left(\epsilon S_w \frac{\delta \rho}{\delta U} \right) \frac{\delta U}{\delta t} \quad (10)$$

While the concepts upon which specific pressure storativity, S_{op} , is based, do not exactly hold for unsaturated media, the error introduced by summing the storativity term with the term involving $(\delta S_w / \delta p)$ is insignificant as $(\delta S_w / \delta p) \gg S_{op}$.

The exact form of the fluid mass balance as implemented in SUTRA is obtained from (9) by neglecting T , substituting (10) and employing Darcy's law, (7), for \underline{v} :

$$\left(S_w \cdot \rho \cdot S_{op} + \epsilon \rho \frac{\delta S_w}{\delta P} \right) \frac{\delta P}{\delta t} + \left(\epsilon \cdot S_w \cdot \frac{\delta \rho}{\delta U} \right) \frac{\delta U}{\delta t} - \nabla \cdot \left[\left(\frac{k \cdot k_r \cdot f}{\mu} \right) \cdot (\nabla P - \rho \underline{g}) \right] = Q_p \quad (11)$$

2.2 Description of Energy Transport in Ground Water

2.2.1 Subsurface energy transport mechanisms

Energy is transported in the water-solid matrix system by flow of ground water, and by thermal conduction from higher to lower temperatures through both the fluid and solid. The actual flow velocities of the ground water from point to point in the three-dimensional space of an aquifer may vary considerably about an average two dimensional velocity uniform in the z -direction, $\underline{v}(x,y,t)$, calculated from Darcy's law (9). As the true, not-average, velocity field is usually too complex to measure in real systems, an additional transport mechanism approximating the effects of mixing of different temperature ground waters moving both faster and slower than average velocity, \underline{v} , is hypothesized. This mechanism, called energy dispersion, is employed in SUTRA as the best currently available, though approximate description, of the mixing process. In the simple dispersion model employed, dispersion, in effect, adds to the thermal conductivity value of the fluid-solid medium in particular directions dependent upon the direction of fluid flow. In other words, mixing due to the existence of nonuniform, non-average velocities in three dimensions about the average-uniform flow, \underline{v} , is conceptualized in two dimensions as a diffusion-like process with anisotropic diffusivities.

The model has, in fact, been shown to describe transport well in purely homogeneous porous media with uniform one-dimensional flow. In heterogeneous field situations with non-uniform flow in, for example, irregular bedding or fractures, the model holds only at the predetermined scale at which dispersivities are calibrated and it must be considered as a currently necessary approximation, and be carefully applied when extrapolating to other scale of transport.

2.2.2 Solid matrix-fluid energy balance

The simulation of energy transport provided by SUTRA is actually a calculation of the time rate of change of the amount of energy stored in the solid matrix and fluid. In any particular volume of solid matrix plus fluid, the amount of energy contained is $[\epsilon \cdot S_w \cdot \rho_w \cdot e_w + (1 - \epsilon) \rho_s \cdot e_s] \cdot \text{VOL}$, where:

- e_w [E/M] energy per unit mass water
- e_s [E/MG] energy per unit mass solid matrix
- ρ_s [MG/LG] density of solid grains in solid matrix

and where [E] are energy units [M.L² / s²].

The stored energy in a volume may change with time due to: ambient water with a different temperature flowing in, well water of a different temperature injected, changes in the total mass of water in the block, thermal conduction (energy diffusion) into or out of the volume, and energy dispersion in or out.

This balance of changes in stored energy with various energy fluxes is expressed as follows:

$$\frac{\delta[\epsilon \cdot S_w \cdot \rho_w \cdot e_w + (1 - \epsilon) \rho_s \cdot e_s]}{\delta t} = - \nabla \cdot (\epsilon \cdot S_w \cdot \rho_w \cdot e_w \cdot \underline{v}) + \nabla \cdot [\lambda \cdot \underline{I} \cdot \nabla T] + \nabla \cdot [\epsilon \cdot S_w \cdot \rho_w \cdot C_w \cdot \underline{D} \cdot \nabla T] + Q_p \cdot C_w \cdot T^* + \epsilon \cdot S_w \cdot \rho_w \cdot r_w + (1 - \epsilon) \rho_s \cdot r_s \quad \text{-----(12)}$$

The time derivative expresses the total change in energy stored in both the solid matrix and fluid per unit total volume. The term involving \underline{v} expresses contributions to locally stored energy from average-uniform flowing fluid (average energy advection). The term involving bulk thermal conductivity, λ , expresses heat conduction contributions to local stored energy and the term involving the dispersivity tensor, \underline{D} , approximately expresses the contribution of irregular flows and mixing which are not accounted

for by average energy advection. The term involving Q_p accounts for the energy added by a fluid source with temperature, T^* . The last terms account for energy production in the fluid and solid, respectively, due to endothermic reactions, for example.

While more complex models are available and may be implemented if desired, SUTRA employs a volumetric average approximation for bulk thermal conductivity, λ :

$$\lambda = \epsilon S_w \lambda_w + (1 - \epsilon) \lambda_s \text{ -----(13)}$$

λ_w [E/ (s.L. °C)] Fluid thermal conductivity

λ_s [E/ (s.L. C)] Solid thermal conductivity
 ($\lambda_w \approx 0.6$ [J/ s.m. °C] at 20°C
 ($\lambda_s \sim 3.5$ [J/s.m. °C]] at 20°C
 for sandstone)

The specific energy content (per unit mass) of the fluid and the solid matrix depends on temperature as follows:

$$e_w = C_w T \text{ -----(14a)}$$

$$e_s = C_s T \text{ -----(14b)}$$

C_s [E/(MG. °C)] Solid grain specific heat
 ($C_s \sim 8.4 \times 10^2$ [J/kg. °C] for sand stone at 20°C)

An expanded form of the solid matrix-fluid energy balance is obtained by substitution of (14) and (13) into (12). This yields:

$$\begin{aligned} & \frac{\delta}{\delta t} [\epsilon S_w \rho C_w + (1 - \epsilon) \rho_s C_s] T + \nabla \cdot (\epsilon S_w \rho C_w \underline{v} T) \\ & - \nabla \cdot \{ [S_w \lambda_w + (1 - \epsilon) \lambda_s] \underline{I} + \epsilon S_w \rho C_w \underline{D} \} \cdot \nabla T \\ & = Q_p C_w T + \epsilon S_w \rho \gamma_0^w + (1 - \epsilon) \rho_s \gamma_0^s \text{ ----- (15)} \end{aligned}$$

2.3 Description of Solute Transport in Ground Water

2.3.1 Subsurface solute transport mechanisms

Solute mass is transported through the porous medium by flow of ground water (solute advection) and by molecular or ionic diffusion, which while small on a field scale, carries solute

mass from areas of high to low concentrations. The actual flow velocities of the groundwater from point to point in three dimensional space of an aquifer may vary considerably about an average, uniform two-dimensional velocity, \bar{v} , which is calculated from Darcy's law (9). As the true, not-average, velocity field is usually too complex to measure in real systems, an additional transport mechanism approximating the effects of mixing of waters with different concentrations moving both faster and slower than the average velocity, $\bar{v}(x,y,t)$, is hypothesized. This mechanism, called solute dispersion, is employed in SUTRA as the best currently available, though approximate, description of the mixing process. In the simple dispersion model employed, dispersion, in effect, significantly adds to the molecular diffusivity value of the fluid in particular directions dependent upon the direction of fluid flow. In other words, mixing due to the existence of non-uniform, non-average velocities in three dimensions about the average flow, \bar{v} , is conceptualized in two dimensions, as a diffusion-like process with anisotropic diffusivities.

The model has, in fact, been shown to describe transport well in purely homogeneous porous media with uniform one-dimensional flows. In heterogeneous field situations with non-uniform flows in, for example, irregular bedding or fractures, the model holds only at the predetermined scale at which dispersivities are calibrated and it must be considered as a currently necessary approximation, and be carefully applied when extrapolating to other scales of transport.

2.3.2 Solute and adsorbate mass balances

SUTRA solute transport simulation accounts for a single species mass stored in fluid solution as solute and species mass stored as adsorbate on the surfaces of solid matrix grains. Solute concentration, C , and adsorbate concentration, $C_s(x,y,t)$ [M/MG] (where [M] denotes units of solute mass, and [MG] denotes units of solid grain mass), are related through equilibrium adsorption isotherms. The species mass stored in solution in a particular volume of solid matrix may change with time due to ambient water with a different concentration flowing in, well water injected with a different concentration, changes in the total fluid mass in the block, solute diffusion or dispersion in or out of the volume, transfer of dissolved species to adsorbed species (or reverse), or a chemical or biological reaction caus-

ing solute production or decay. The species mass stored as adsorbate on the surface of solid grains in a particular block of solid matrix may change with time due to a gain of adsorbed species by transfer of solute from the fluid (or reverse), or a chemical or biological reaction causing adsorbate production or decay.

The separate balances for a single species stored in solution (solute) and on the solid grains (adsorbate), are expressed, respectively, as follows:

$$\frac{\delta(\epsilon S_w \rho C)}{\delta t} = -f - \nabla(\epsilon S_w \rho \cdot \underline{v} \cdot C) + \underline{v}[\epsilon S_w \rho \cdot (D_m \underline{I} + \underline{D}) \cdot \underline{v} C] + \epsilon S_w \rho \cdot \underline{T}_w + Q_p \cdot C \quad \text{-----(16)}$$

$$\frac{\delta[(1-\epsilon)\rho_s C_s]}{\delta t} = +f + (1-\epsilon)\rho_s \cdot \underline{T}_s \quad \text{-----(17)}$$

- $f(x,y,t)$ [Ms/ (L .S)]² volumetric adsorbate source
- D_m [L /S] apparent molecular diffusivity
- \underline{I} [1]² identity tensor
- $\underline{D}(x,y,t)$ [L /s] dispersion tensor
- $\underline{T}_w(x,y,t)$ [Ms/M.s] solute mas source in fluid due to production reaction.
- $C(x,y,t)$ [Ms/M] Solute concentration of fluid sources
- $C_s(x,y,t)$ [Ms/MG] specific concentration of adsorbate on solid grains
- $\rho_s = (MG/LG)$ ³ Density of soild grains in soild matrix
- $\underline{T}_s(x,y,t)$ [Ms/MG.s] Adsorbate mass source due to production reactions withion material itself.

where [LG]³ is the volume of solid grains.

Equation (16) is the solute mass balance in terms of the dissolved mass fraction (solute concentration), C. The time

derivative expresses the total changes in solute mass with time in a volume due to the mechanisms represented by terms on the right side of the equation. The term involving $f(x,y,t)$ represents the loss of solute mass from solution which becomes fixed on the solid grain surfaces as adsorbate. The adsorbate source, f , may, in general, depend on solute concentration, C , adsorbate concentration, C_s , and the rate of change of these concentrations, depending on either an equilibrium adsorption isotherm or on non-equilibrium adsorption processes. SUTRA algorithms are structured to directly accept non-equilibrium sorption models as an addition to the code. However, the current version of SUTRA assumes equilibrium sorption as shown in the following section, "Adsorption and production/decay processes."

The term involving fluid velocity, V represents average advection of solute mass into or out of the local volume. The term involving molecular diffusivity of solute, and dispersivity, D , expresses the contribution of solute diffusion and dispersion to the local changes in solute mass. The diffusion contribution is based on a true physical process often negligible at the field scale. The dispersion contribution is an approximation of the effect of solute advection and mixing in irregular flows which are not accounted for by solute advected by the average velocity. The solute mass source term involving the solute mass production rate per unit mass of fluid, expresses the contribution to dissolved species mass of chemical, biological or radioactive reactions in the fluid. The last term accounts for dissolved species mass added by a fluid source with concentration, C .

Equation (17) is the balance of mass which has been adsorbed by solid grain surfaces in terms of species concentration on the solid (specific adsorbate concentration), C_s . The change in total adsorbate mass is expressed by the time derivative term. It may increase due to species leaving solution as expressed by adsorbate mass (per unit solid matrix mass), T_s , by radioactive or chemical processes within the adsorbate. Note that mass becomes immobile once adsorbed, and is affected only by possible desorption or chemical and biological processes.

The total mass of a species in a volume is given by the sum of solute mass and adsorbate mass. A balance of the total mass of a species is obtained by addition of (17) and (16). The general form of the total species mass balance used in SUTRA is

$$\text{this: } \frac{\partial(\epsilon \cdot S_w \rho C)}{\partial t} + \frac{\partial[(1-\epsilon) \rho_s \cdot C_s]}{\partial t} = -\nabla \cdot (\epsilon S_w \cdot \rho \cdot \underline{v} \cdot C)$$

$$+ \nabla \cdot [\epsilon S_w \cdot \rho \cdot (D_m \cdot \underline{I} + D) \cdot \nabla C] + \epsilon S_w \cdot \rho \cdot f_w$$

$$+ (1-\epsilon) \rho_s \cdot T_s + Q_p \cdot C \text{ -----(18)}$$

Equation (18) is the basis for SUTRA solute transport simulation. In cases of solute transport where adsorption does not occur ($C_s = 0$) the adsorbate source term, f , simply has the value zero ($f=0$), and the terms that stem from equation (17) are ignored. Further discussion of solute and adsorbate mass balances may be found in Bear (1979).

2.3.3 Adsorption and production/decay processes

The volumetric adsorbate source, f , of (16) and (17) may be expressed in terms of a specific sorption rate, as:

$$f = (1-\epsilon) \rho_s \cdot f_s \text{ -----(19a)}$$

$f_s(x,y,t)$ [Ms/M .s] specific solute mass production rate
G
 (per unit mass solid matrix)

A particular non-equilibrium (kinetic) model of sorption is obtained by defining the functional dependence of the sorption rate, f_s , on other parameters of the system. For example, for a linear reversible non-equilibrium sorption model, the expression is: $f_s = m_1(C - m_2 \cdot C_s)$ where m_1 & m_2 are sorption parameters. This particular model and a number of other non-equilibrium sorption models are accommodated by a general expression for f_s as follows:

$$f_s = \kappa_1 \frac{\partial C}{\partial t} + \kappa_2 C + \kappa_3 \text{ ----- (19b)}$$

where: $\kappa_1 = \kappa_1(C, C_s)$, $\kappa_2 = \kappa_2(C, C_s)$, $\kappa_3 = \kappa_3(C, C_s)$

κ_1, κ_2 & κ_3 are First, Second & Third general sorption coefficient

Through a suitable definition of the general coefficients, a number of non-equilibrium sorption models may be obtained. For example, the linear reversible non-equilibrium model mentioned above requires the definitions: $\kappa_1 = 0$, $\kappa_2 = m_1$, and $\kappa_3 = -m_1 \cdot m_2 \cdot C_s$. The general coefficients κ_1 , κ_2 and κ_3 are included in the

SUTRA code to provide generality for possible inclusion of such non-equilibrium (kinetic) sorption models.

The equilibrium sorption models are based on definition of the general coefficients through the following relation:

$$\frac{\partial C_s}{\partial t} = K_i \cdot \frac{\partial C}{\partial t} \text{-----(20)}$$

Only general sorption coefficient, K_i , need be defined on various equilibrium sorption isotherms as shown in the following. The other coefficients are set to zero,

The linear equilibrium sorption model is based on the linear sorption isotherm assuming constant fluid density:

$$C_s = (X_1 \rho_f) C \text{-----(21a)}$$

$$\frac{\partial C_s}{\partial t} = (X_1 \rho_f) \frac{\partial C}{\partial t} \text{-----(21b)}$$

where:

X_1 [L /MG] Linear distribution coefficient and ρ_f is the fluid base density.

For linear sorption, general coefficient, K_i takes on the definition:

$$K_i = X_1 \cdot \rho_f \text{----- (21c)}$$

The Freundlich equilibrium sorption model is based on the following isotherm which assumes a constant fluid density,

where

$$X_1 \left[\frac{L^3}{MG} \right] \text{ Freundlich distribution coefficient (22a)}$$

$$X_2 [1] \text{ Freundlich Coefficient (22b)}$$

when $X_2 = 1$, the Freundlich isotherm is equivalent to the linear isotherm. For Freundlich sorption, then, the general coefficient, takes the definition:

$$K_1 = \left(\frac{x_1}{x_2}\right) \cdot \rho_0^{\left(\frac{1}{x_2}\right)} C^{\left(\frac{1-x_2}{x_2}\right)} \quad (22c)$$

The Langmuir equilibrium sorption model is based on the following isotherm which assumes a constant fluid density.

$$C_s = \frac{x_1(\rho_0 C)}{1 + x_2(\rho_0 C)} \quad (23a)$$

$$\frac{\partial C_s}{\partial t} = \frac{x_1 \rho_0}{(1 + x_2 \rho_0 C)^2} \frac{\partial C}{\partial t} \quad (23b)$$

Where:

For very low solute concentrations, C , Langmuir sorption becomes linear sorption with linear distribution coefficient X_1 . For very high solute concentrations, C , the concentration of adsorbate mass, C_s , approaches an upper limit equal to (x_1/x_2) . The general SUTRA coefficient, K_1 , is defined for Langmuir sorption as:

$$K_1 = \frac{x_1 \rho_0}{(1 + x_2 \rho_0 C)^2} \quad (23c)$$

The production terms for solute, T_w , and adsorbate, T_s , allow for first-order mass production (or decay) such as linear BOD (Biochemical Oxygen Demand) or radioactive decay, biological or chemical production, and zero-order mass production (or decay).

$$f_w = \gamma_1^\omega \cdot C + \gamma_0^\omega \quad (24a)$$

$$\int_S = \int_1^S C_S + \int_0^S$$

(24b)

2.4 Description of Dispersion

2.4.1 Pseudo-transport mechanism

Dispersion is a pseudo-transport process representing mixing of fluids which actually travel through the solid matrix at velocities different from the average velocity in two space dimensions, v , calculated from Darcy's law, (7). Dispersion is a pseudo-flux in that it only represents deviations from an average advective flux of energy or solute mass and as such does not represent a true mechanism of transport. Should it be possible to represent the true, complex, non-homogeneous velocity field in, for example, in the layers of an irregularly bedded field system, then the dispersion process need not be invoked to describe the transport, as the local variations in advection would provide the true picture of the transport taking place. However, as available data almost never allows for such a detailed velocity description, an approximate description, which helps to account for observed temperatures or concentrations different from that expected based on the average, fluid advection, must be employed.

Current research trends are to develop dispersion models for various hydrogeological conditions, and SUTRA may be updated to include these new results as they become available. Currently, SUTRA dispersion is based on a new generalization for anisotropic media of the standard description for dispersion in isotropic homogeneous porous media. The standard description is, in fact, the only model available today for practical simulation. Because any inconsistencies which may arise in applying this dispersion model to particular field situation often would not be apparent due to the poor quality or small amount of measured data, the user is warned to exercise good judgement in interpreting results when large amounts of so-called dispersion are required to explain the field measurements.

In any case, the user is advised to consult up-to-date literature on field-scale dispersion, before employing this

transport model.

2.4.2 Isotropic-media dispersion model

The dispersion tensor, D , appearing in both energy and solute balances, (15) and (18), is usually expressed for flow in systems with isotropic permeability and isotropic spatial distribution of inhomogeneities in aquifer materials as:

$$\underline{D} = \begin{bmatrix} D_{xx} & D_{yy} \\ D_{yx} & D_{yy} \end{bmatrix} \text{-----} (22)$$

where, \underline{D} is, in fact, symmetric and the diagonal elements are:

$$D_{xx} = (1/v) \left(d_L^2 v_x + d_T^2 v_y \right) \text{----} (23)$$

$$D_{yy} = (1/v) \left(d_T^2 v_x + d_L^2 v_y \right) \text{-----} (24)$$

and the off-diagonal elements are:

$$D_{ij} = (1/v)^{1/2} (d_L - d_T) (v_i v_j) \text{-----} (25)$$

$$i = j, i=x,y, j=x,y$$

$v(x,y,t)$ [L/S] magnitude of velocity v ,

$v_x(x,y,t)$ [L/S] magnitude of x-component of v

$v_y(x,y,t)$ [L/S] magnitude of y-component of v

$d_L(x,y,t)$ [L²/S] Longitudinal dispersion coefficient

$d_T(x,y,t)$ [L²/S] Transverse dispersion coefficient

The terms d_L and d_T [L²/S] are called longitudinal and transverse dispersion coefficients, respectively. These terms are analogous to typical diffusion coefficients. What is special, is that these are directional in nature. The term, d_L , acts as a diffusion coefficient which causes dispersion forward and backward along the local direction of fluid flow, and is called the longitudinal dispersion coefficient. The term, d_T , acts as a diffusion coefficient causing dispersion evenly in the

directions perpendicular to the local flow direction, and is called the transverse dispersion coefficient. Thus, if d_L and d_T were of equal value, a circular disk of tracer released (in the x-y plane) in ground water flowing, on the average uniformly and unidirectionally, would disperse in a perfectly symmetric circular manner as it moved downstream. However, if $d_L > d_T$, then the tracer would disperse in an elliptical manner with the long axis oriented in the flow direction, as it moved downstream.

The size of the dispersion coefficients are, in this model, for dispersion in isotropic permeability systems, dependent upon the absolute local magnitude of average velocity in a flowing system (Bear, 1979):

$$d_L = \alpha_L \cdot v \quad (26a)$$

$$d_T = \alpha_T \cdot v \quad (26b)$$

$\alpha_L(x,y)$ [L] Longitudinal dispersivity of solid matrix
 $\alpha_T(x,y)$ [L] Transverse dispersivity of solid matrix

when the isotropic-media dispersion model is applied to a particular field situation where aquifer inhomogeneities are much smaller than the field transport scale, then dispersivities α_L and α_T may be considered to be fundamental transport properties of the system just as, for example, permeability is a fundamental property for flow through porous media. In cases, where inhomogeneities are large or scales of transport vary, dispersivities may possibly not be representative of a fundamental system property. In this case, dispersion effects must be interpreted with care, because dispersivity values are the only means available to represent the dispersive characteristics of a given system to be simulated.

2.4.3 Anisotropic-media dispersion model

In a system with anisotropic permeability or anisotropic spatial distribution of inhomogeneities in aquifer materials, dispersivities may not have the same values for flows in all directions. In a case such as a layered aquifer, longitudinal dispersivity would clearly not have the same value for flows parallel to layers and perpendicular to layers. The isotropic-

media dispersion model, described in the previous section, does not account for such variability as α_L is isotropic (direction-independent). Transverse dispersivity would also tend to be dependent on the flow-direction, but because it typically is only a small fraction of longitudinal dispersivity, especially in anisotropic media (Gelhar and Axness, 1983), its variability is ignored here. This does not imply that transverse dispersion is an unimportant process, but the approximation is made because accurate simulation of low transverse dispersion is already limited, due to the requirement of a fine mesh for accurate representation of the process. The effect of any direction-dependence of transverse dispersivity would be obscured by the numerical discretization errors in a typical mesh.

An ad-hoc model of flow-direction-dependent longitudinal dispersion is postulated. In this model, longitudinal dispersivity is assumed to have two principal directions (in two space dimensions) aligned with principal directions of permeability. The principal values of longitudinal dispersivity, are α_{Lmax} and α_{Lmin} in these principal directions (see Figure 2). Note that the subscripts, L_{max} and L_{min} , refer only to the maximum and minimum permeability directions, and are not intended to imply the relation in magnitude of α_{Lmax} and α_{Lmin} the principal values of longitudinal dispersivity.

If F_s is the dispersive flux of solute (or energy) along a stream line of fluid flow, then

$$F_s = - \alpha_L \frac{\partial U}{\partial s} \text{-----(27)}$$

where :

$$\alpha_L (x, y, t)$$

and U represents either concentration or temperature, and s is distance measured along a streamline. The dispersive flux components in the principal permeability directions X_p and X_m are:

$$F_p = - \alpha_{Lmax} \frac{\partial U}{\partial x_p} = F_s \cdot \cos \theta_{kv} \text{ (28a)}$$

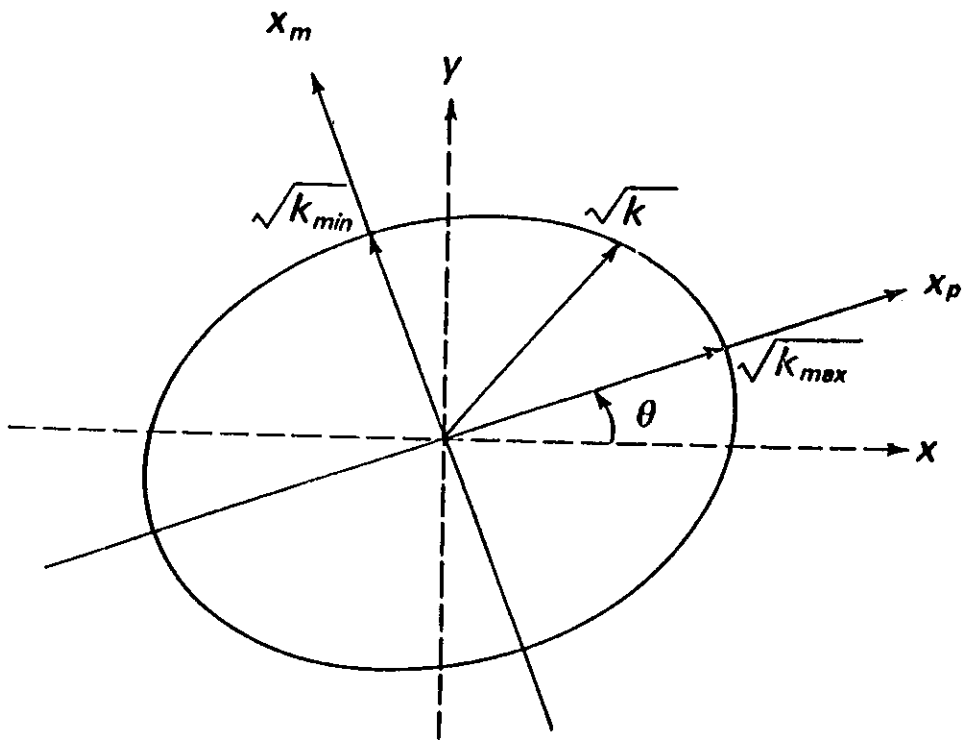


Figure 1
Definition of anisotropic permeability and effective permeability, k .

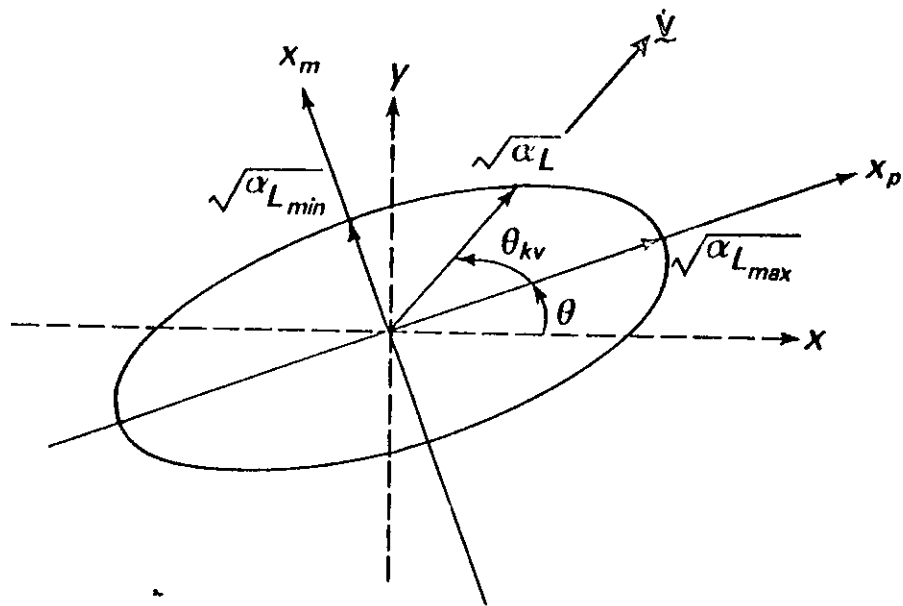
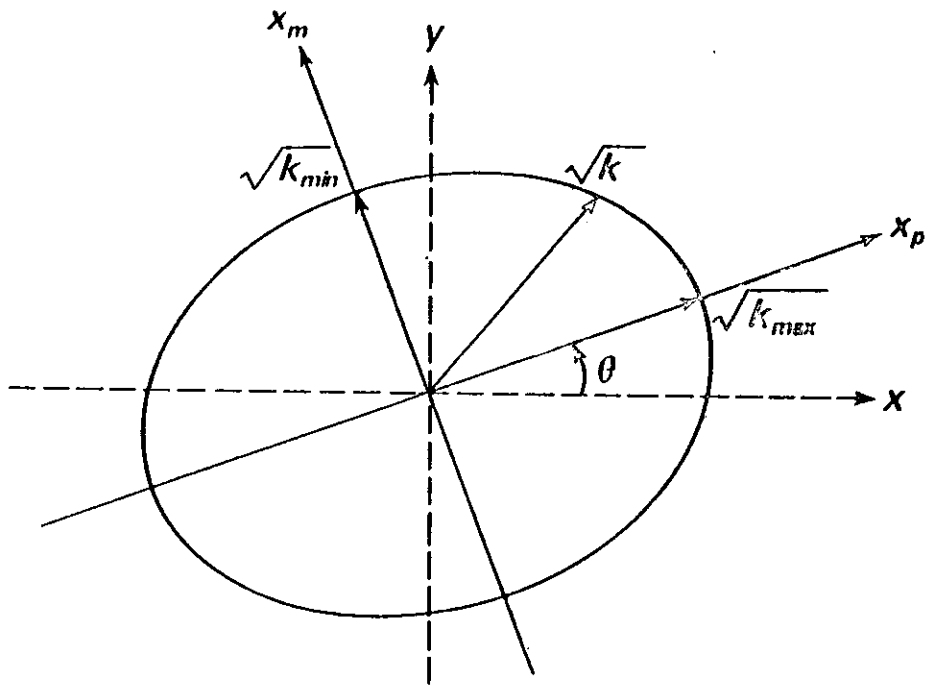


Figure 2
 Definition of flow-direction-dependent longitudinal dispersivity, $\alpha_L(\theta)$.

$$F_m = - \alpha_{Lmin} \frac{\partial U}{\partial x_m} = F_s \cdot \sin \theta_{kv} \text{ ----- (28b)}$$

where,

$\alpha_{Lmax} (x,y)$ [L] Longitudinal dispersivity in the max. permeability direction, x_p

$\alpha_{Lmin} (x,y)$ [L] Longitudinal dispersivity in the minimum permeability direction, x_m .

$\theta_{kv} (x,y,t)$ [$^\circ$] Angle from maximum permeability direction, x_p , to local flow direction ($v/|v|$)

(U varies with x and y, $U = U(x,y,t)$):

$$\frac{\partial U}{\partial s} = \frac{\partial U}{\partial x_p} \cdot \frac{\partial x_p}{\partial s} + \frac{\partial U}{\partial x_m} \cdot \frac{\partial x_m}{\partial s} \text{ ----- (29a)}$$

$$\frac{\partial U}{\partial s} = \frac{\partial U}{\partial x_p} \cdot \cos \theta_{kv} + \frac{\partial U}{\partial x_m} \cdot \sin \theta_{kv} \text{ ----- (29b)}$$

and:

$$F_s = -\alpha_L \left(\cos \theta \cdot \frac{\partial U}{\partial x_p} + \sin \theta \cdot kv \cdot \frac{\partial U}{\partial x_m} \right) \text{ ----- (30a)}$$

$$F = \alpha_L \left[\cos^2 \theta_{kv} \left(\frac{F_s}{\alpha_{Lmax}} \right) + \sin^2 \theta_{kv} \left(\frac{F_s}{\alpha_{Lmin}} \right) \right] \text{ ----- (30b)}$$

This defines an ellipse as:

$$\left(\frac{1}{\alpha_L} \right) = \left(\frac{\cos^2 \theta_{kv}}{\alpha_{Lmax}} \right) + \left(\frac{\sin^2 \theta_{kv}}{\alpha_{Lmin}} \right) \text{ ----- (31)}$$

with semi-major axis $(\alpha_{Lmax})^{1/2}$ and semi-minor axis $(\alpha_{Lmin})^{1/2}$

The length of a radius is $(\alpha_L)^{1/2}$ as shown in Figure 2. This ellipse is analogous in concept to that which gives effective permeability in any direction in an anisotropic medium.

The value of effective longitudinal dispersivity as dependent on the flow direction is:

$$\alpha_L = \frac{\alpha_{Lmax} \alpha_{Lmin}}{(\alpha_{Lmin} \cos^2 \theta_{kv} + \alpha_{Lmax} \sin^2 \theta_{kv})} \quad \text{-----(32)}$$

which is used by SUTRA to compute, α_L , for the anisotropic-media dispersion model. Note that if $\alpha_{Lmax} = \alpha_{Lmin}$ then the isotropic dispersion-media model is obtained. This form of longitudinal dispersivity dependence on direction of flow relative to the principal permeability directions is similar to that obtained for a transversely isotropic medium in a stochastic analysis of macro-dispersion by Gelhar and Axness (1983).

CHAPTER III

3.0 Program Algorithms

Sutra is structured in a modular , top-down programming style that allows for code readability , ease in tracing logic , and hopefully , ease in eventual modifications. Each subroutine carries out a primary function that is clearly distinguished from all other program functions. User required program changes are limited to :

- 1) dimensioning three storage arrays in the main routine , and
- 2) coding portions of a subroutine which is used to control time-dependent sources and boundary conditions (when they are used) and a subroutine which sets the unsaturated flow functions when unsaturated flow is simulated. The code consists of approximately 3000 statements and includes one main program and 23 subroutines. The program is commented to aid in tracing logic.

SUTRA is written in FORTRAN-77; however, few structures are used which are not compatible with FORTRAN-66. Modifications of the code required to compile in FORTRAN-66 would not be major.

The code runs accurately when it employs "double-precision" real variables (64 bit words with 47 bit mantissa) with a precision of about 15 significant figures, and 32 bit word integer variables. Should the code require modification to run on machines with other word lengths or other bit to byte ratios, the number of significant figures in a real variable should be preserved, if not increased.

Input and output is also somewhat modularized. Input is through Fortran unit numbers 5 and 55. Unit-55 contains only data on initial conditions for a simulation at the nodes for p and U. Unit-5 contains all other data required for a simulation. Unit-555 is used to impose time dependent boundary conditions. Output is to Fortran unit number 6 and 66. Unit-66 receives the result of the final time step in a format equivalent to that of Unit-55, for later use as the initial conditions file if the simulation is to be restarted. Unit-6 receives all other simulation output usually to be printed on a line printer.

A schematic diagram of the code is shown in Figure 3 .The purpose of each subroutine is given in the following sections.

Main Program

- 1) To dimension and allocate space for the main storage arrays.
- 2) To divide the storage arrays into their component arrays. (User up pointers.)
- 3) To start and stop the simulation.

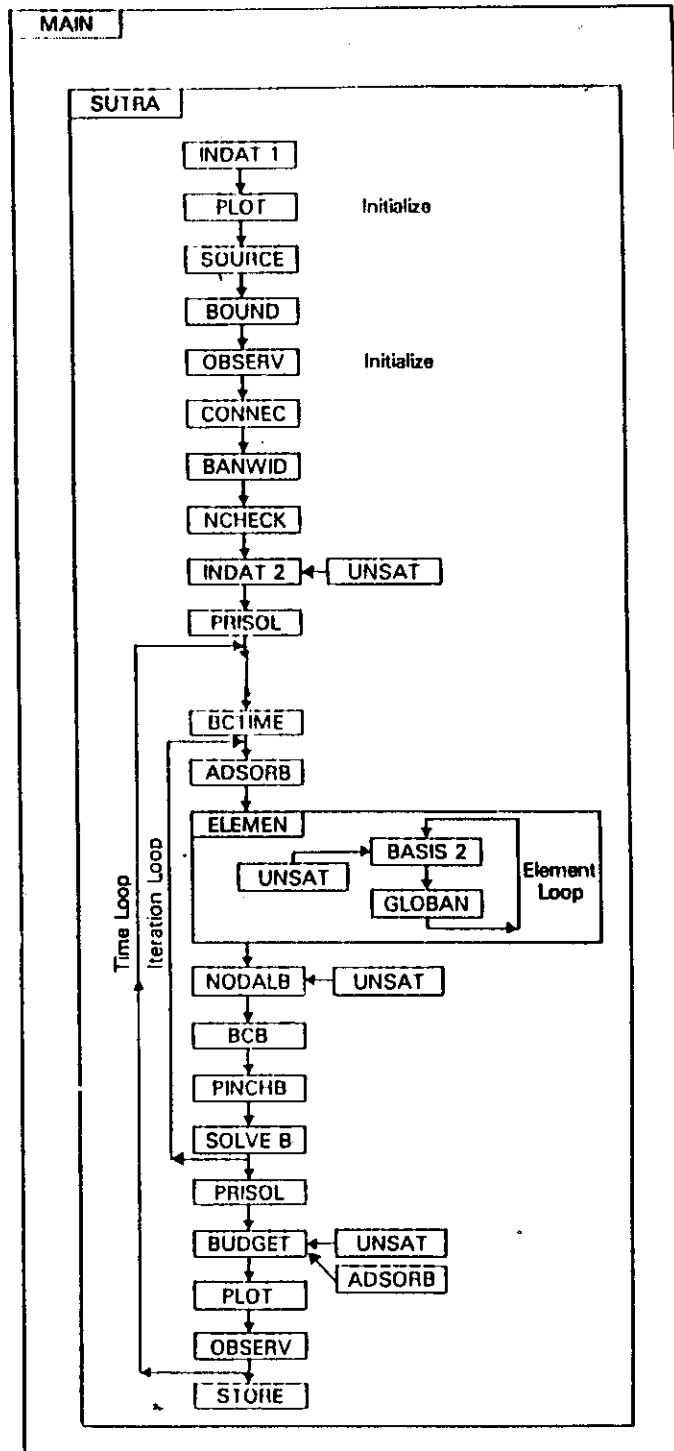


Figure 3-3
SUTRA logic flow.

Subroutine SUTRA

- 1) To act primary control on SUTRA simulation, cycling both iterations and time steps.
- 2) To sequence program operations by calling subroutines for input, output and most program calculations.
- 3) To carry out minor calculations.

Subroutine INDATI

- 1) To read simulation and mesh data from the Unit-5 data file, and print out this information.
- 2) To initialize some variables and carry out minor calculations.

Subroutine PLOT

To provide maps on printer output paper of the finite-element mesh, pressure values at nodes, and U values at nodes.

Subroutine SOURCE

- 1) To read source node numbers and source values for fluid mass sources and boundary fluxes and for diffusive and productive U sources, as well as fluxes of U at boundaries; to check the data, and to print information.
- 2) to set up pointer arrays which track the source nodes for the simulation.

Subroutine BOUND

- 1) To read specified pressure node numbers and pressure values, check the data, and print information.
- 2) To read specified concentration or temperature node numbers and the values, to check the data, and print information.
- 3) To set up pointer arrays which track the specified p and U nodes for the simulation.

Subroutine OBSERV

- 1) To save p and U values at chosen observation nodes as a function of the time.
- 2) To report the observations after the simulation has been completed.

Subroutine CONNEC

- 1) To read, output, and organize node incidence data.
- 2) To read, output, and organize pinch-node incidence data.

Subroutine BANWID

To calculate the band width of the mesh and check the value specified by the user.

Subroutine NCHECK

To check that pinch nodes are neither assigned sources, nor have specified p or U.

Subroutine INDAT2

- 1) To read initial conditions from Unit-55.
- 2) To initialize some arrays.

Subroutine PRISOL

To output the following to Unit-6:

- Initial conditions
- Pressure solutions
- Saturation values
- Concentration and temperature solutions
- Steady-state pressure solution
- Fluid velocities (magnitude and direction)

Subroutine BCTIME

A user-programmed routine in which time-dependent sources and boundary conditions are specified.

Subroutine ADSORB

To calculate and supply values from adsorption isotherms to the simulation.

Subroutine ELEMEN

- 1) To carry out all elementwise calculations required in the matrix equations.
- 2) To calculate element centroid velocities for output.

Subroutine BASIS2

To calculate values of basis functions, weighting functions, their derivatives, Jacobians, and coefficients at a point in a quadrilateral element.

Subroutine UNSAT

A user-programmed routine in which unsaturated flow functions are specified.

Subroutine GLOBAN

To assemble elementwise integrations into global matrix form.

Subroutine NODALB

To calculate and assemble all nodewise and cellwise terms in the matrix equation.

Subroutine BCB

- 1) To implement specified pressure node conditions in the matrix equations.
- 2) To implement specified temperature or concentration node conditions in the matrix equations.

Subroutine PINCHB

To implement pinch-node conditions in both matrix equations.

Subroutine SOLVEB

To solve a matrix equation with a non-symmetric banded matrix.

Subroutine BUDGET

- 1) To calculate and output a fluid mass budget on each time step with output.
- 2) To calculate and output a solute mass or energy budget on each time step with output.

Subroutine STORE

To store p and U results as well as other parameters on Unit-66 in a format ready for use as initial conditions in Unit-55. This acts as a backup for re-start in case a simulation is unexpectedly terminated before completion by computer malfunction.

3.1 Solution Sequencing

On any given time step, the matrix equations are created and solved in the following order: (1) the matrix equation for the fluid mass balance is set up, (2) the transport balance matrix equation is set up, (3) pressure is solved for, and (4) concentration or temperature are solved for. Both balance are set up on each pass such that the elementwise calculations only need be done once per pass. However, SUTRA allows the p or U equation to be set up and solved only every few time steps in a cyclic manner based on parameters NPCYC. These values represent the solution cycle in this steps. For example, setting up and solving for both P and U each time step (NPCYC=NUCYC=1):

3.2 Specification of boundary conditions

Before solving the matrix equation as described above, information about boundary conditions must be included. At a point of fixed head in an aquifer, a particular value of fluid inflow or outflow occurs at that point in order to keep the head constant when the aquifer is stressed. It is this flux of fluid which is added to the model aquifer in order to obtain fixed heads at nodes.

Consider the closed system of Figure 4 in which head at node i , h_i , is to have a specified value, h_{BC} , for all time. A well is removing water from the system at an internal node. A core of porous medium with conductance V is connected to node i . The head outside the core is held at the specified value, h_{BC} . The head at node i , h_i , is calculated by the model. A flow of Q_{BCi} [L³/s] enters through the core at node i in order to balance the rate of fluid removal at the well. The resulting head at node i depends on the conductance value V of the core. If V is very small, then a large head drop is required across the core in order to supply fluid at the rate the pumping well requires. This results in h_i having quite a different value from h_{BC} . If however, V is very large, then the value of head at node i , is very close to h_{BC} , as only a minute head drop across the core supplies the fluid required by the well. Therefore, by applying flux to a node through a highly conductive core, the out side of which is held at a specified head value, the node responds with a head value nearly equal to that specified.

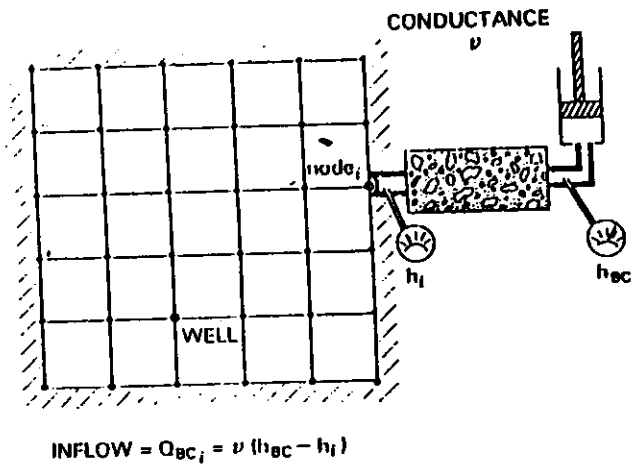


Figure 4
Schematic representation of specified head (or pressure) boundary condition.

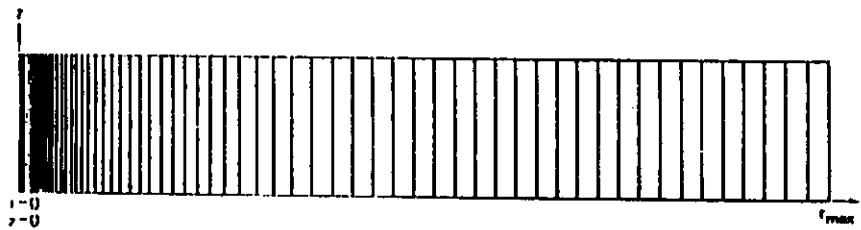


Figure 5
Radial finite-element mesh for constant-density solute and energy transport examples.

CHAPTER IV

4.0 Development and Application of the Model

4.1 Programme Compilation

Sutra source file has been developed through line to line typing of the programme listing available in the documentation manual of Sutra(Saturated Unsaturated Transport) model published as Voss,Clifford I.,1984,SUPRA:A Finite-Element Simulation Model for Saturated-Unsaturated Fluid-Density-Dependant Ground-water Flow with Energy Transport or Chemically-Reactive Single-Species Solute Transport,U.S.Geological Survey Water-Resources Investigations Report B4-4369.It has been compiled on PC-386 with Fortran compiler version 5.1 after making following alterations and additions.

1.Incorporated following Input/Output files:

- PKM.DAT to work as unit-5 input file.
- PKM1.DAT to work as unit-55 input file.
- PKM2.DAT to work as unit-555 input file.
- PKM.OUT to work as unit-6 to receive the output.
- PKM.USE to work as unit-66 to store the latest simulation results.

2.Removed the Subroutine-Zero ,and incorporated alternative statements to initialise different variables.

3.Codes for supplying time variant values of source/sink,and boundary conditions is generated in subroutine BCTIME for the specified problem taken up for simulation.

4.2 Test Run

4.2.1 Energy Transport

A complete Sutra input data set and Model output is provided for the example of section 6.3 , "Radial Flow With Energy Transport," of chapter 6, "Simulation Examples", in Appendix B and Appendix C of the documentation report.The same set of data has been generated for the test run of the recently compiled PC version of Sutra.

The mesh consists of one row of elements with element width expanding from $r = 2.5$ [m] by a factor, 1.06, to $r = 395$ [m], and then maintaining constant element width of $r = 24.2$ [m] to $r = 1000$ [m]. Element height, b , is 10. [m] Mesh thickness is set for radial coordinates, $Bi = 2$, with the number of nodes and elements given by $NN = 132$, $NE = 65$. see Figure 5.

The time step is constant at $t = 4021$ [s]. One pressure solution is carried out to obtain a steady-state. ($ISSFLO = 1$). and one concentration solution is done per time step. ($NUCYC = 1$). Different parameters adopted are as below. (For notations see Appendix I)

$$\begin{aligned}
 C_w &= 4182. \text{ [J/Kg. C]} & S_{op} &= 0. \\
 C_s &= 840. \text{ [J/Kg. C]} & k &= 1.02 \times 10^{-11} \text{ [m}^2\text{]} \\
 \lambda_w &= 0.6 \text{ [J/s.m. C]} & \epsilon &= 0.2 \\
 \rho &= 1000. \text{ [Kg/m}^3\text{]} & & \\
 \lambda_s &= 3.5. \text{ [J/s.m. C]} & & \\
 \rho_s &= 2650. \text{ [Kg/m}^3\text{]} & g &= 9.8 \text{ [m/s}^2\text{]} \\
 \delta\rho/\delta\tau &= 0.0 & \alpha_L &= 10. \text{ [m]} \\
 & & \alpha_r &= 0.0 \text{ [m]} \\
 \mu &= \mu(T) = (239.4 \times 10^{-7}) 10^{248.37/(T+133.15)} \text{ [kg/(m.s)]} \\
 Q_{TOT} &= 312.5 \text{ [Kg/s]} \text{ (one half at each well node)} \\
 T^* &= 1.0 \text{ C}
 \end{aligned}$$

Boundary Conditions:

No flow occurs across any boundary except where hydrostatic pressure is specified at r_{max} . At the top outside corner of the mesh, pressure is held at zero. a source is specified at $r = 0.0$ to represent the injection well. Further, the system is thermally insulated along the top and bottom of the mesh.

Initial Conditions:

Initially, hydrostatic pressure is set with $p = 0.0$ at the top of the aquifer. the initial temperature is $T_i = 0.0$ C.

4.2.2 Solute Transport

The same problem has been solved for solute transport also, with following parameters.

Storativity = 0.0

Permeability = 1.02×10^{-11} [m²]

Fluid mass density = 1000.0 [kg/m³]

Void ratio = 20%

Fluid viscosity = 1.0×10^{-3} [kg/m.s]

molecular diffusivity = $1. \times 10^{-10}$ [m²/s]

longitudinal dispersion = 10.0 [m]

transverse dispersion = 0.0 [m]

Rate of injection of fluid at zero radial distance = 62.5 [kg/s]

Specified concentration = 1.0

Initial concentration is set to zero.

The results are matched with the approximate analytical solutions of Hopes and Harleman (1967) and Gelhar and Collins (1971).

The solution of Gelhar and Collins (1971) is

$$\left(\frac{c - c_0}{c^* - c_0} \right) = \frac{1}{2} e_{r/c} \cdot \left\{ \frac{(r^2 - r^{*2})}{2 \left[\left(\frac{4}{3} \alpha_L \right) r^{*3} + \left(\frac{D_m}{A} \right) r^{*4} \right]^{1/2}} \right\}$$

where:

$$r^* = (2At)^{1/2}$$

$$A = \left(\frac{Q_{TOT}}{2\pi e b f} \right)$$

The Hopes and Harleman (1967) solution is obtained by replacing r^* in the denominator of above equation with r .

Results:

Output results of the test run for energy transport has been compared with the model output available in the documentation report for the same problem. However number of time steps is curtailed to 90 instead 225 due to the storage limitation of PC-

386. Steady state pressures at all nodes before first time step and the budgeted values of pressures and temperatures at node no. 34, 52, 64 and 72 after time step 1, 45 and 90 are quite comparable and all these results are shown in Table 1 and can be compared with the results of section 6.3 of the documentation report. Whatever minor differences are there it is due to the need of using double precision statements very frequently. This arises differences in the calculated values of different variables on different machines due to rounding-off errors.

Results of solute transport problem after 15, 30, 45 time steps are compared with the approximate analytical solutions of Gelhar and Collins (1971) and Hopes and Harleman (1967) in Fig 6, 7, and 8 respectively. All solutions compare well with each other. Due to finer spatial and temporal discretization the Sutra solution may be considered as more accurate as compared to both the approximate analytical solutions.

4.3 Numerical Simulation

4.3.1 Study Area

Upper Palar zone in Palar river basin (fig. 9 a & b) lies between longitude 79 22' 30" and latitude 15 13 05 . It is located in North Arcot district in Tamilnadu. Area of the zone is 1255 sq miles. Morphometric parameters indicate that the basin yield is low but it has an extended peak flow and good drainage.

Two types of soil covers are encountered in the zone . First is red loamy soil with thickness more than 90 cm in the flood plains of rivers and along the stream course. Both the type of soil is having good permeability.

Geologically, in the upper Palar zone , three types of rock formations are observed (i) Peninsular gneiss, which are granitic rocks such as massive or porphyritic biotite granite, biotite granite gneiss and foliated varieties. These type of rocks may be seen mainly around Vaniyambadi, Ambur, Gudiyattam, Arani and Arcot. The general trend of this group of rocks are NNE-SSW and dip at fairly steep angles to ESE , (ii) Charnockites , these are holocrystalline , hypersthene granites. The general trend of the rock type is NE-SW and dips south eastern direction with amounts of 40 to 50, (iii) Leptynites , generally these are associated with charnockites. In the study area these formations are found

STEADY - STATE PRESSURE

NODE	NODE	NODE	NODE	NODE	NODE	NODE					
1	6.56282930D+06	2	6.46478375D+06	3	4.85060247D+06	4	4.75254390D+06	5	4.25720373D+06	6	4.15910333D+06
7	3.89002232D+06	8	3.79180813D+06	9	3.62002744D+06	10	3.52149801D+06	11	3.40422699D+06	12	3.30475849D+06
13	3.40261009D+06	14	3.30458356D+06	15	3.40091398D+06	16	3.30438953D+06	17	3.26035974D+06	18	3.16268601D+06
19	3.13251466D+06	20	3.03457995D+06	21	3.01490065D+06	22	2.91691231D+06	23	2.90558992D+06	24	2.80759175D+06
25	2.80311221D+06	26	2.70511246D+06	27	2.70633554D+06	28	2.60833557D+06	29	2.61438325D+06	30	2.51638325D+06
31	2.52655936D+06	32	2.42855936D+06	33	2.44229912D+06	34	2.34429912D+06	35	2.36114617D+06	36	2.26314617D+06
37	2.28271747D+06	38	2.18471747D+06	39	2.20669428D+06	40	2.10869428D+06	41	2.13280867D+06	42	2.03480867D+06
43	2.06083052D+06	44	1.96283052D+06	45	1.99056233D+06	46	1.89256233D+06	47	1.92183268D+06	48	1.82383268D+06
49	1.85449399D+06	50	1.75649399D+06	51	1.78841525D+06	52	1.69041525D+06	53	1.72348148D+06	54	1.62548148D+06
55	1.65959211D+06	56	1.56159211D+06	57	1.59665675D+06	58	1.49865675D+06	59	1.53459458D+06	60	1.43659458D+06
61	1.47333382D+06	62	1.37533382D+06	63	1.41281021D+06	64	1.31481021D+06	65	1.35296477D+06	66	1.25496477D+06
67	1.29374505D+06	68	1.19574505D+06	69	1.23510388D+06	70	1.13710388D+06	71	1.17699708D+06	72	1.07899708D+06
73	1.11938572D+06	74	1.02138572D+06	75	1.06223325D+06	76	9.64233254D+05	77	1.00550681D+06	78	9.07506807D+05
79	9.49176569D+05	80	8.51176569D+05	81	8.93214484D+05	82	7.95214484D+05	83	8.42312704D+05	84	7.44312704D+05
85	7.94267520D+05	86	6.96267520D+05	87	7.48775345D+05	88	6.50775345D+05	89	7.05578542D+05	90	6.07578542D+05
91	6.64456603D+05	92	5.66456603D+05	93	6.25219347D+05	94	5.27219347D+05	95	5.87701587D+05	96	4.89701587D+05
97	5.51758945D+05	98	4.53758945D+05	99	5.17264492D+05	100	4.19264492D+05	101	4.84106048D+05	102	3.86106048D+05
103	4.52183721D+05	104	3.54183721D+05	105	4.21409149D+05	106	3.23409149D+05	107	3.91702429D+05	108	2.93702429D+05
109	3.62991942D+05	110	2.64991942D+05	111	3.35213039D+05	112	2.37213039D+05	113	3.08307164D+05	114	2.10307164D+05
115	2.82221114D+05	116	1.84221114D+05	117	2.56906406D+05	118	1.58906406D+05	119	2.32318736D+05	120	1.34318736D+05
121	2.08417507D+05	122	1.10417506D+05	123	1.85165430D+05	124	8.71654324D+04	125	1.62528092D+05	126	6.45280834D+04
127	1.40473969D+05	128	4.24740059D+04	129	1.18973735D+05	130	2.09735790D+04	131	9.79998009D+04	132	4.68379798D-01

OBSERVATION MODE DATA

TIME STEP	TIME(SEC)	NODE 34		NODE 52		NODE 64		NODE 72	
		PRESSURE	TEMPERATURE	PRESSURE	TEMPERATURE	PRESSURE	TEMPERATURE	PRESSURE	TEMPERATURE
1	4.02100D+03	2.34430D+06	2.37787D-12	1.69042D+06	2.39597D-23	1.31481D+06	6.33246D-34	1.07900D+06	2.24979D-42
45	1.80945D+05	2.34430D+06	4.84787D-04	1.69042D+06	1.79440D-09	1.31481D+06	7.72387D-17	1.07900D+06	2.00668D-23
90	3.61890D+05	2.34430D+06	9.10646D-03	1.69042D+06	3.27523D-06	1.31481D+06	5.97689D-12	1.07900D+06	1.62741D-17

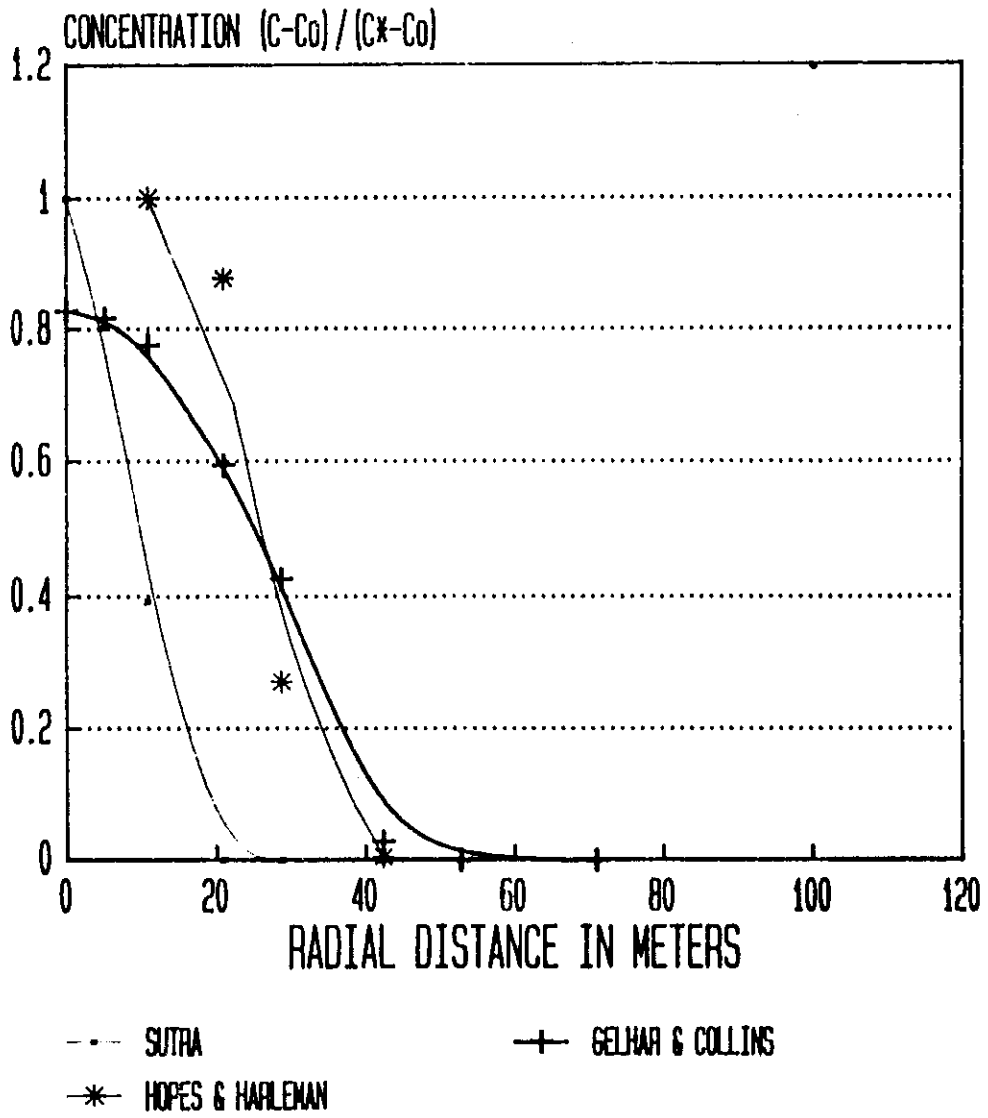


Fig.6 Comparison of sutra solution with analytical Solution in time step 15

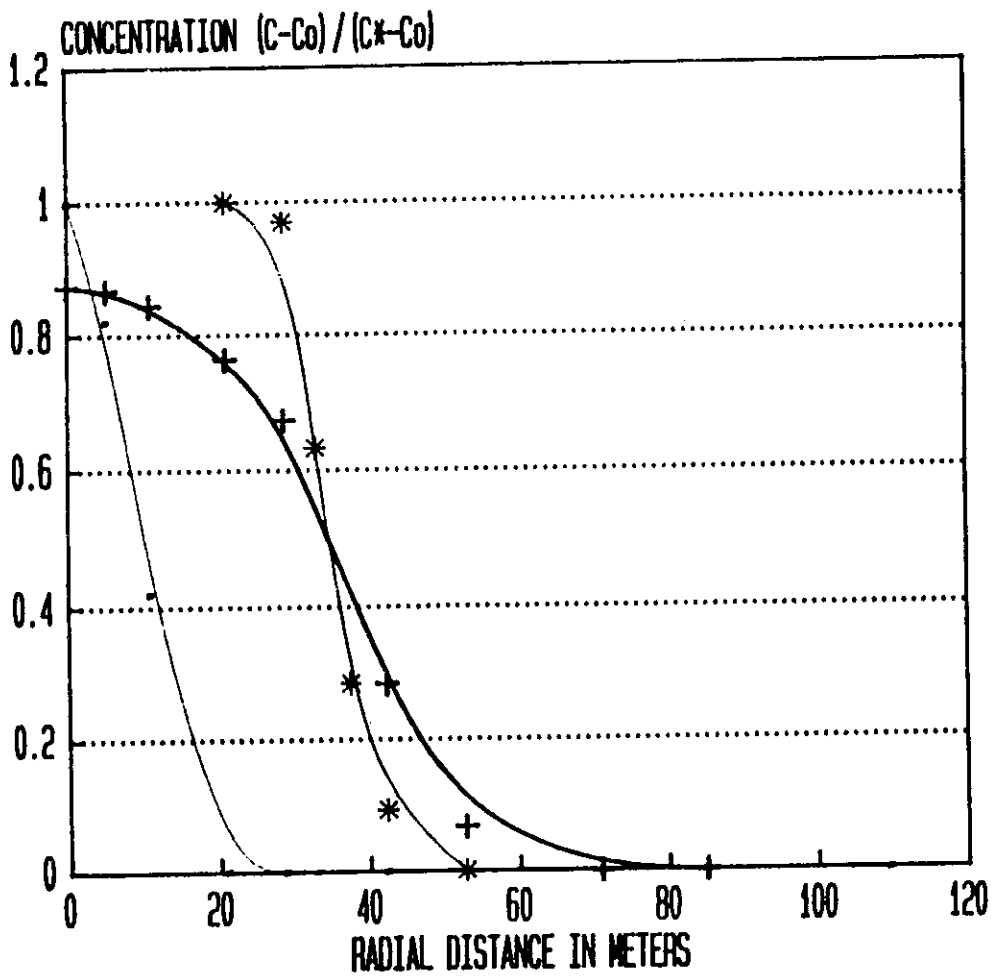


Fig.7 Comparison of sutra solution with analytical solution in time step 30

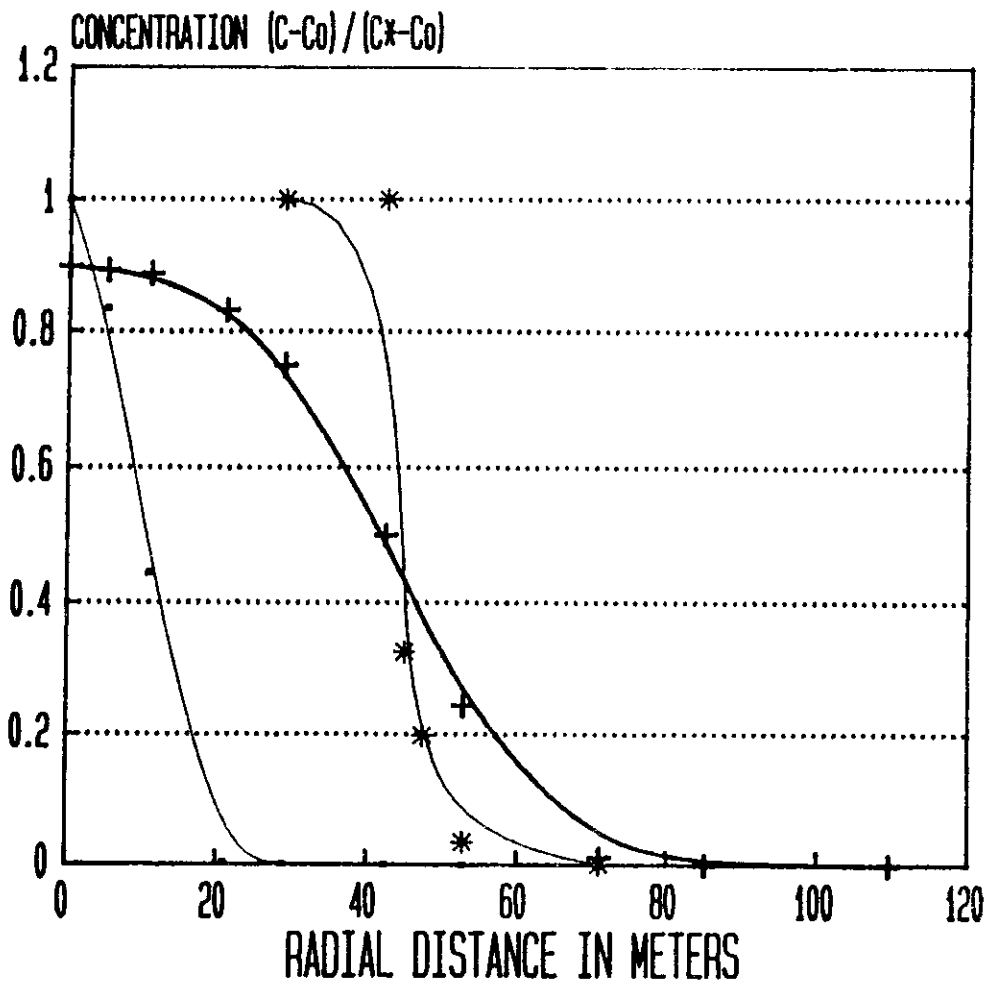
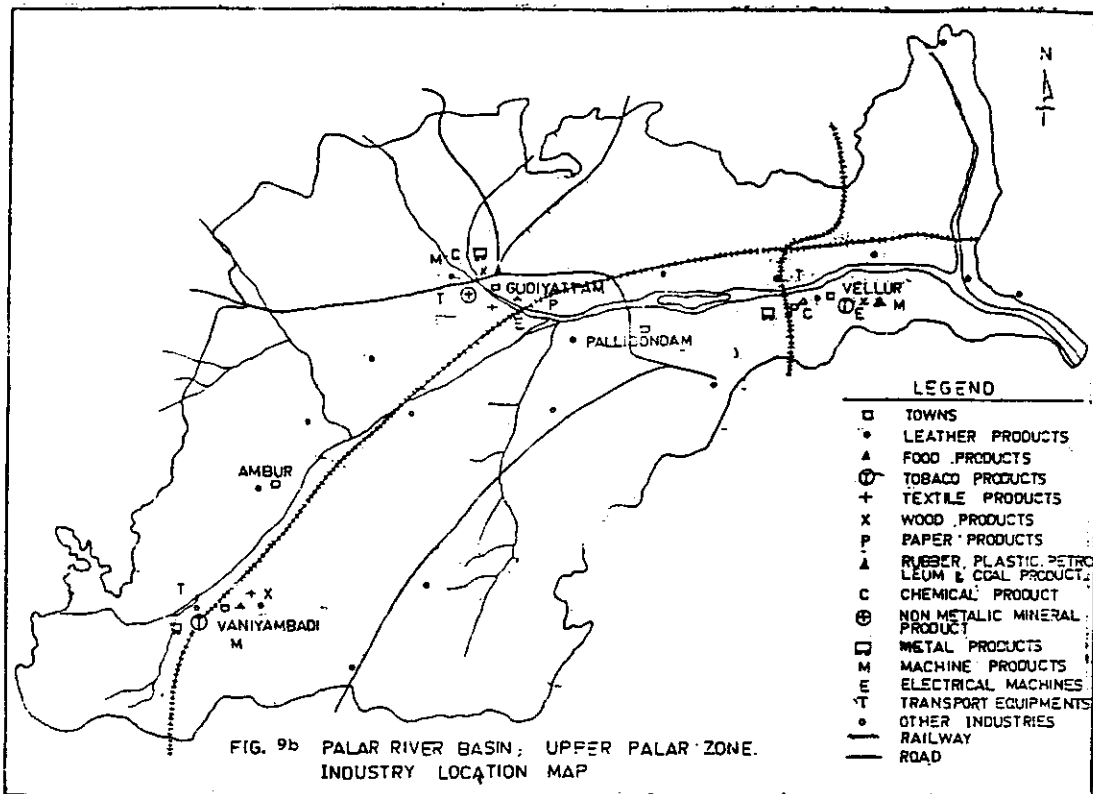
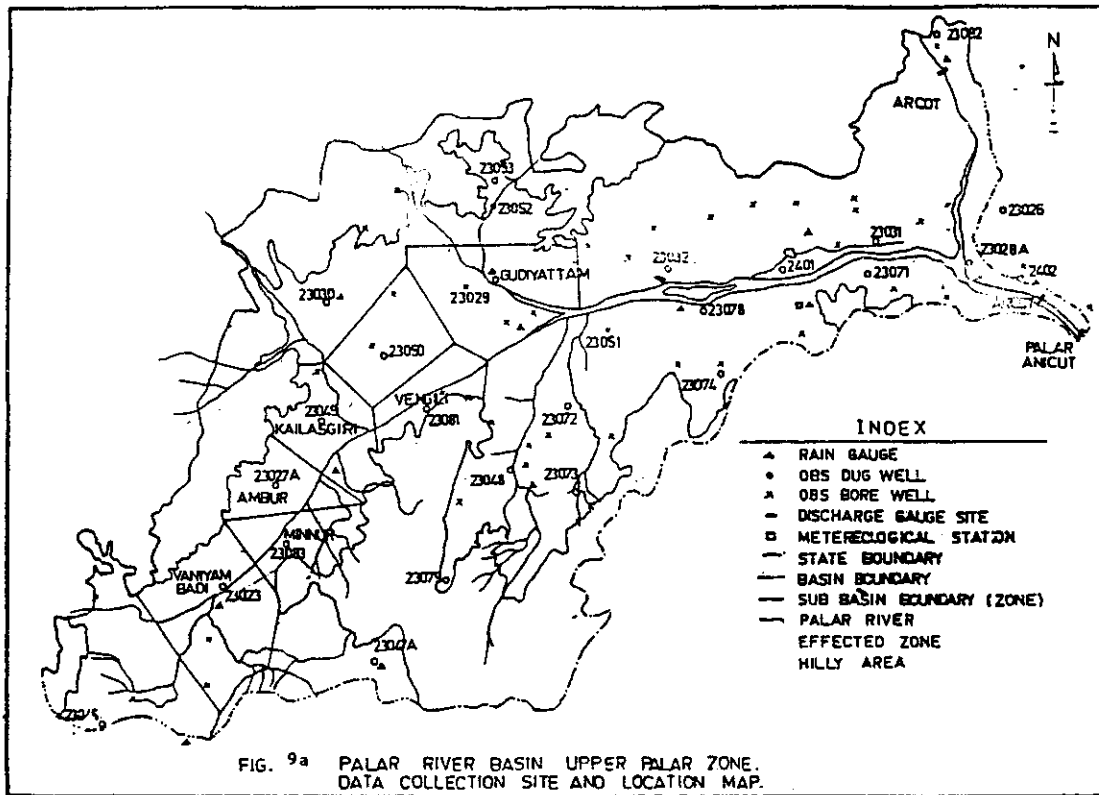


Fig. 8 Comparison of sutra solution with analytical solution in time step 45



in isolated patches surrounded by charnockite on the eastern side of the Vellore town in the hills.

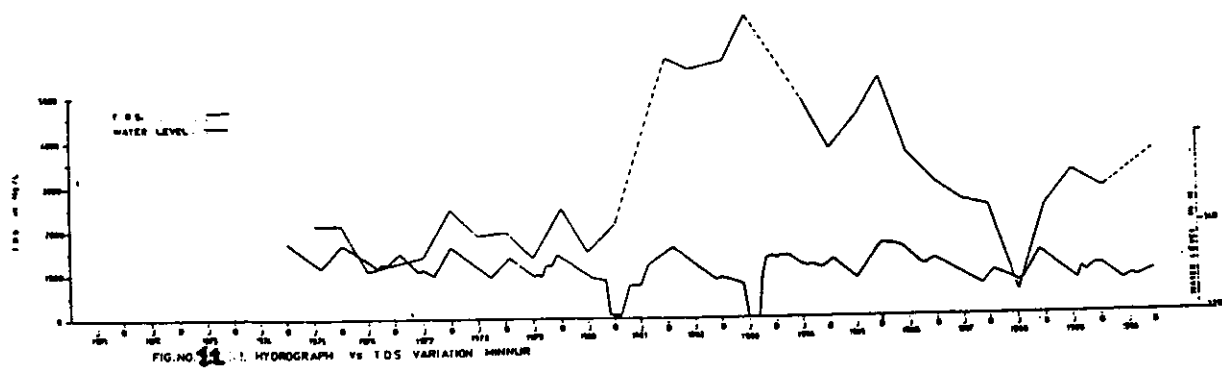
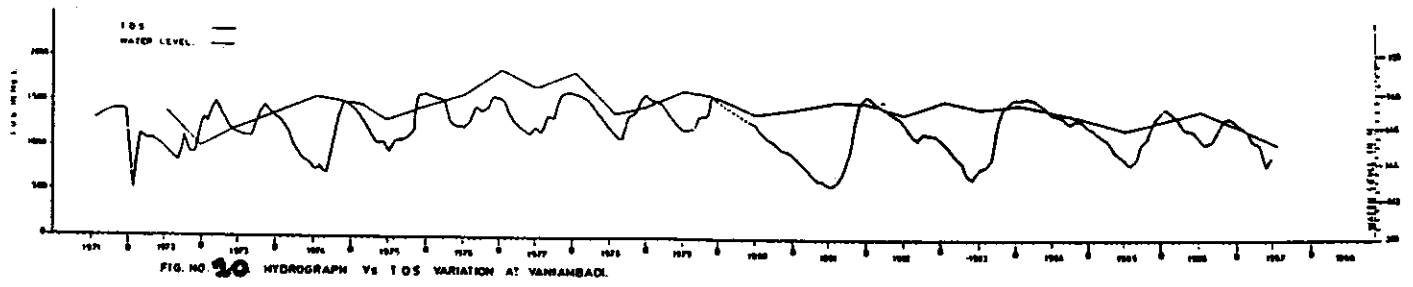
Land use pattern reveal that 62.7% of the total area is covered by cultural command area and the rest is covered by forests . The agricultural land is generally double cropped (khariff + Rabi). Mostly the forest land is deciduous , but small patches of evergreen/ semi-evergreen , degraded /scrubs are also existing in the zone. Paddy, pulses, groundnut , ragi, gingelly, vegetables and sugarcane are the predominant crops.

Rainfall is the major source of recharge to ground water storage. rainfall occurs due to SW and NE monsoon from June to December. River flows only for about 15 days in a year during normal monsoon season. Minimum water level fluctuation recorded in the well situated at Vaniyambadi located in weathered granitic gneiss formation, in year 1977 is recorded as 5.54 m and the maximum fluctuation is 11.89 m in the well situated at Vellore in weathered charnockite formation in year 1977. Monthly water level fluctuations are shown in Fig.10 for vaniyambadi and in fig.11 for Minnur.

The seasonal fluctuation of water level in alluvial aquifer ranges from 0.6 to 4.5 m below ground level. In Palar river alluvium the ground water level decline from January to October and then NE monsoon push the recharge rate eventually reaches its original position. In upper Palar zone , bed rocks are available at depth ranging from 20m to 40m . It covers 14 sub basins and according to December 1991, census 80136 numbers of wells are existing in the region out of which 62% are electrically driven , 5% on diesel and 33% by bullocks.

Number of industries are located in Vaniyambadi- Walajapet area, of which the tanneries constitute 90% and rest are chemicals, sugar , soaps, leather goods and paper industries . No treatment plant was in existence till December 1992 and tannery effluents were found disposed directly into the river. Dry waste disposals were also seen in the banks of the Palar river. In upper Palar zone of Palar river basin, in Tamil nadu, surface water as well as ground water are experiencing drastic change in terms of quality so as to render it unuseful for domestic and irrigation purposes.

Hydrological feature of Palar river basin is an unique one, as the river flows only for 15 days in a year during heavy and



long durational storm. Moreover it lies in the upper reach of the basin in Tamil Nadu thereby no other source of domestic and irrigation water supply, other than sub surface water is available. Not long back in North Arcot district, of which the study area is an integral part, had a reputation of being one of the best for its agricultural production capability, but subsequently during last 5-10 years, the ground water quality deteriorated to such an extent that the socioeconomic condition of the locality got badly effected to a larger extent. Results of the analysis are discussed below.

Rainfall pattern of the study area is more or less of well distributed nature. 75% dependable rainfall on the basis of last 20 years data comes out to be 800 mm which is quite normal. It has been noticed that hardly any periods of dry years lasted more than one year. Always there is a year of less rainfall followed by a good rainfall year. Ground water level fluctuation in the key locations suggest that ground water level attains the original status just after the monsoon season. No noticeable over extraction is seen in the study area. Ground water level contour reveal that the direction of ground water movement is from NW to SE and the trend is more or less same as the ground level contours. Hydraulic gradient of ground water as suggested by IWS, Madras is 2.39 m/km.

4.3.2 Objectives of the simulation

(1) To demonstrate the applicability of SUTRA to an areal constant density solute transport problem.

(2) To simulate the flow and contaminant transport in the alluvium of palar river basin in steady state as well as transient condition.

(3) To simulate various pollution creating activities on the model.

4.3.3 Simulation Set-up

Palar River basin is mostly comprised of hard rocks having discontinuities like dykes, faults, fissures and fractured zones with bed rock available at a depth ranging from 20 to 40 mts. An

alluvium runs all along the river with an average width of 120 mts approximately. The river stretch between Vaniyambadi and Minnur is chosen for the simulation study as shown in fig.12.

The area has been discretised in 144 equal rectangular elements of 100 x 60 mts. dimensions, each along the river and across the river respectively. Discretisation is done with a view to satisfy the criteria of mesh Peclet number, given by:

$$Pe_m = \frac{\epsilon S_w / |V| \Delta L_L}{[\epsilon S_w (\sigma_w + \alpha_L |V|) + (1 - \epsilon) \sigma_s]}$$

Where ϵ = Volumetric Porosity of solid matrix at each node
 S_w = Degree of saturation
 V = Darcy Velocity
 ΔL_L = Distance between element side along stream line
 σ_w = Molecular diffusivity
 α_L = Longitudinal dispersivity
 σ_s = Thermal conductivity (Zero for solute transport)

Stability is guaranteed in all cases when $Pe_m \leq 2$, and is usually obtained with $Pe_m \leq 4$. When concentrations or temperatures exhibit small changes along streamlines, then above criterion may safely be violated, even by a few orders of magnitude, without inducing spatial instability.

When longitudinal dispersion causing the transport is mainly due to longitudinal mixing, the mesh Peclet number becomes:

$$Pe_m \approx \frac{\Delta L_L}{\alpha_L}$$

A discretization rule of thumb for simulation with SUTRA which guarantees spatial stability in most cases is:

$$\Delta L_L \leq 4 \alpha_L$$

Criteria for transverse discretization is given by:

$$\Delta L_T \leq \alpha_T + \frac{1}{|V|} [\epsilon S_w \sigma_w + (1 - \epsilon) \sigma_s]$$

Where L_T is the local element dimension transverse to the flow direction. In the case where the transverse mixing rather than

diffusion dominates the transverse dispersion an adequate but stringent rule-of-thumb may be $\Delta L_T \leq 10 \alpha_T$.

With the above criteria a size of 400x400 meters would have been the upper limit for stability, but having only 120mts of width and to keep atleast one row of non-boundary nodes in the alluvium rectangular elements of size 100 x 60 mt. have been preferred (fig 12). Depth varies all along the river bed starting from 13 mts to finally 20 mts. In all 219 nodal points are available out of which 148 nodes are boundary nodes where time dependent pressures and concentration have been specified. Only two observation wells are available within the mesh area. Vaniyambadi well is adjacent to node no.1 and well at Minnur is near by node no.217. Simulation is basically based upon the observation data available for these two wells. Total area for the mesh is 0.6912 sq.km. only.

Source of flow and contamination transport is through rainfall recharge only as there is no cultivation in the river bed. Recharge is considered as 20% of the rainfall occurred during the time step. No abstraction has been presumed as hardly there is any type of well available on the river bed. Apart from this, disposals from the small scale industries situated mostly on the left bank also add to it both in term of quantity and quality. Time dependent Source values through rainfall recharge have been calculated nodewise by distributing the estimated elemental recharge to four nodes as shown in fig 13 for each time step. A computer code for this purpose has been appended in subroutine BCTIME.

Monthly water level observations are available for both the observation wells. Therefore monthly time step has been chosen to simulate the flow, as well as contamination throughout the simulation. However concentration values are only available on pre and post monsoon basis. The same has been interpolated for monthly values considering the premonsoon values for the month of June and post monsoon values for the month of December, as and wherever required. In the case of steady state flow and transient transport, pressure is calculated once before first time step, and only concentration on each time step, where as in the case of transient flow and transport both pressure and concentration is calculated for each time step.

No. of elements = 144

No. of nodes = 219

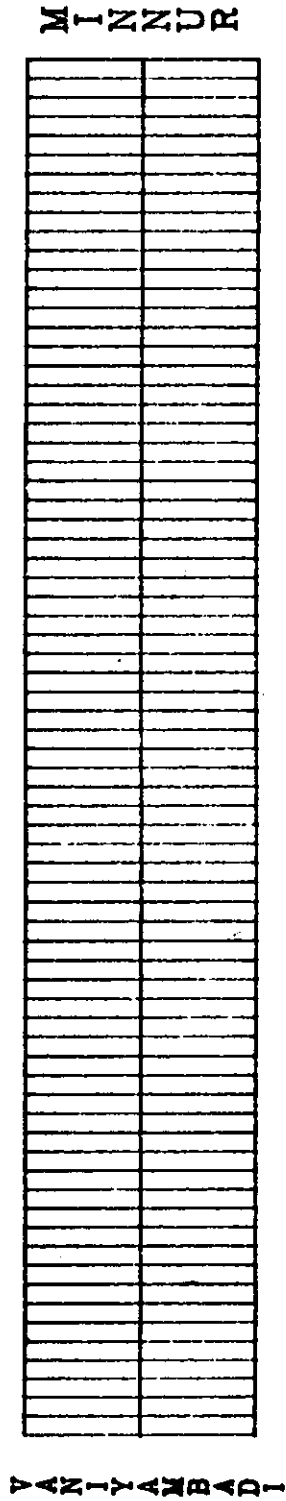


Fig.12 Discretized mesh of the study area in Palar river basin
(NOT TO THE SCALE)

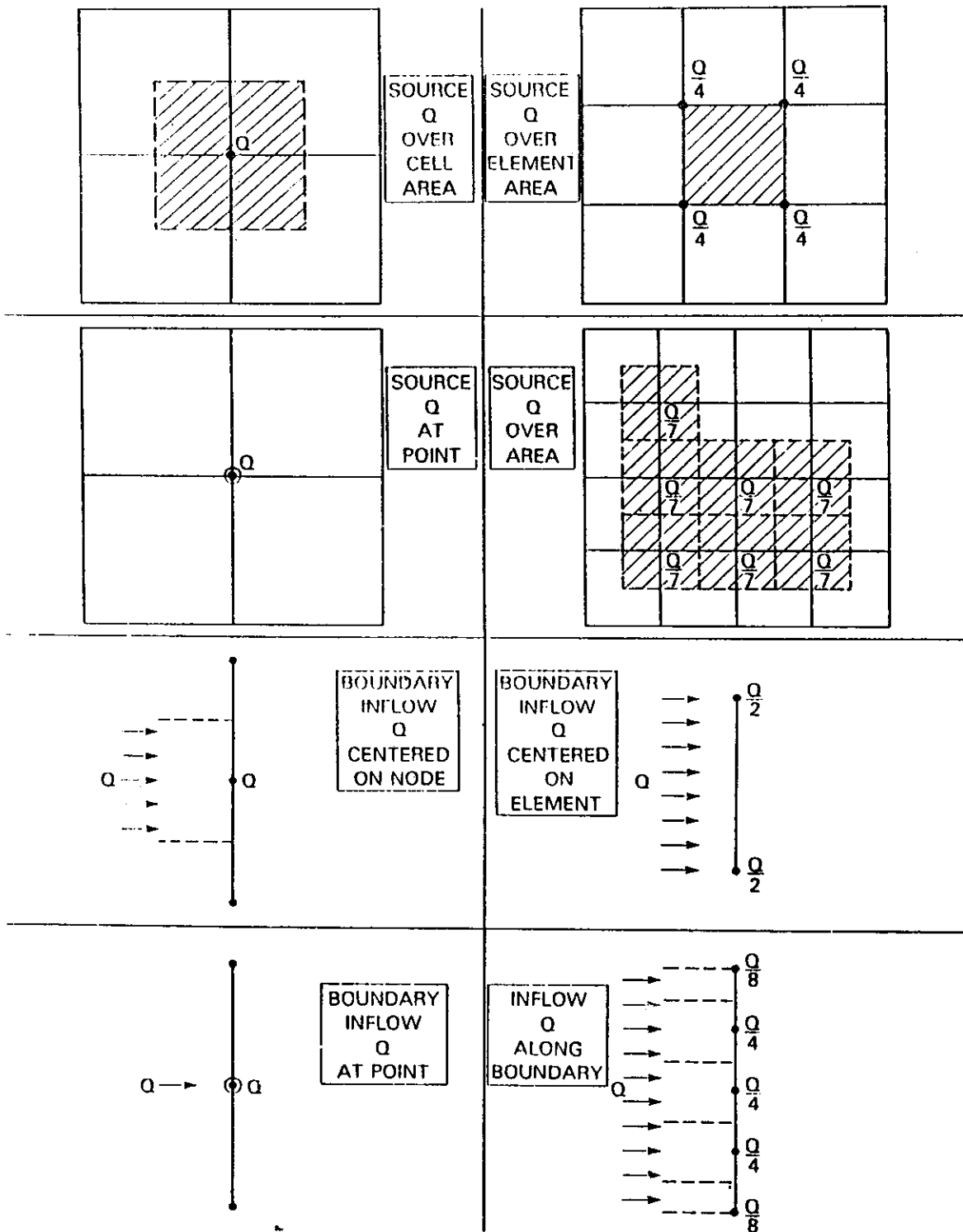


Figure 13
Allocation of sources and boundary fluxes
in equal-sized elements.

4.3.4 Parameters

On the basis of collected information following parameters are considered to start the simulation and subsequently some of the parameters are modified accordingly to have an approximate real aquifer system response to a certain degree of certainty.

(a) Flow Properties:

Porosity = 0.4

Fluid compressibility = 4.47×10^{-10}

Solid matrix compressibility = 4.8286×10^{-5}

Estimated Storativity = 2.8972×10^{-5}

Molecular diffusivity = 1.0×10^{-10}

Density of fluid at base concentration = 1000.0

Base value of solute concentration = none

Coefficient of density change with concentration = none

Viscosity = 1.0×10^{-3}

Density of solid grains = 2.65

Isotropic permeability = 6.8796×10^{-7} sq.mts.

(b) Transport Properties:

Isotropic longitudinal dispersivity = 100 mt

Transverse dispersivity = 10 mt

Adsorption parameters = None

Production of Solute mass = None

4.3.5 Boundary Conditions

Flow has been allowed to occur from all boundaries where time dependent pressures and concentration in mass fraction are specified. Constant head and contamination is assumed on the two sides of the mesh directed across the river and varying values all along the river course. Pressure and concentration values are estimated per time step on the basis of the available water levels of the two wells at node no.1 and 217. A computer code is established for this matter of fact in subroutine BCTIME, which interpolates at all other boundary nodes by using input data file

PKM2.DAT (Unit=555).

4.3.6 Initial conditions

Initial pressures and concentrations are specified for all nodes in pressure unit for pressure values and in mass fraction units for concentration values. Again these values are estimated by simple interpolation technique on the basis of the values observed at node no. 1 and 217, considering that there is no change in the values in the direction across the river. These data are conveyed to the computer code through input data file PKM1.DAT (Unit=55)

4.3.7 Problem Dimensions

Dimensions of all vectors and arrays are accommodated in three large arrays, RM, RV, and IMV. These arrays are dimensioned in the main routine. RM contains all of the real matrices in the code, RV contains all of the real vectors, and IMV contains all of the integer matrices and vectors. The dimensions required for these arrays, RMDIM, RVDIM, and IMVDIM must be specified in the main program to value greater or equal to those required. The required values are estimated as below.

$$\text{RMDIM} = 2(\text{NN})(\text{NBI})$$

$$\text{RVDIM} = (\text{NNV})(\text{NN}) + (\text{NEV} + 8)(\text{NE}) + (\text{NBCN})3 \\ + (\text{NOBS} + 1)(\text{NTOBS} + 2)2 + \text{NTOBS} + 5$$

$$\text{IMVDIM} = (\text{NE})8 + \text{NN} + (\text{NPINCH})3 + \text{NSOP} + \text{NSOU} \\ + (\text{NBCN})2 + \text{NOBS} + \text{NTOBS} + 12$$

Where

NN = number of nodes
NE = number of elements
NBI = full band width of matrix
NSOP = number of fluid source nodes.
NSOU = number of solute or energy source nodes
NPBC = number of specified pressure nodes
NUBC = number of specified solute or energy nodes
NBCN = NPBC + NUBC
NPINCH = number of pinch nodes
NOBS = number of observation nodes
NTOBS = number of observation time steps(max)
NNV = number of vectors NN long = approx. 30 (fixed)
NEV = number of vectors NE long = approx. 10 (fixed)

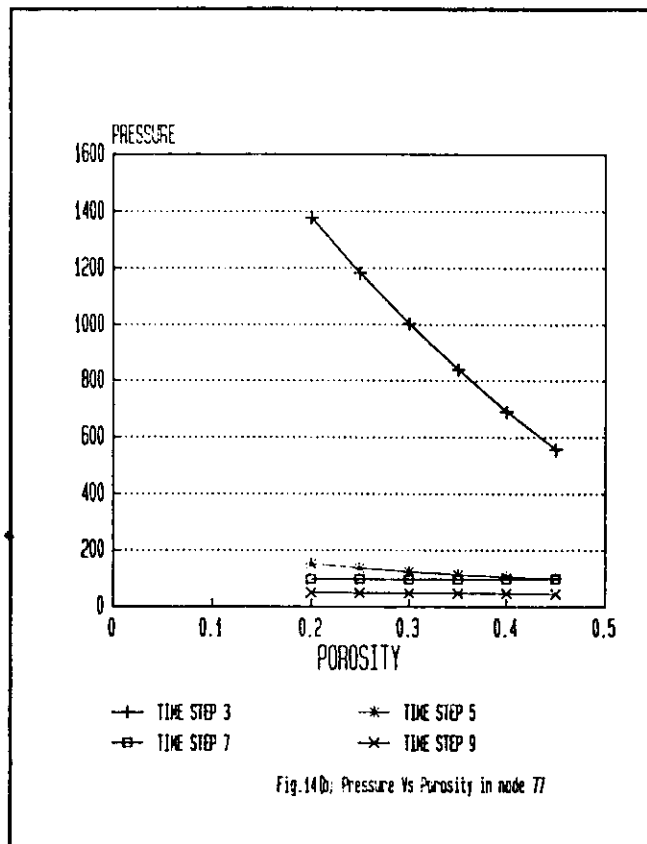
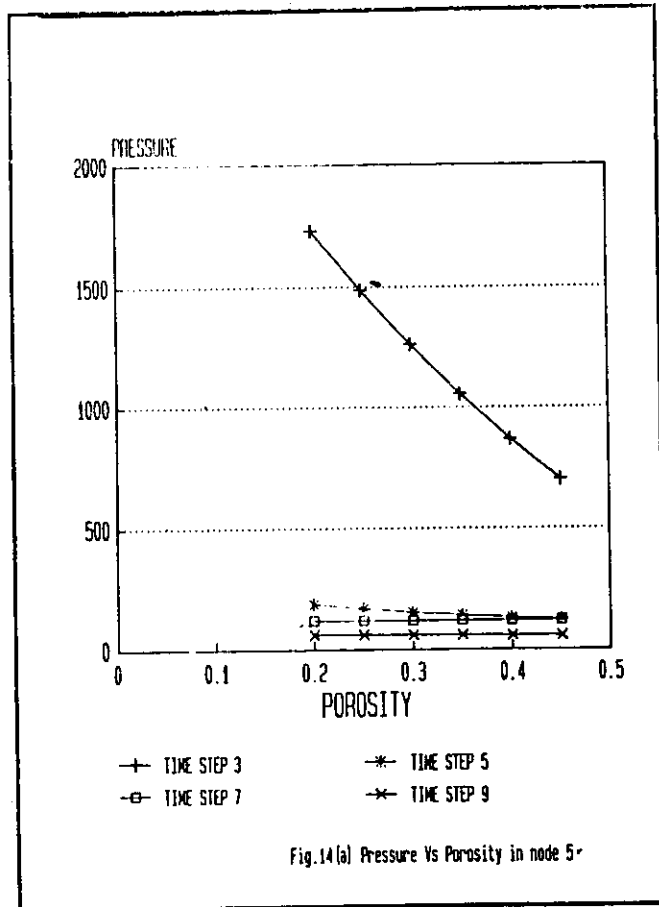
Therefore for the present simulation set-up problem dimensions are calculated as RMDIM = 3942 , RVDIM = 10284 ,IMVDIM = 1961 Program dimensions should be more than these values.

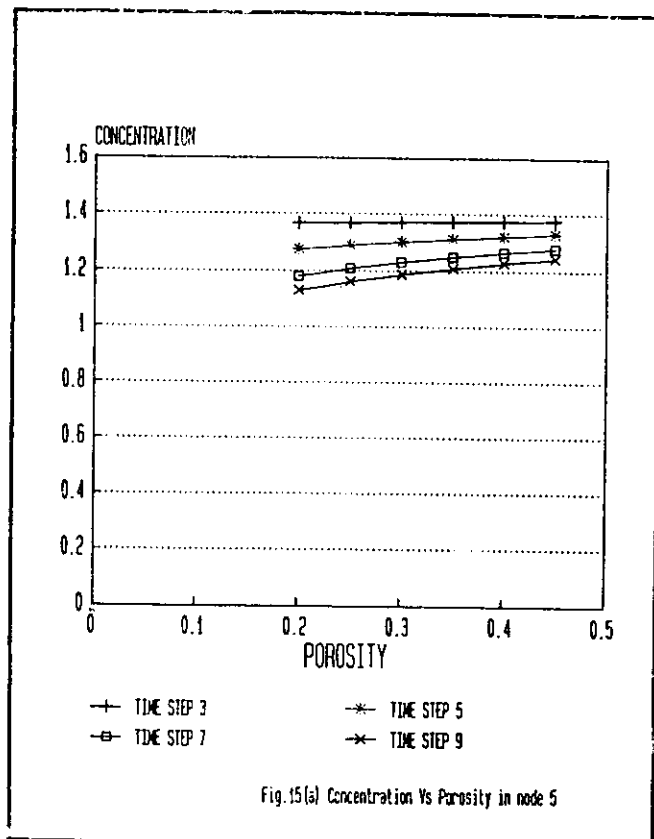
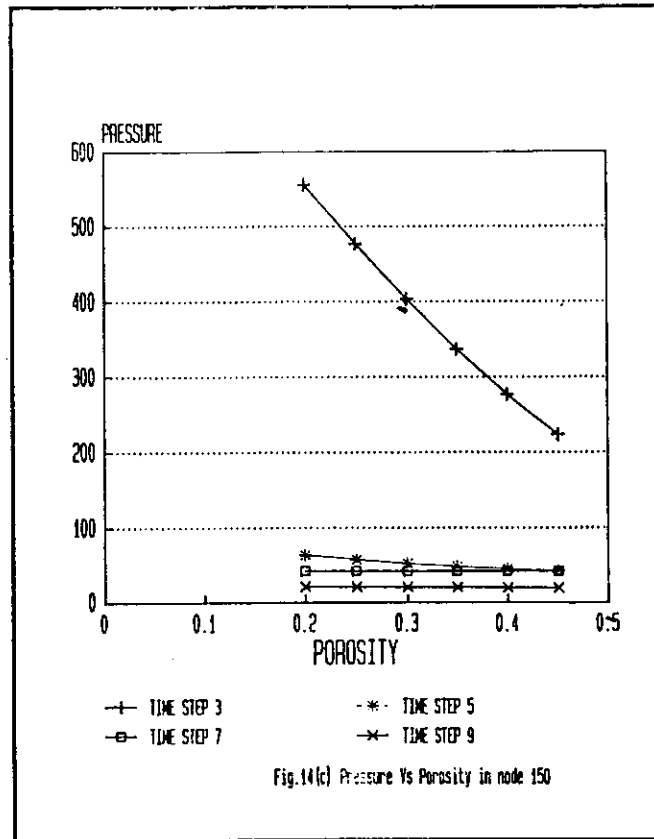
4.3.8 Sensitivity Analysis

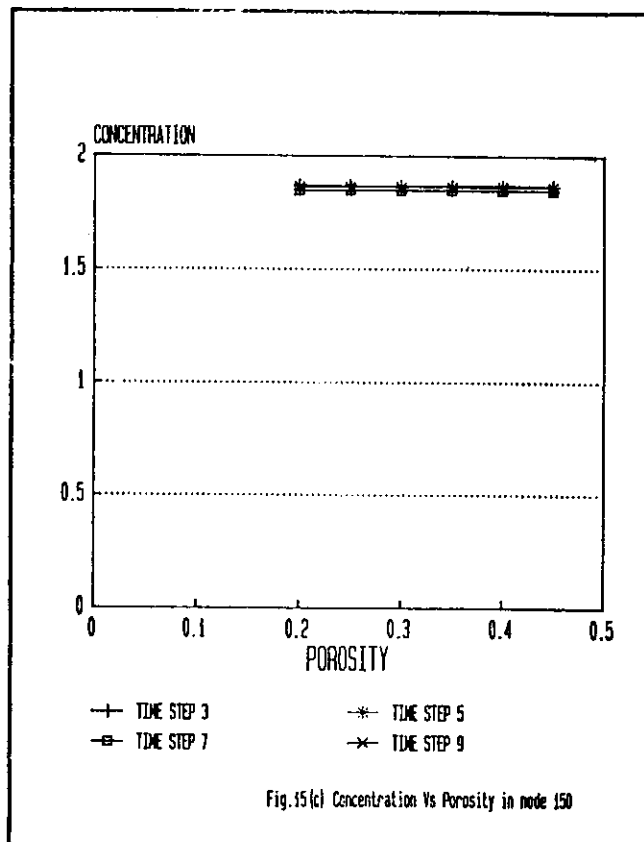
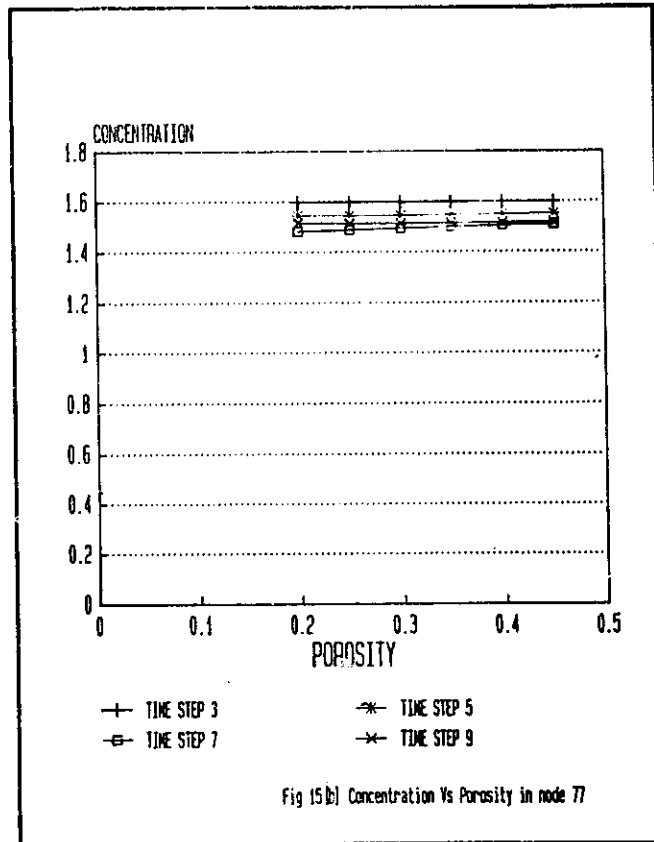
The numerical model has its own sets of coefficients that have to be identified before the model can be used for any particular problem. Parameter identification is full of uncertainty which can lead to a doubt that whether the selected conceptual model indeed represents what happens in the real aquifer system, to the accepted degree of approximation. Possible errors in observed data also contribute to the uncertainty in model parameters. However numerical simulation can be a useful tool in understanding the hydrogeological systems by conducting sensitivity analysis to examine the effect of variables in the values of the system parameters and boundary conditions.

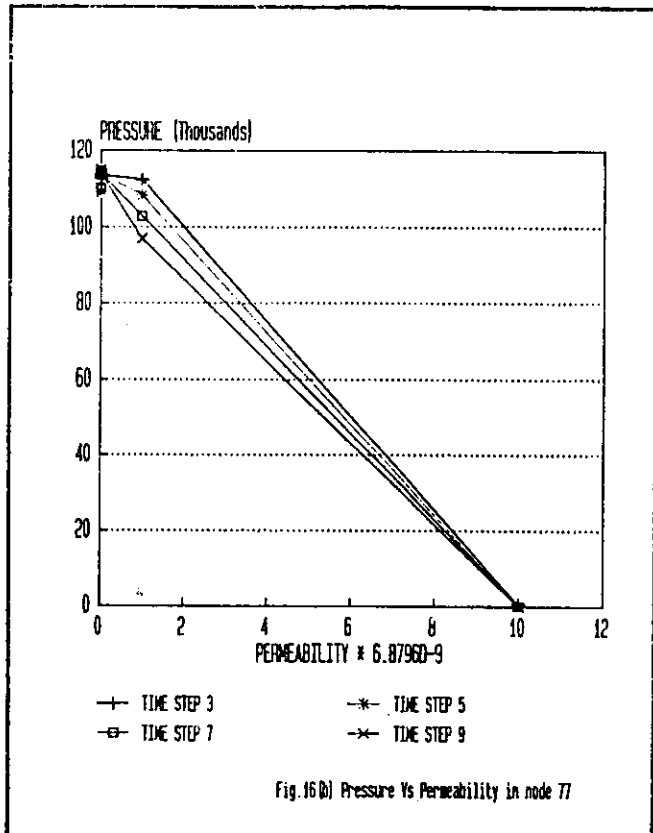
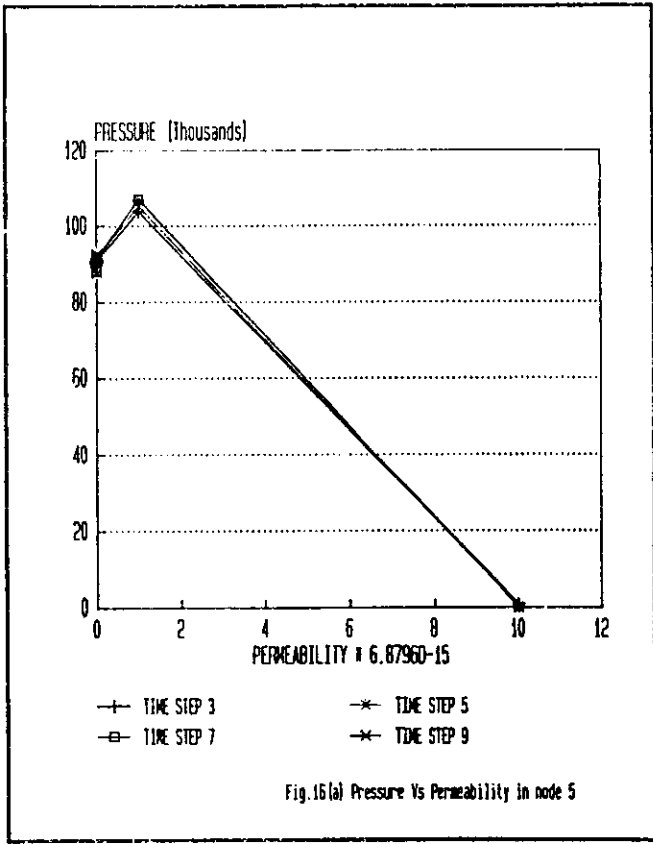
Degree of Sensitivity of different flow and transport parameters have been checked through numerical simulation of the proposed model. These input parameters are porosity, permeability, storativity, longitudinal and transverse dispersivity and molecular diffusivity. Model is first simulated for Steady state condition by December 1974 time step data and then run for transient condition considering the initial condition as on December 1974 and for next 12 monthly timesteps with time variant boundary and source/sink conditions. Each parameter is changed one by one within a range keeping others as constant value as stipulated in para 4.3.4 .

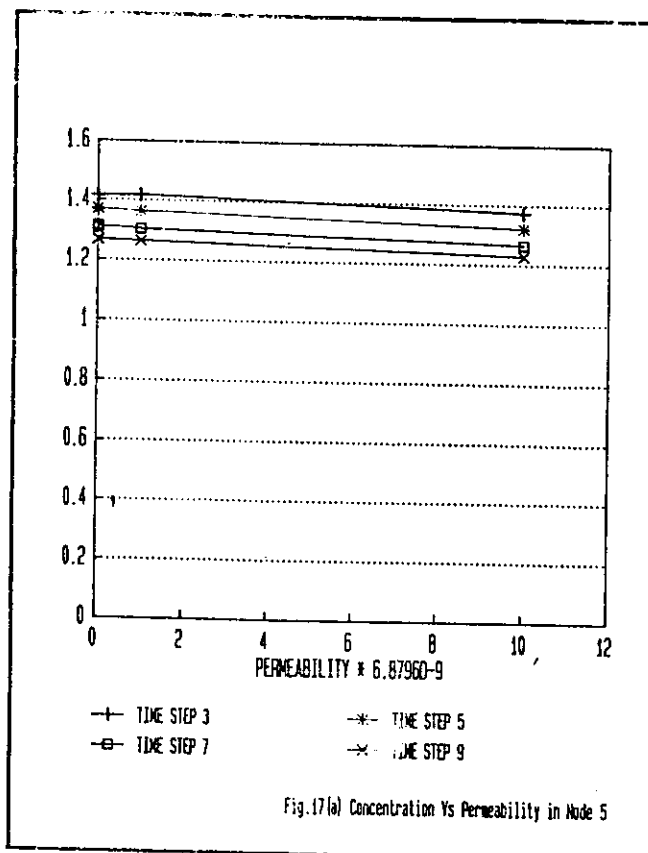
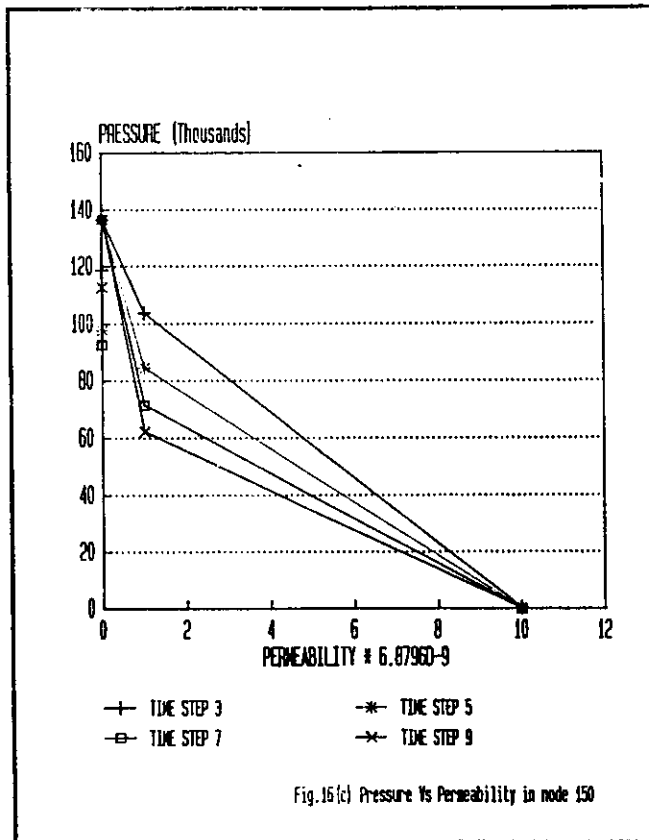
Porosity values are ranged between 20% to 45% and the resulting pressures and concentration values at selected node nos. 5, 77 and 150 are plotted in the fig.14 (a) to (c) and fig 15 (a) to (c) respectively, on four different time steps, i.e. 3, 5, 7, and 9. Likewise permeability values are ranged from 6.8796×10^{-7} sq.mt. to 6.8796×10^{-15} sq.mt. and the pressure and concentration variations are plotted in fig 16 (a) to (c) and fig 17 (a) to (c) respectively. Storativity values are changed through solid matrix compressibilities ranging from 4.8086×10^{-5} to 4.8086×10^{-10} keeping fluid compressibility and porosity value as constant on 4.47×10^{-10} and 0.40 respectively. This ultimately gives a variation of storativity ranging between 2.8972×10^{-5} to 4.6708×10^{-10} units. Results are shown in fig 18 (a) to (c) and fig 19 (a) to (c) for pressure and concentration respectively.

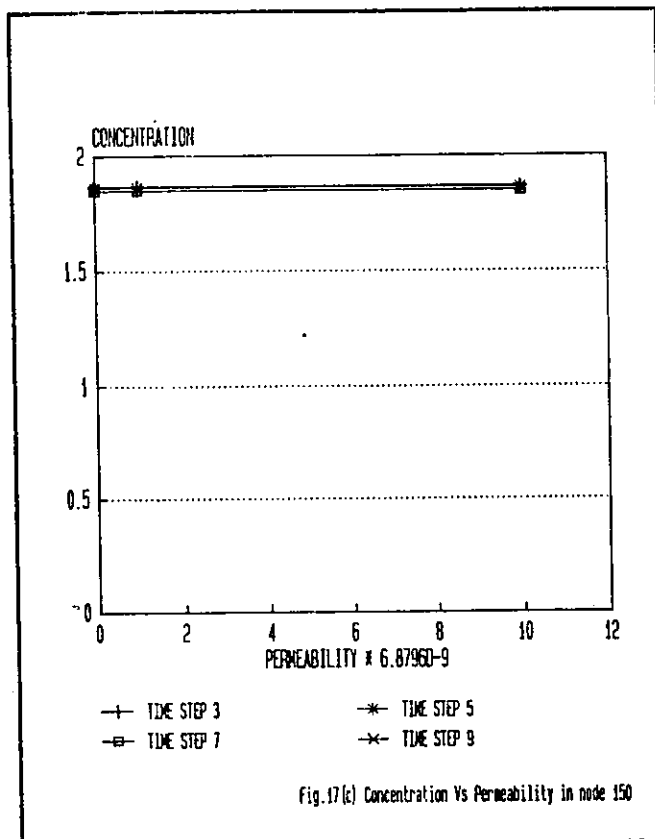
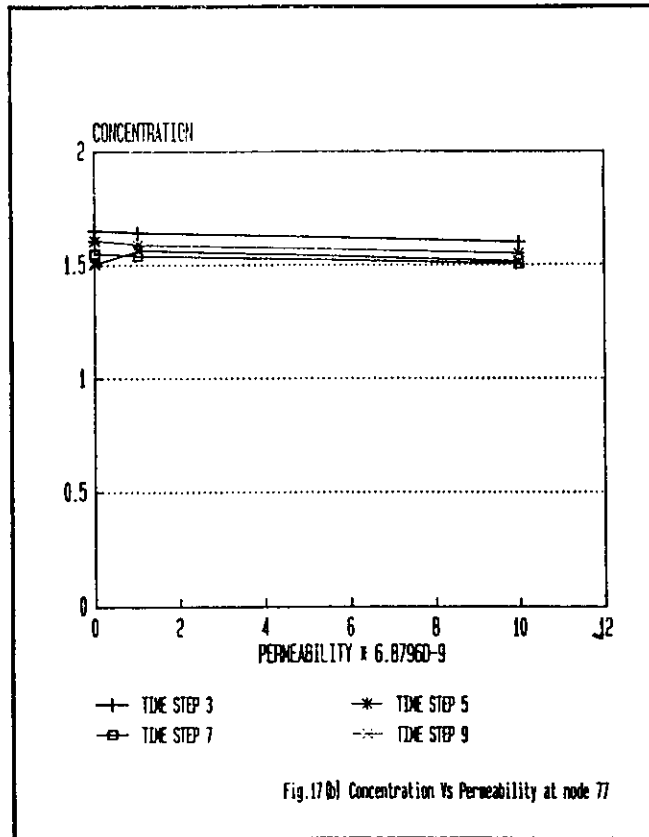


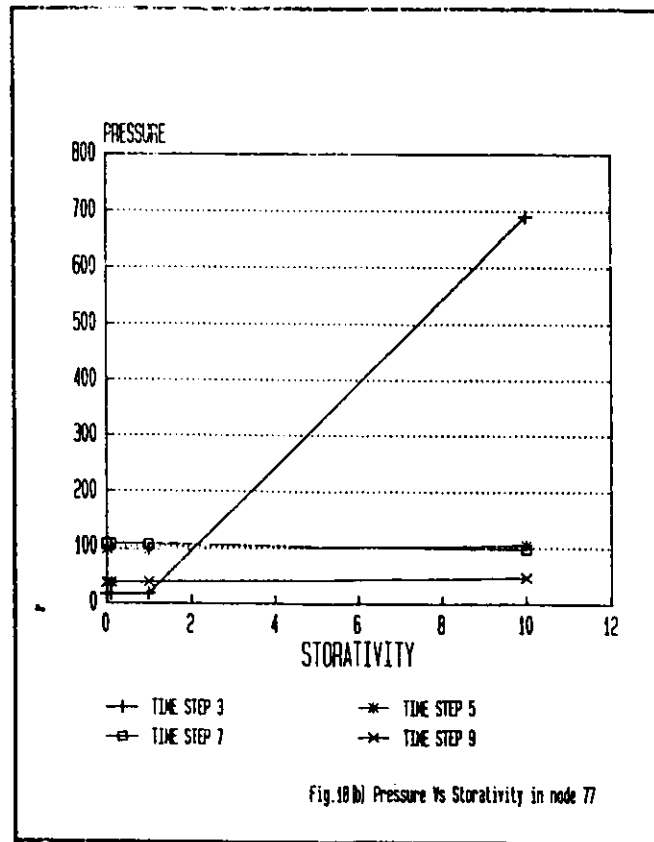
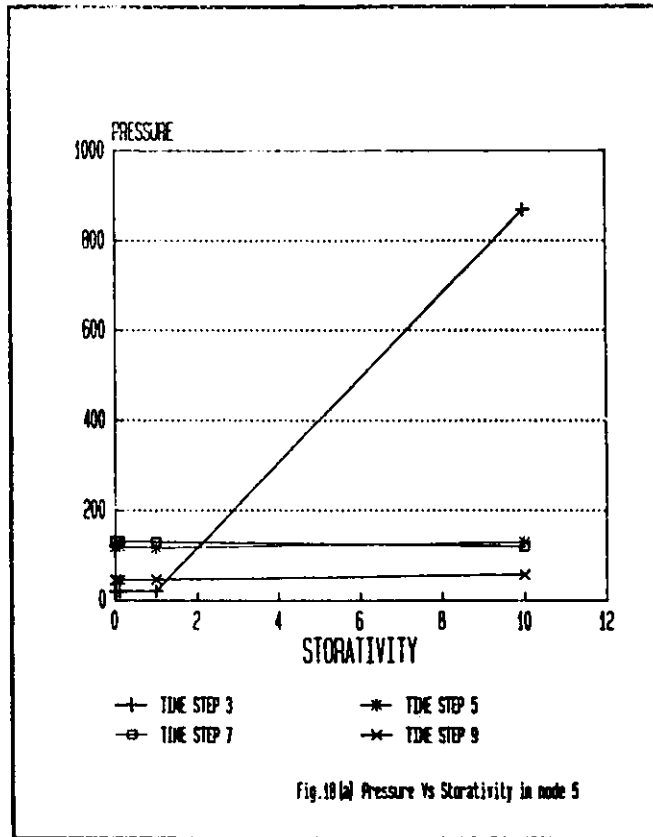


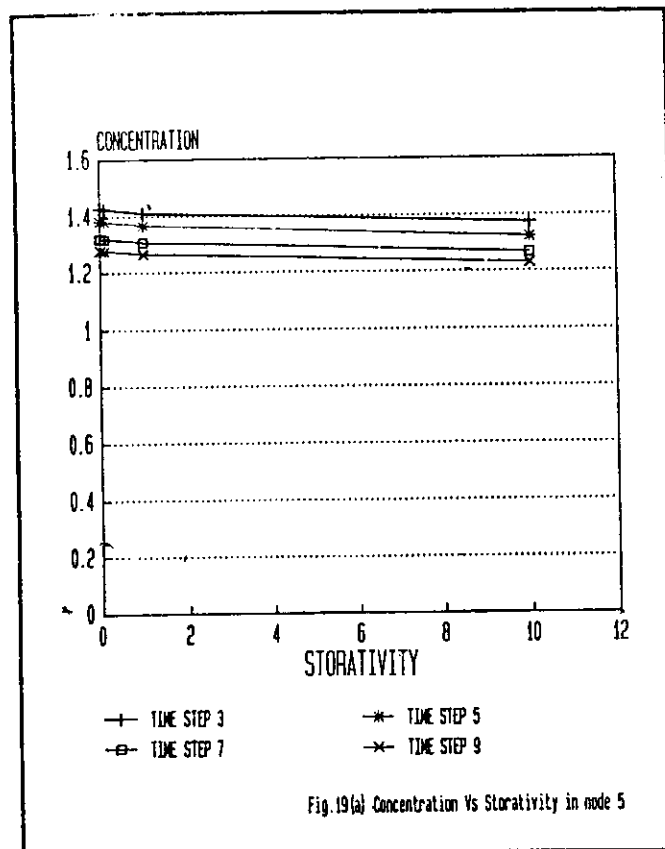
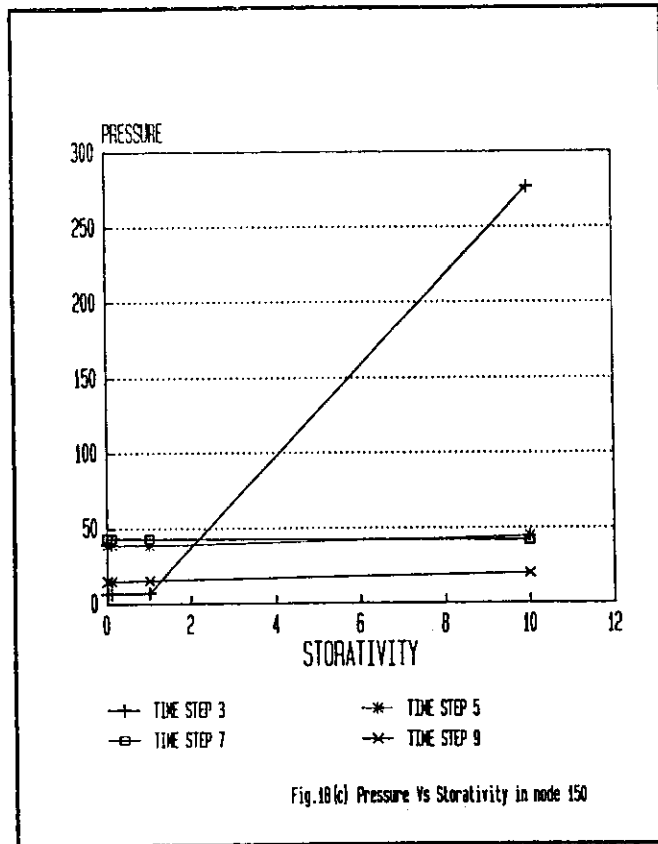


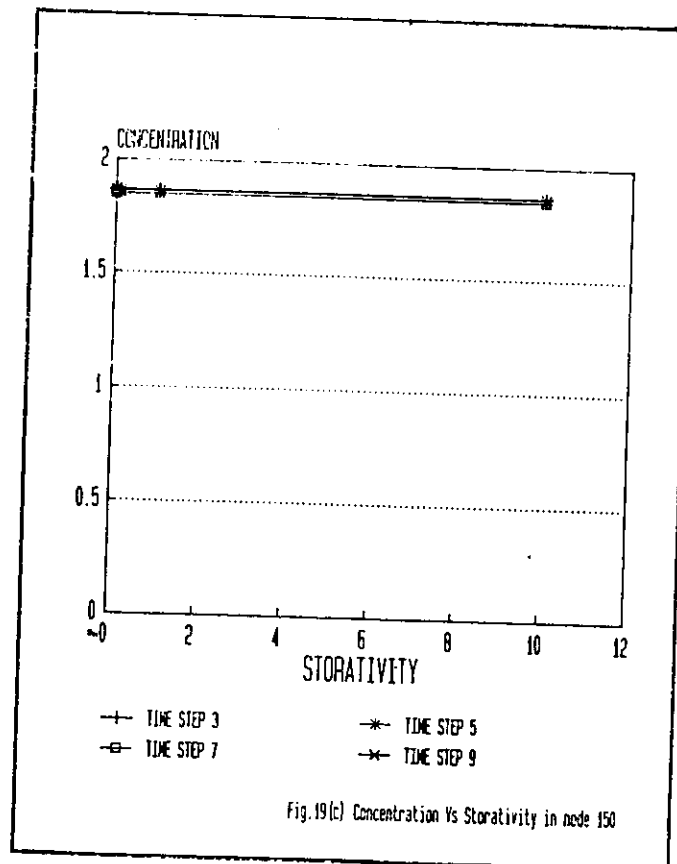
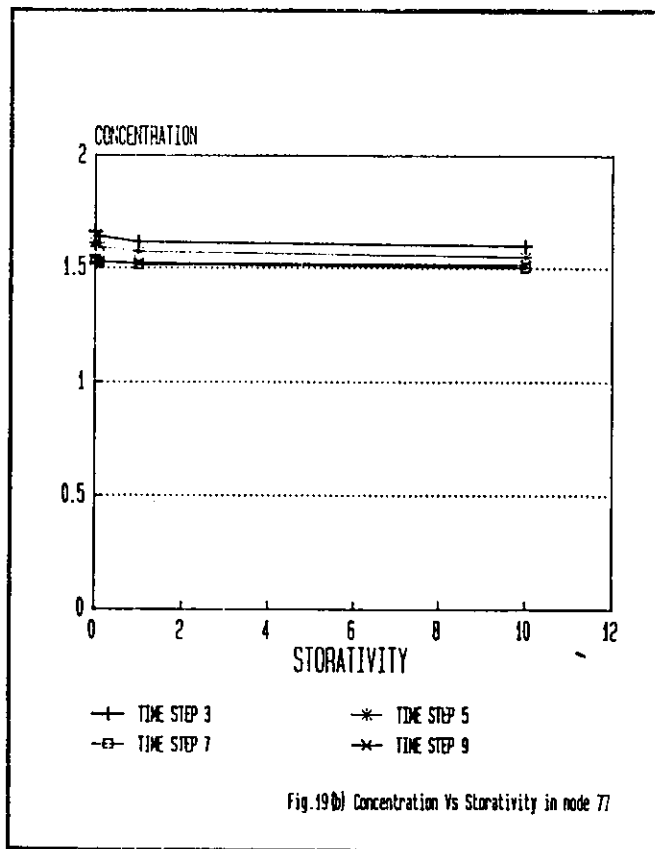












Variation in concentration values are checked by putting different values of longitudinal dispersivity ranging between 10 mt to 100 mt. with corresponding values of transverse dispersivity as 10% of longitudinal value and the plots are shown in fig 20 (a) to (c). There is no significant changes noticed with variation of molecular diffusivity values, therefore those plots are overlooked. All these results of the sensitivity analysis signifies more or less some trend and it can be viewed that permeability parameter has greater impact than parameters like porosity or storativity on pressure results. Concentration values are mostly governed by the dispersivity values.

4.3.9 Steady state Model calibration

Alluvium river stretch from Vaniyambadi to Minnur is simulated considering it as an hypothetical case based on actual field data as far as possible. The model is simulated for steady state condition first for the period January 1975 to January 1980 for 61 monthly time steps. Parameters are taken as shown in para 4.3.4 to start with. Aquifer is considered as fully saturated and isotropic. Initial condition for the model calibration is that of December 1984. Pressures and concentrations at different nodes of which, are interpolated using simple interpolation technique. Time dependent pressures and concentration values are specified in all boundary nodes, which are again the interpolated values based upon the values at node no.1 and 217. A time dependent recharge value is given to all nodes considering it as 20% of the monthly rainfall value at Vaniyambadi.

Simulated steady state boundary pressure values are adjusted through the parameter such as conductance value described in sub head 3.2, to bring it to the specified boundary pressures. Fluid mass budget is then corrected through permeability value. Model resulted in comparatively higher pressure values in the inner nodes. Recharge value has been modified to 0.25 kg/sec per element to attain comparatively normal pressure values, as shown in fig 21. This additional recharge may take care of the tannery effluents disposed directly in to the river. Being a hypothetical case and having no observation node in side the mesh, comparison between observed and computed values could not be possible but overall result shows converging nature and realistic system response.

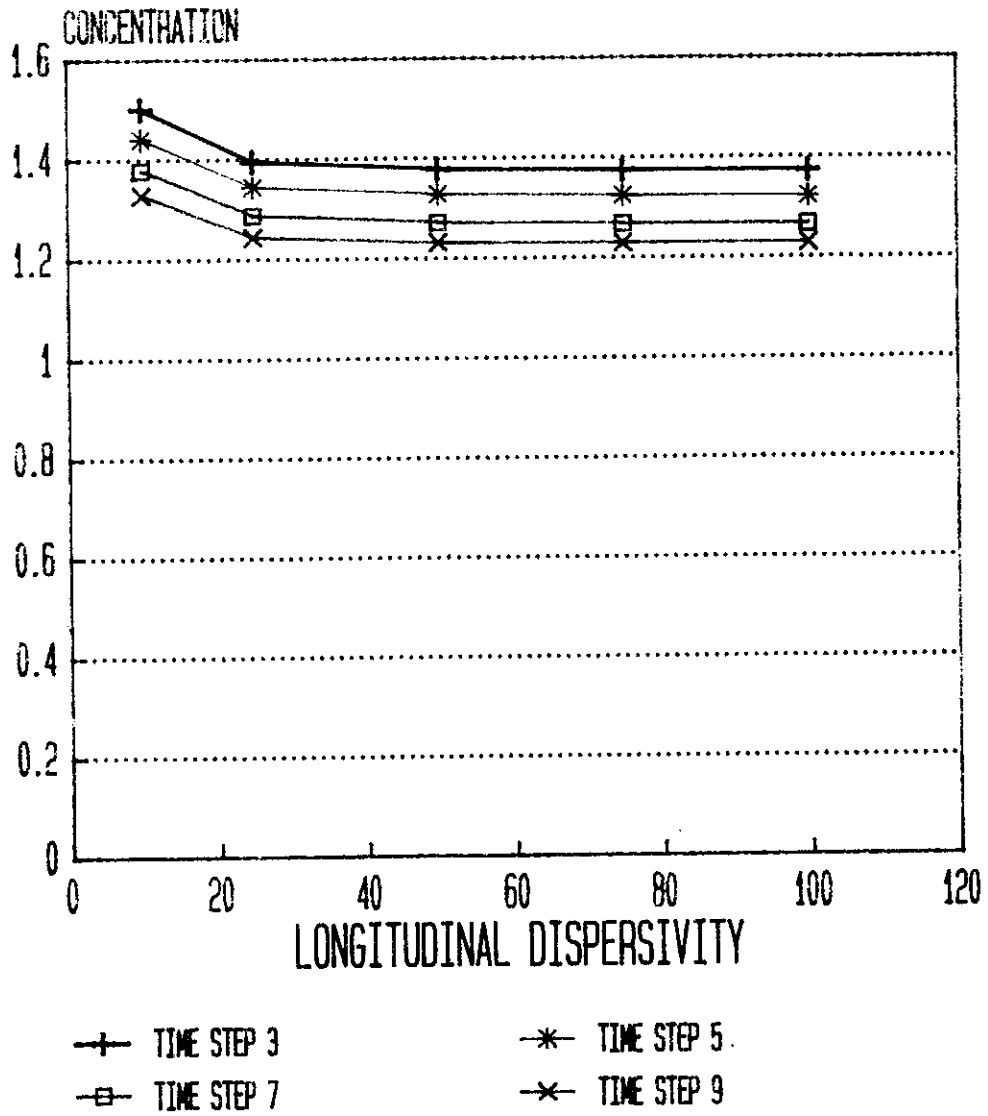


Fig.20(a) Concentration Vs Dispersivity in node 5

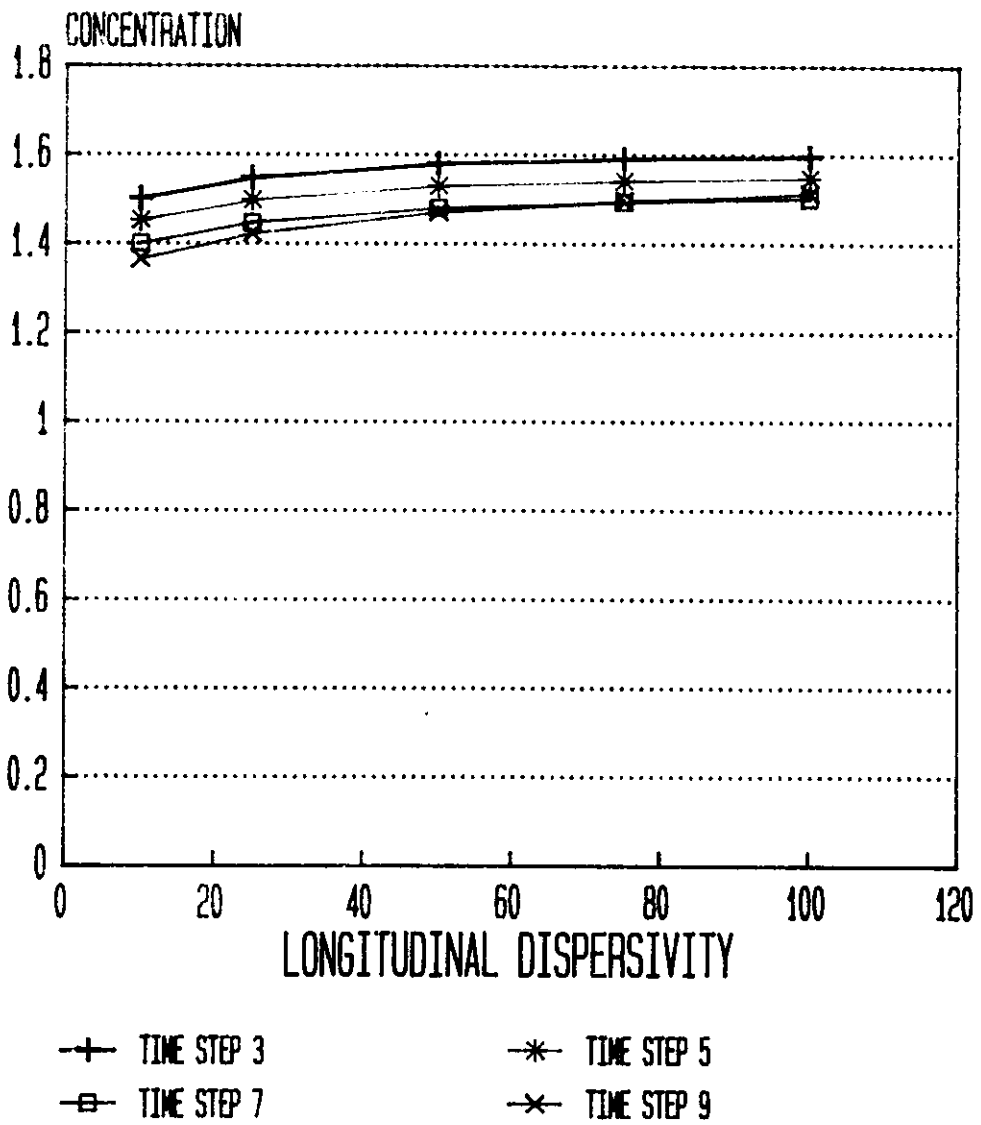


Fig.20 (b) Concentration Vs Dispersion in node 77

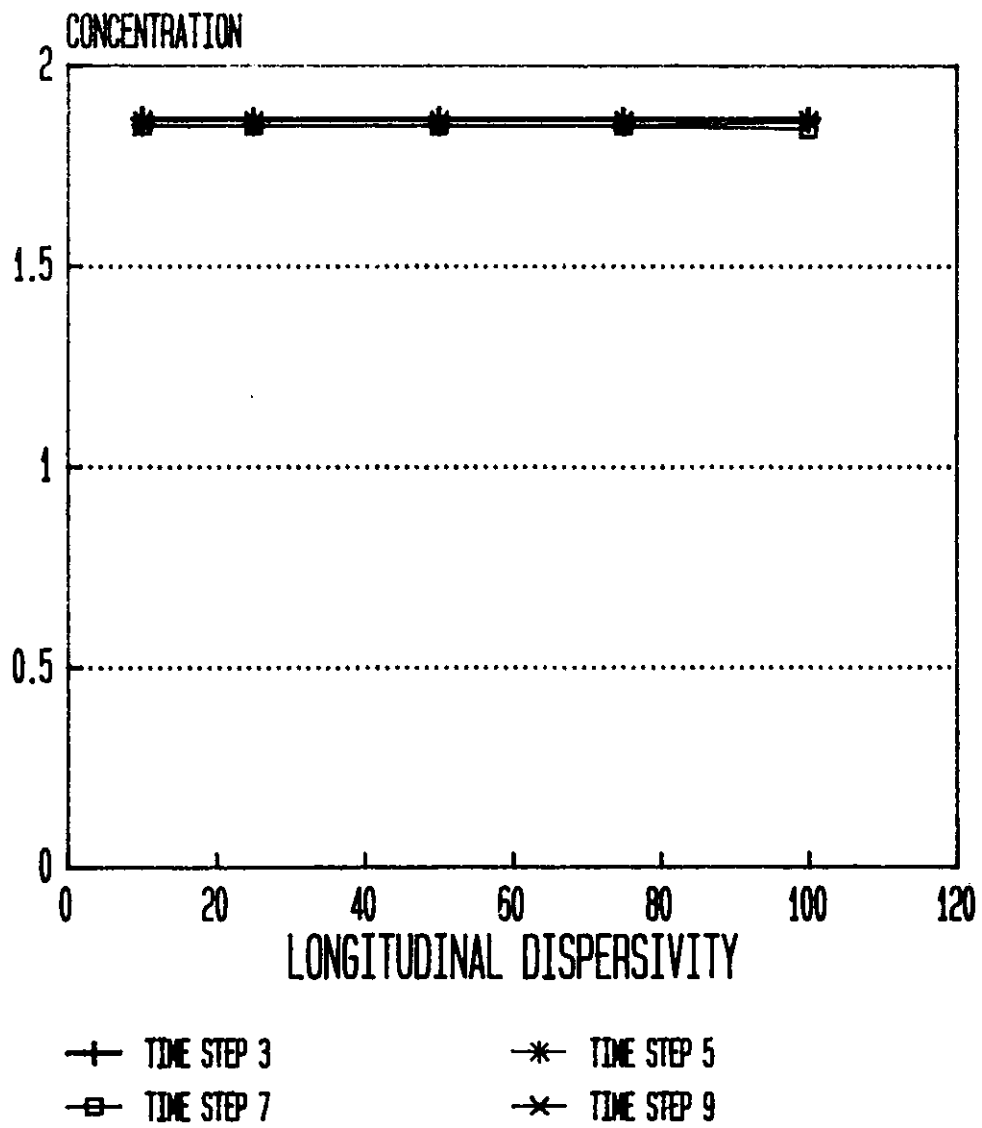


Fig.20(c) Concentration Vs Dispersivity in node 150

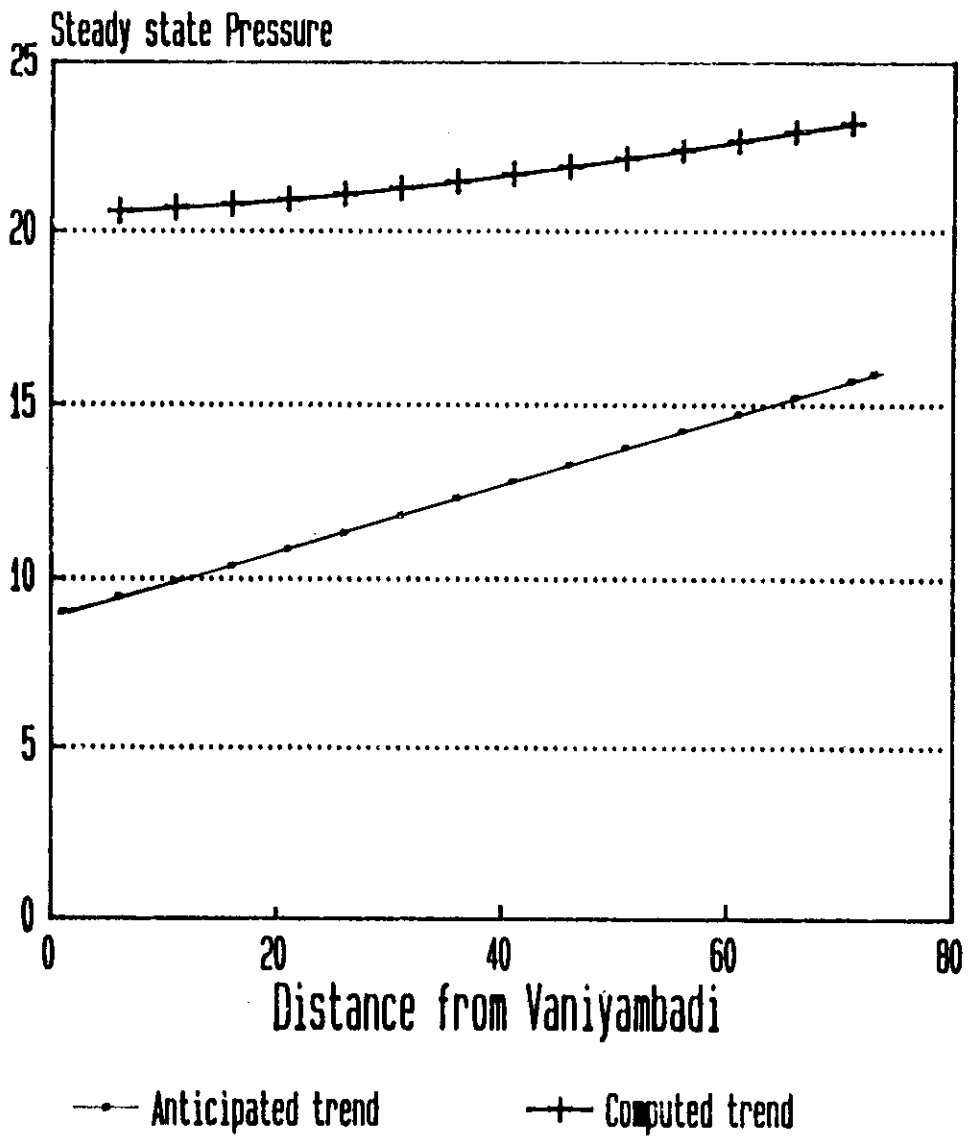


Fig.21 Arial steady state pressure distribution

Simulated concentration values are automatically found to be converging with specified boundary values at the boundaries and to the acceptable limit in the inner nodes in all the 61 time steps (fig.22). Results of the analysis after 1st, 30th and 61st time step along with the initial time step are shown in fig. 23. The values plotted are those of node nos. 2, 5, 77, 150, 215 and 218 out of which 2 and 218 are boundary specified values. During the steady state calibration the permeability value has to be modified from 6.8796×10^{-7} sq.mt. to 5.0×10^{-14} mt², which is inside the range shown in the table 1 comprising the results of some of the pump tests carried out by the state departments in the region.

4.3.10 Transient model calibration:

A storativity value of 2.8972×10^{-5} is considered for the transient model calibration with all other simulation parameters and condition remain same as mentioned in steady state simulation. Pressure values at all time steps seem to be converging with the specified values at the boundaries and to the anticipated values at the inner nodes. A portion of output is appended as appendix VIII. Fluid mass budget also satisfies physicality of the domain. Concentration values are also converging with the specified values. Variation in pressures and concentrations at different nodes and time steps are shown in fig.24 and fig.25 respectively. Areal variation of concentration on 1st, 30th and 61st time steps are shown in fig.26.

This simulated model has been tested for the following cases of solute injection to verify the contamination transport responses of the model. These Test runs are executed with Time dependent specified concentrations only on two nodes i.e. on node nos.1 and 219, where the observation wells at vaniyambadi and minnur are situated.

(1) A mass fraction of 10 units are specified for the source entering per element on first time step. Variation in concentration in some of the observed nodes with different time steps is shown in fig 27. Areal variation of concentration on time steps 31st and 61st can be compared by fig 28(a) and 28(b).

(2) A mass fraction of 10 units are specified for the source entering each element on each time step. Results are shown in fig 29 for temporal variation and in fig 30(a) and 30(b) for areal variations on 31st and 61st time step.

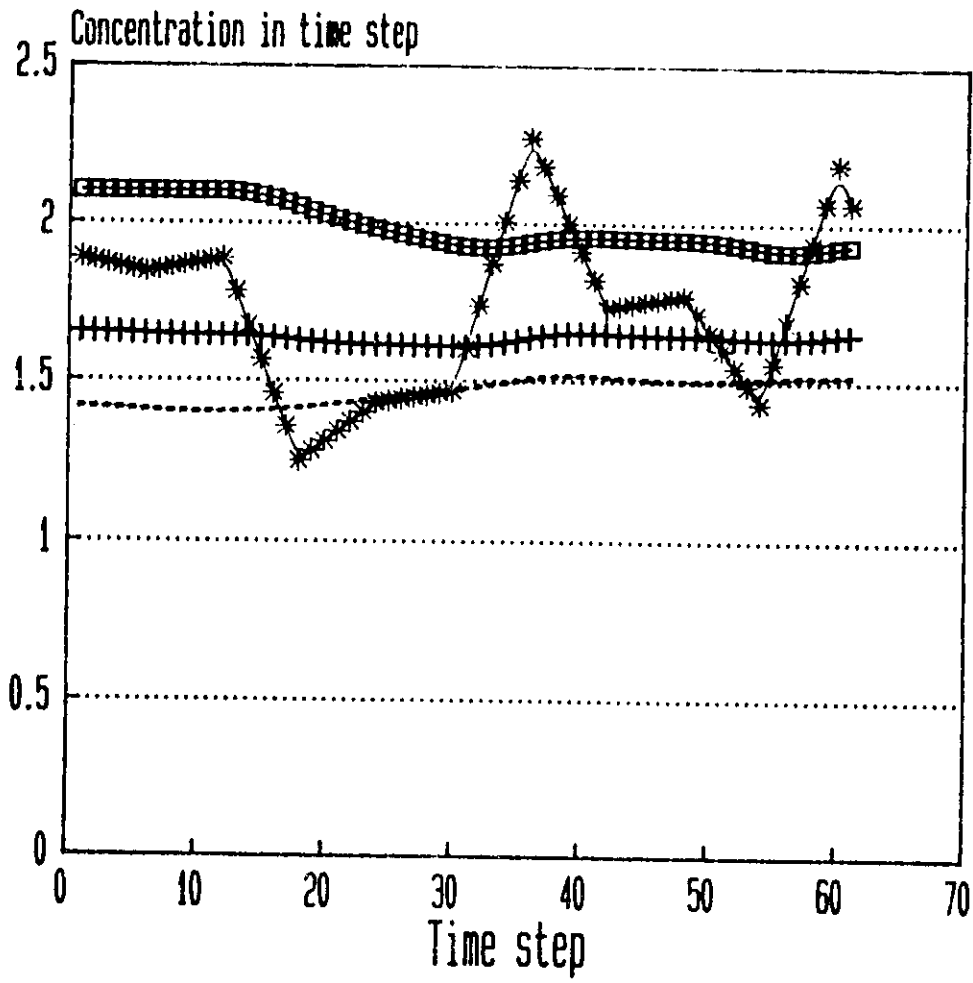


Fig.22 Temporal concentration variation in steady state condition

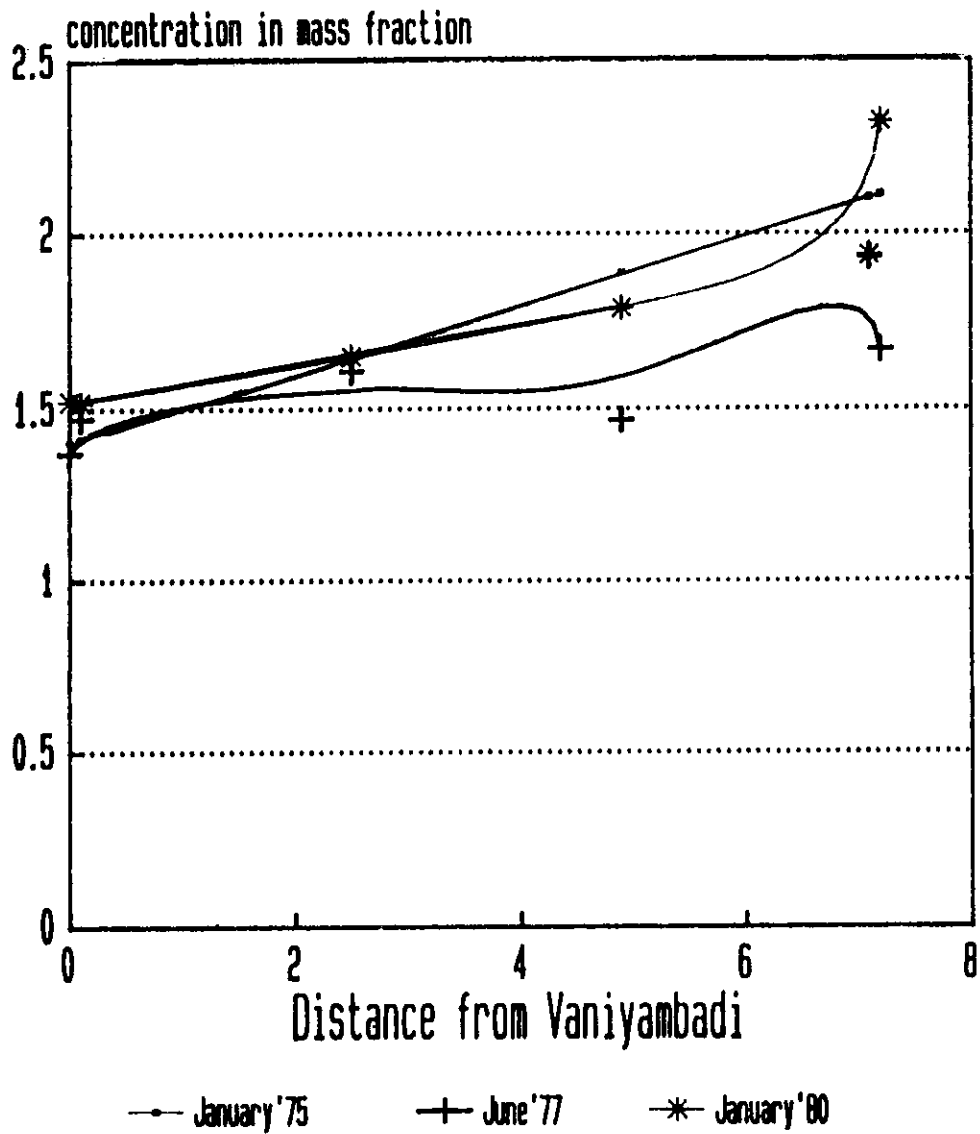


Fig.23 Aerial variation of concentration in steady state flow condition

Table 2 Pump Test Results of bore wells in Palar river basin.

Sl no	Location	Duration of pumping	Q (pump) Cumec	T (pump) Sq.mt/day	Storativity Sq.mt/day	Permeability Sq.mt.
1.	Velur(Velur)	60 min.	2.515E-3	1639	3.04E-4	1.913-11
2	Thuthukodi (Velur)	60 min.	3.373E-3	6.735	1.25E-6	1.35E-11
3.	Rangapuram (Kudiyattam)	30 min.	4.907E-4	0.5215	9.68E-8	5.08E-14
4.	Madhanur (Kudiyattam)	30 min.	5.520E-4	0.457	8.49E-8	4.05E-14
5.	Usm(Vellore)	30 min.	6.748E-4	655.6	1.21E-4	1.42E-11
6.	Arumpakkam (Arcot)	240 min.	6.103E-4	0.160	2.97E-8	4.02E-13
7.	Narasingapuram(Gudiyattam) 21077	855 min.	1.840E-3	156.45	2.90E-5	7.61E-12

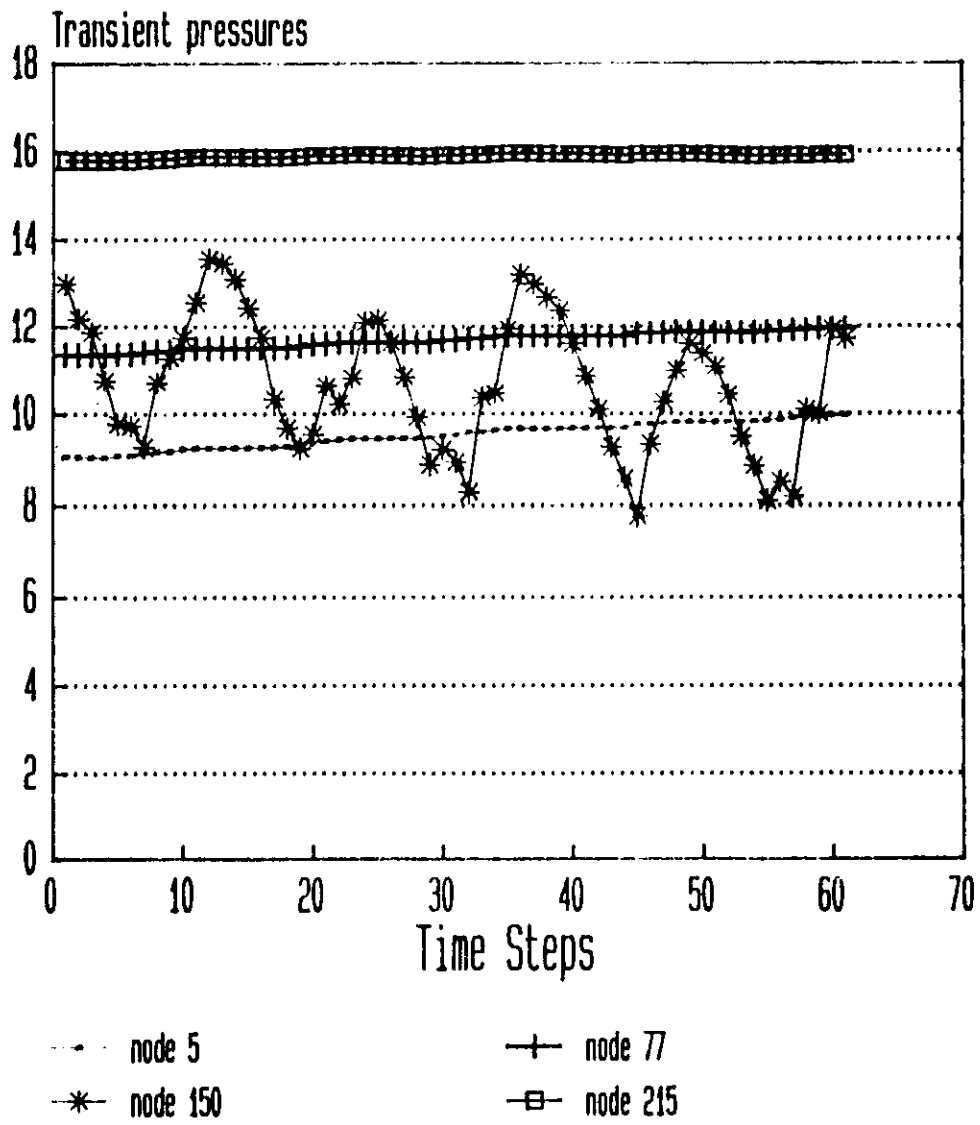


Fig 24 Temporal pressure variation in Transient-condition

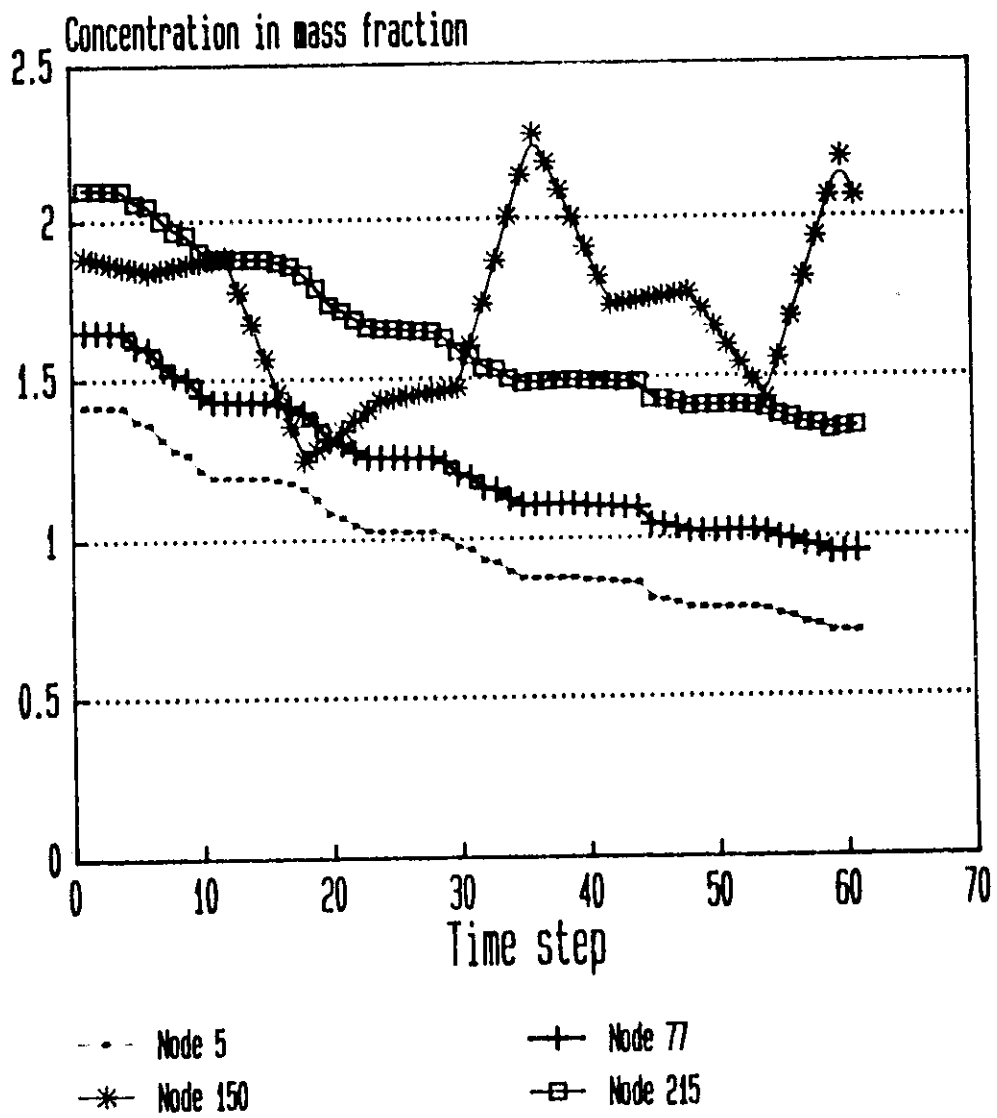


Fig. 25 Temporal concentration variation in Transient condition

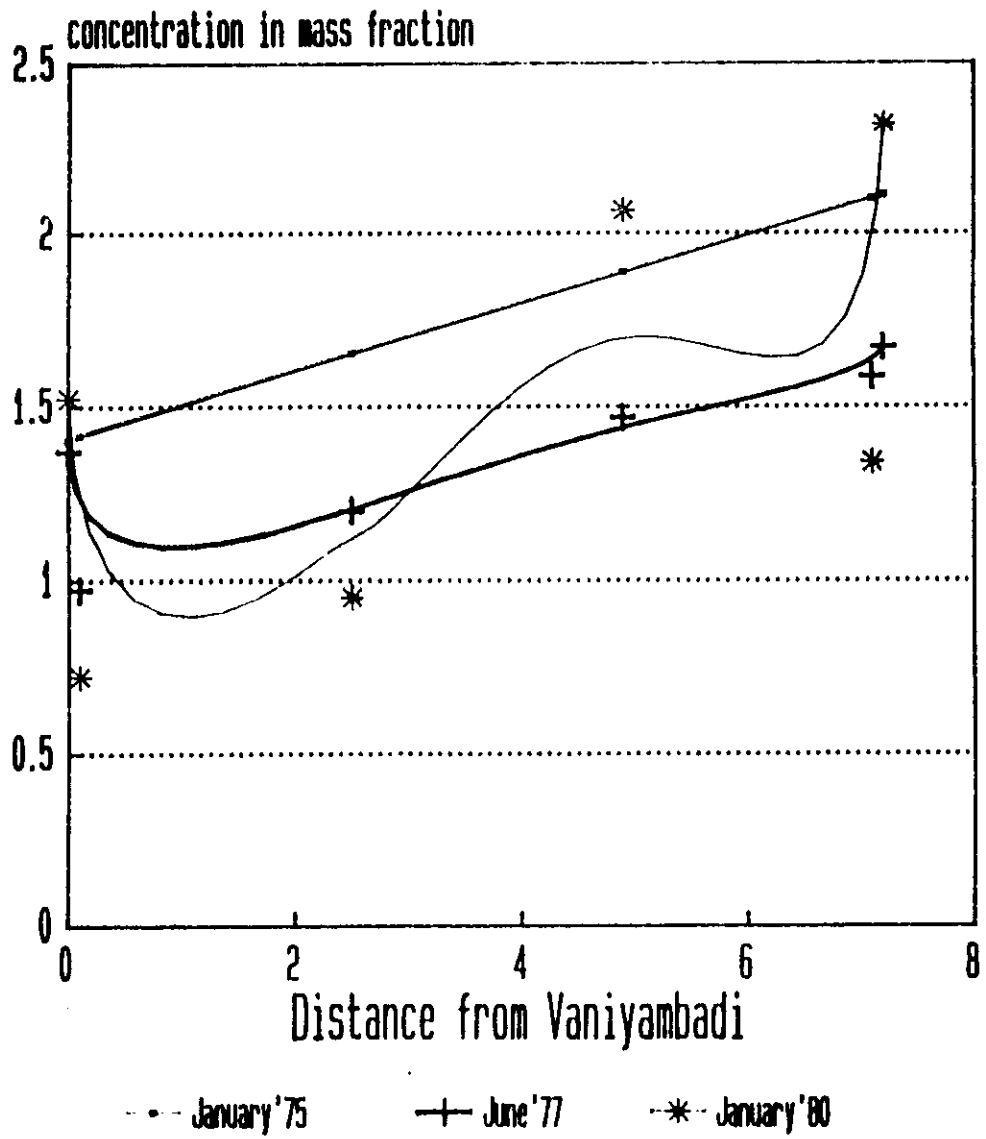


Fig.26 Arial variation of concentration in transient condition

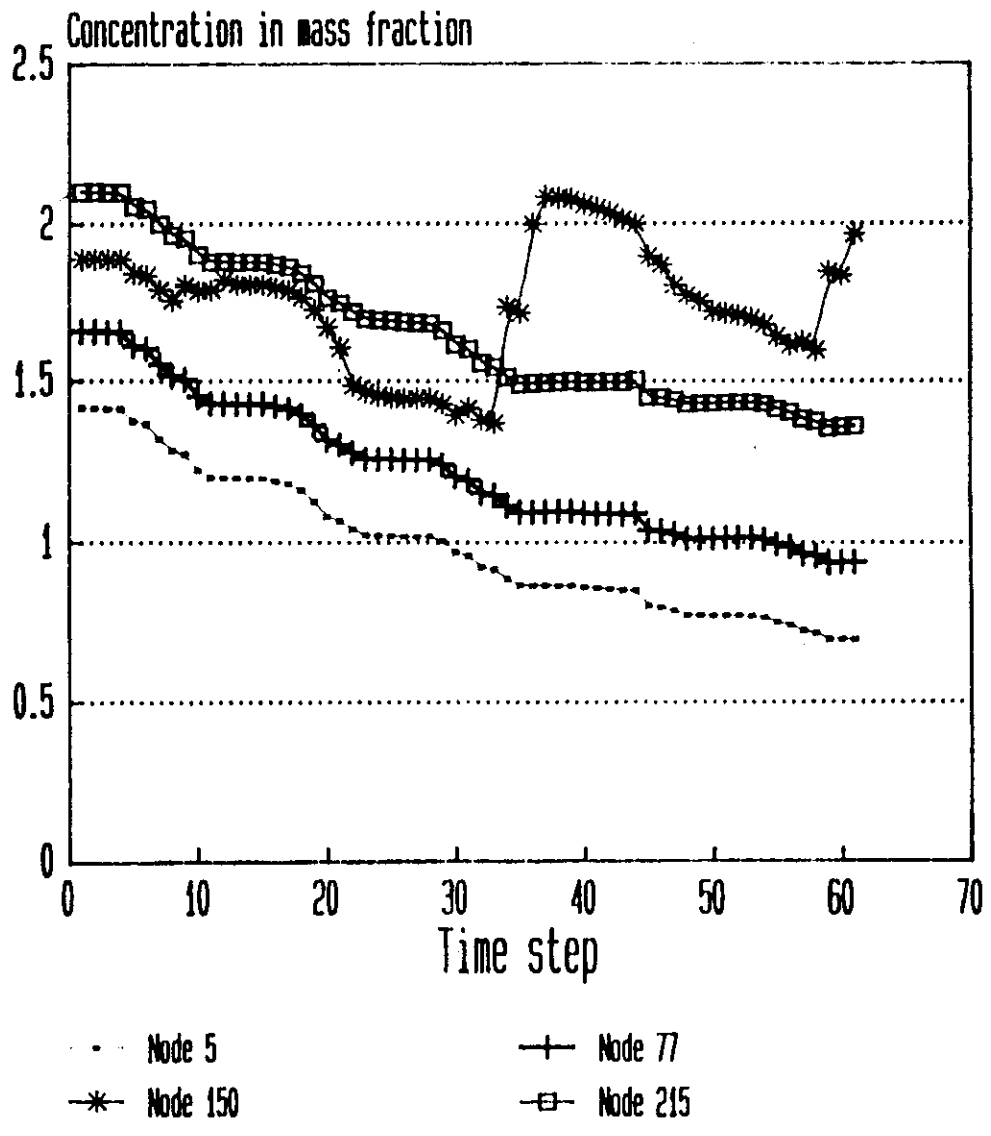


Fig.27 Temporal concentration variation in case 1

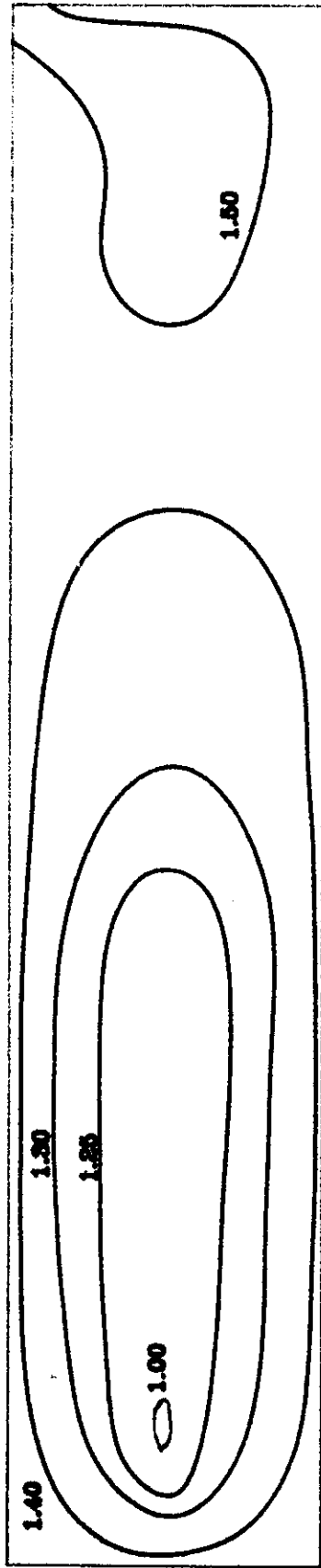


FIG. 28(a) ARIAL VARIATION OF CONCENTRATION IN MASS FRACTION
FOR CASE 1 FOR TIME STEP 31

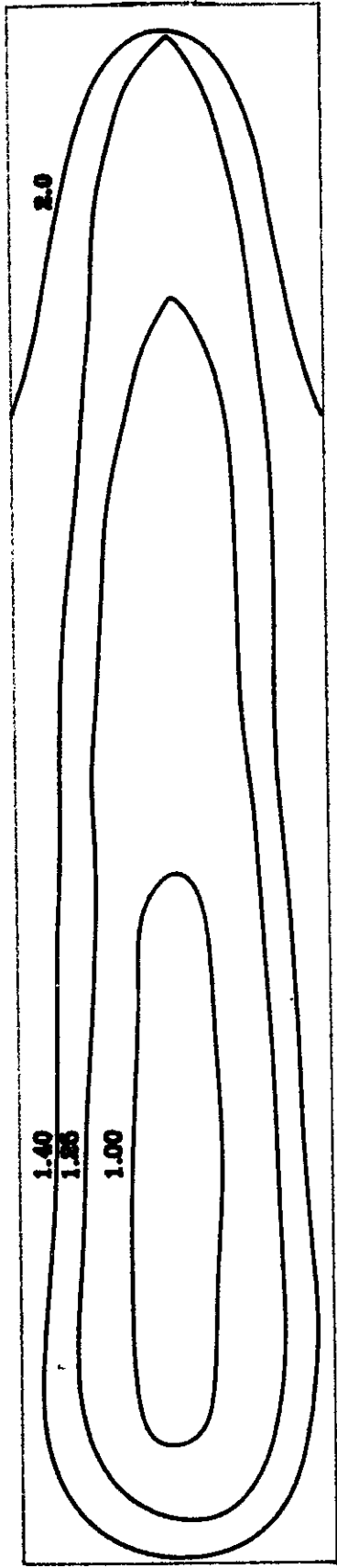


FIG. 28(b) ARIAL VARIATION OF CONCENTRATION IN MASS FRACTION FOR CASE 1 FOR TIME STEP 61

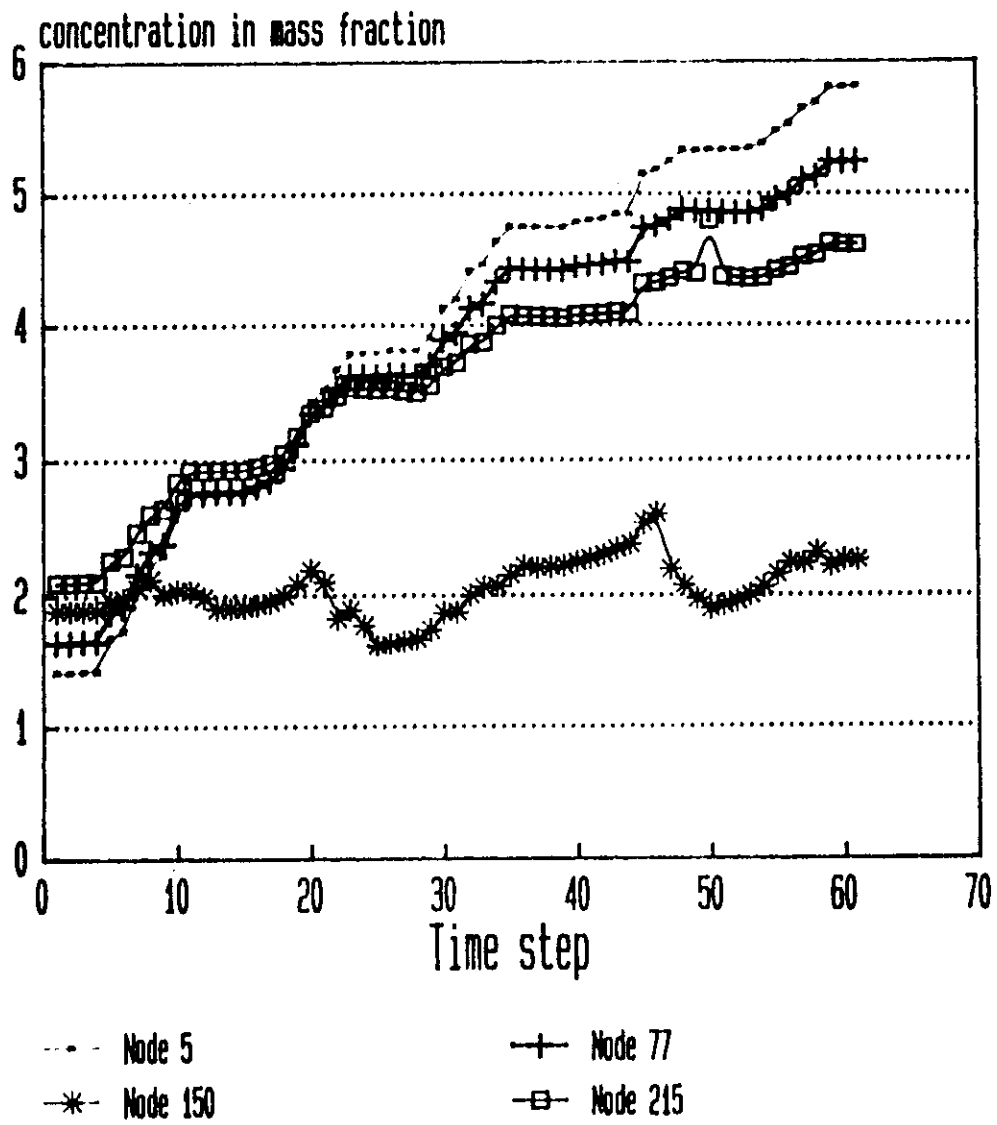


Fig.29 Temporal concentration variation in case 2

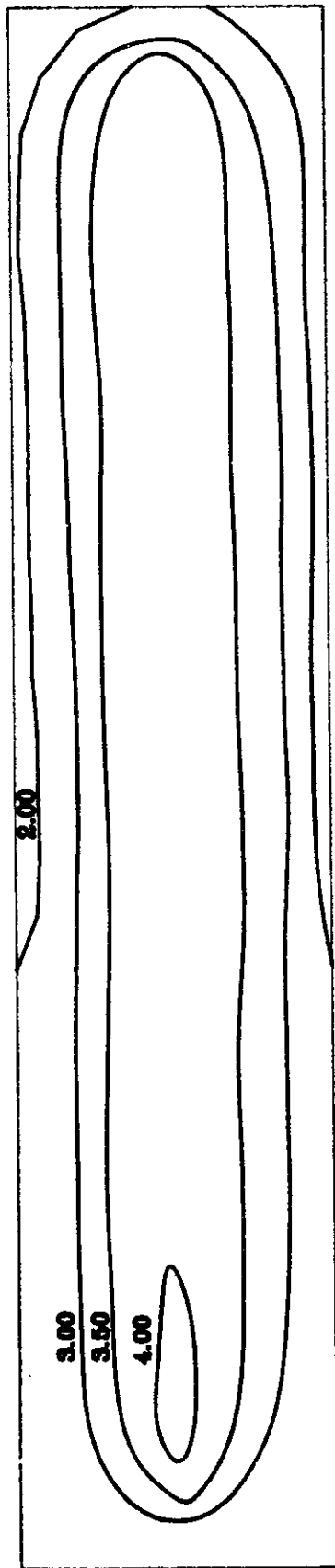


FIG. 30(α) ARIAL VARIATION OF CONCENTRATION IN MASS FRACTION
FOR CASE 2 TIME STEP 31

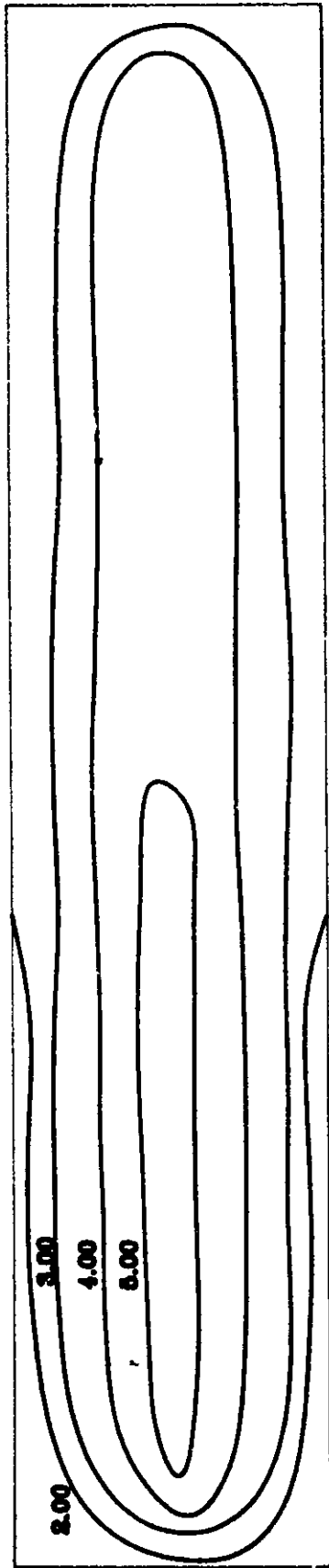


FIG. 30(b) ARIAL VARIATION OF CONCENTRATION IN MASS FRACTION
FOR CASE 2 TIME STEP 61

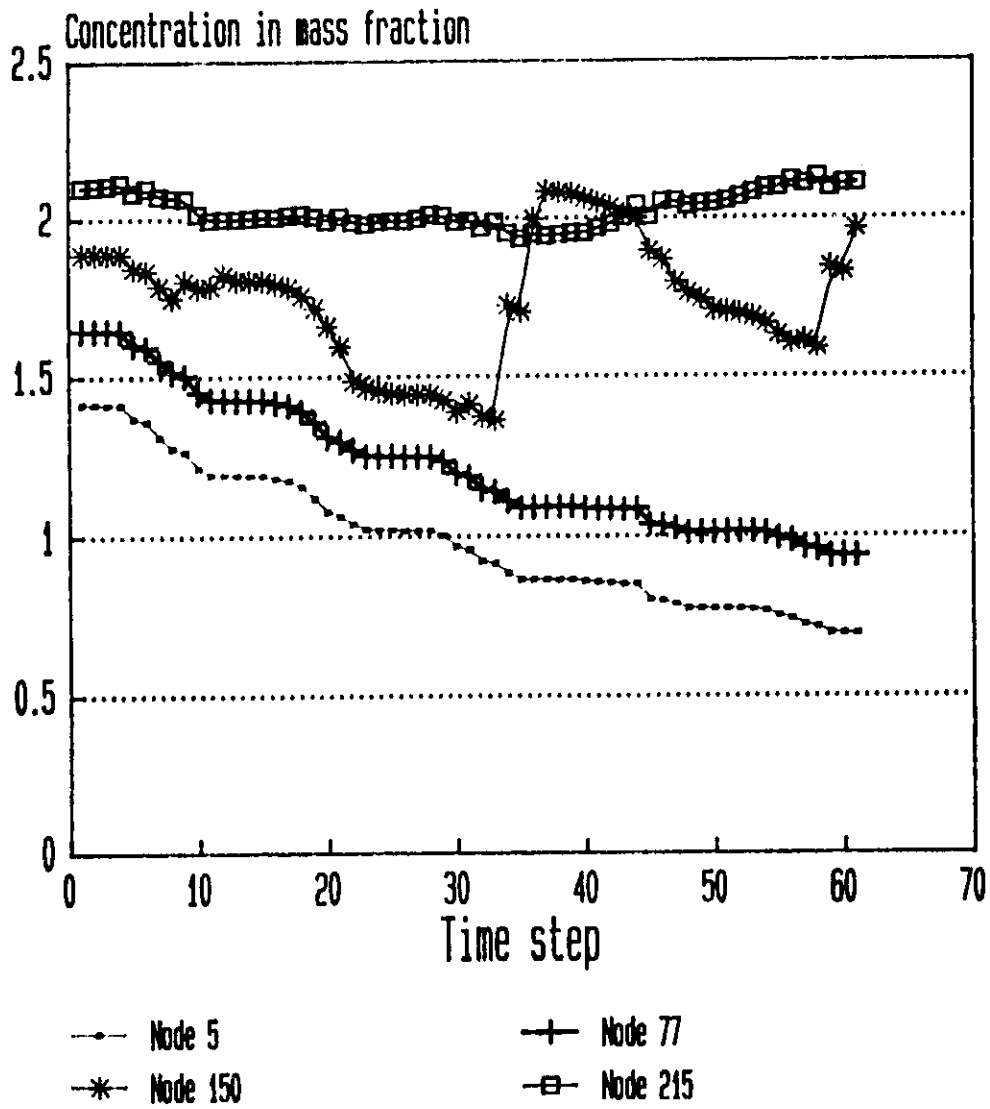


Fig.31 Temporal concentration variation in case 3

(3) Constant solute mass source fraction of 10 units specified on 10 nodes near Minnur well i.e. on node nos. 219, 216, 213, 210, 207, 204, 201, 198, 195 and 192 to represent a situation where 1 Km of the length from minnur is experiencing constant disposal of untreated effluent from left bank. Results are plotted in fig 31 for temporal variation and in fig 32(a) and 32(b) for areal variation on 31st and 61st time steps.

(4) A mass fraction of 2 units are specified for the source entering each element on each time steps in addition to the conditions specified at (3). Results are depicted in fig 33 for temporal variation and in fig 34(a) and 34(b) to represent areal variation on 31st and 61st time step respectively.

4.3.11 Results of the simulation

Steady state pressure results in fig 21 are quite comparable with the anticipated trend which is nothing but the trend which has been adopted while interpolating initial pressures in the inner nodes. Computed values are on higher side which can be adjusted through authentic values of recharge and discharge. The impact of this irrelevant recharge value may be the reason behind comparatively more vibrant nature of concentration variation in node 150 in fig 22. Excess system responses are segregated around the zone near node 150 otherwise response at other three nodes are quite encouraging. Areal variations are quite convergent in nature in fig 23.

Simulated Transient pressures on all 61 time steps are of converging nature except and again in node 150 in fig 24 where comparatively more vibrant trend is noticed. Reason is same that specified in the case of steady state simulation. This trend is evident in all the test runs and will be ignored due to the same reason and to avoid repetition. Concentrations are also simulated to represent smooth and converging trend and no numerical oscillations are noticed. This can be concluded from fig 25 and 26. Only shortcoming of the simulation is that due to lack of any observation well inside the mesh, comparison with field observation could not be possible.

Solute transport phenomena is evident in all the four test runs with different solute injection conditions. Temporal variation in all the nodes for case 1 shown in , where solute is injected only on first time step is on reducing trend. In case 2 where

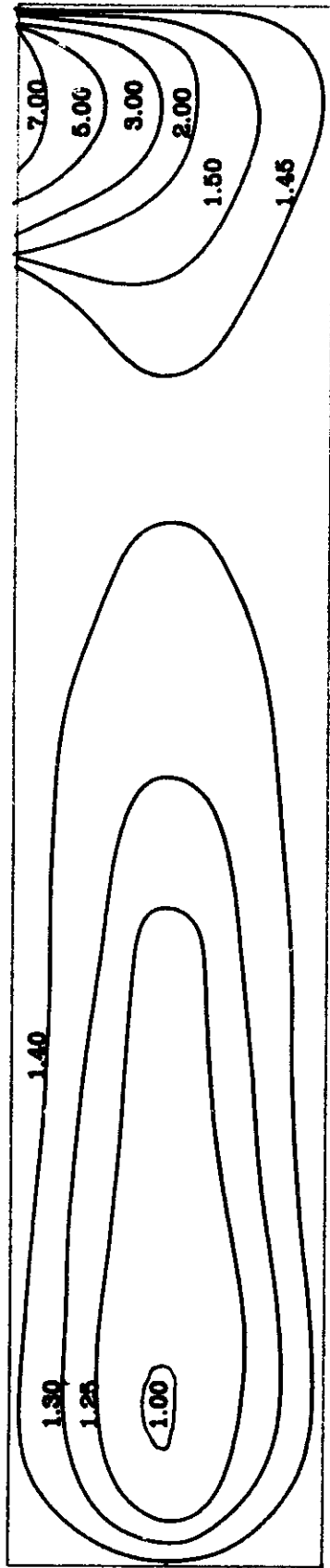


FIG. 32(a) ARIAL VARIATION OF CONCENTRATION IN MASS FRACTION
FOR CASE 3 TIME STEP 31

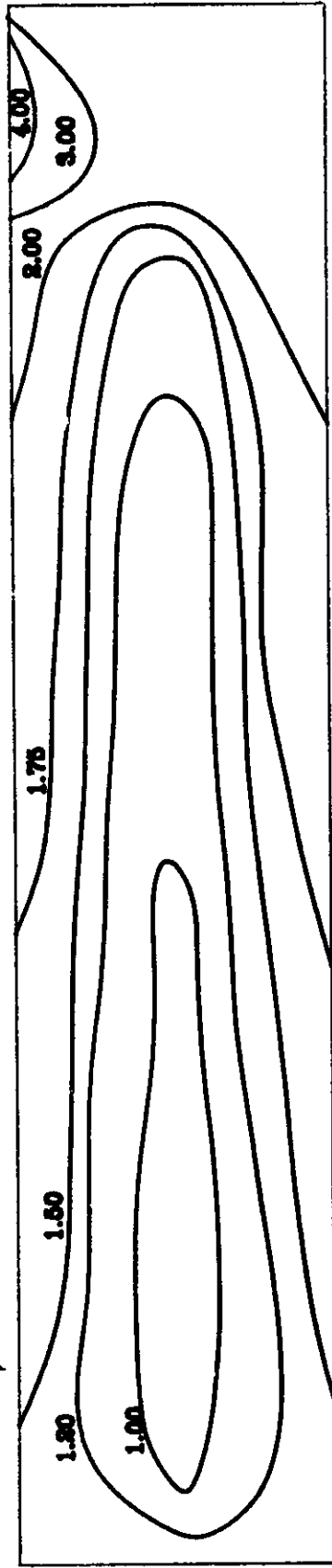


FIG. 32(b) ARIAL VARIATION OF CONCENTRATION IN MASS FRACTION
FOR CASE 3 TIME STEP 61

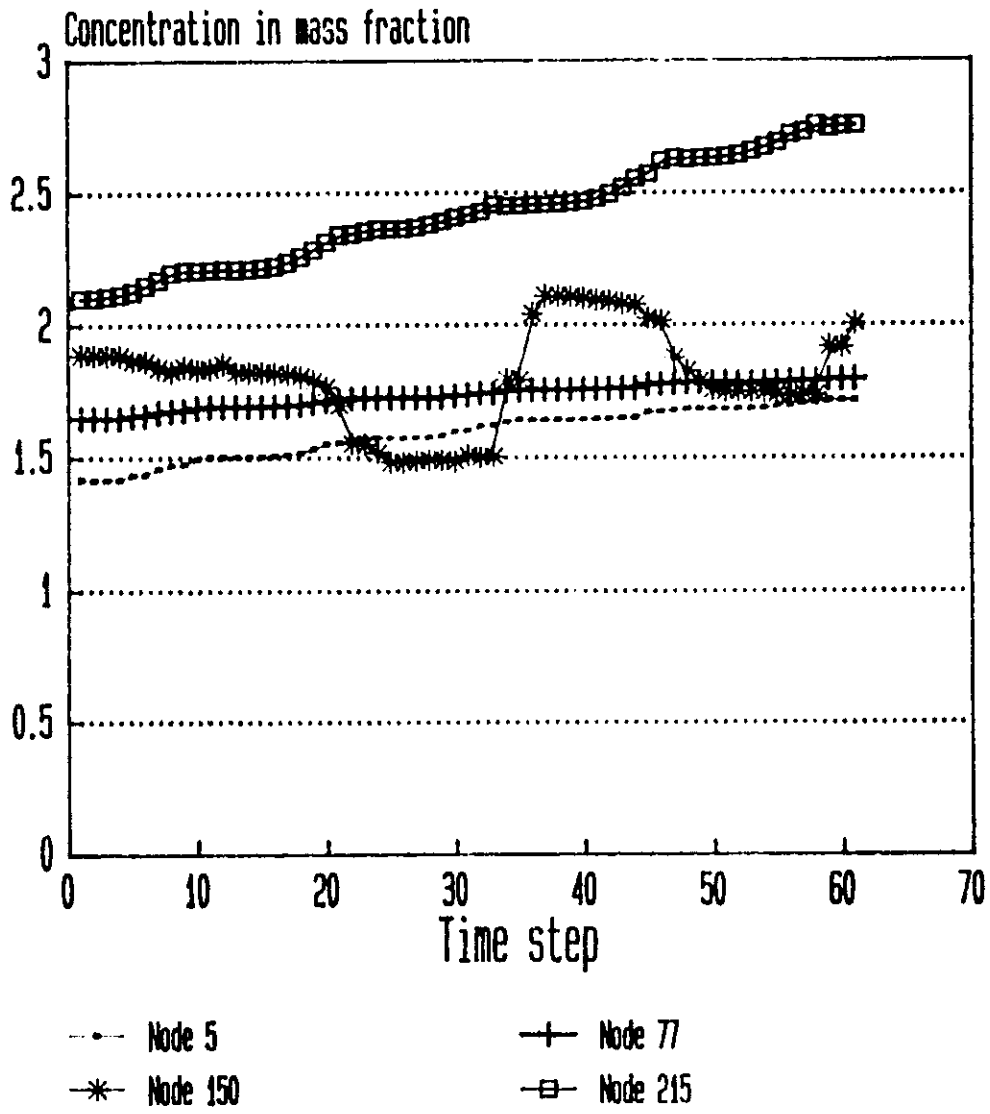


Fig.33 Temporal concentration variation in case 4

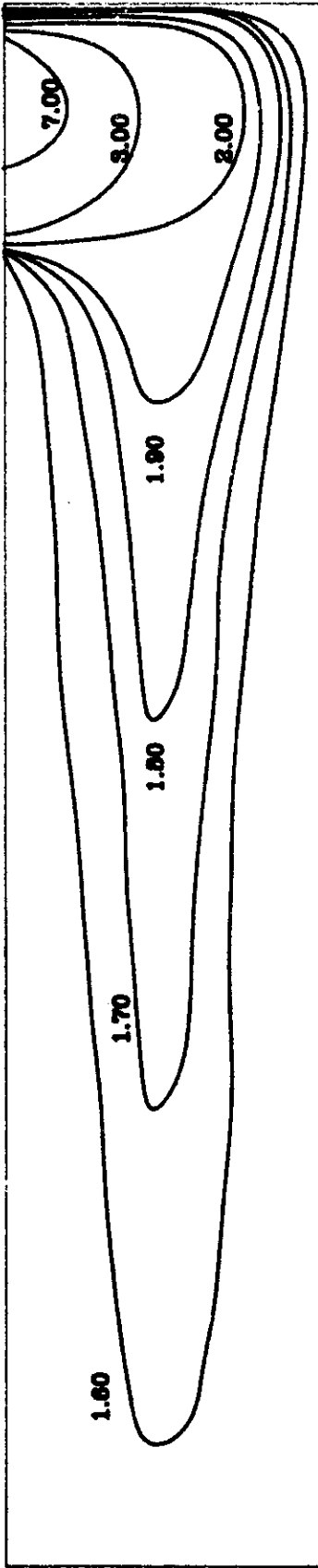


FIG. 34(a) ARIAL VARIATION OF CONCENTRATION IN MASS FRACTION
FOR CASE 4 TIME STEP 31

solute injection is in all the time steps concentration is on increasing trend. In case 3, where 10 nodes near Minnur on the left bank is assigned with some solute mass source shows increasing trend of solute concentration in node 215 which is nearest to Minnur and rest of the nodes behaves just like case 1. Case 4 is mixing of case 2 and 3. Results are also just like addition of the results of those two cases.

Areal transport of contaminants can be realised by comparing the plumes that has been plotted for 31st and 61st time steps. This again claim support to the outcome that has been extracted from the analysis of temporal variations. In all, the results of the simulation are quite convincing one towards the physicality of the system. Again the sole limitation is that these concentration values could not be compared with some of the observed values inside the mesh.

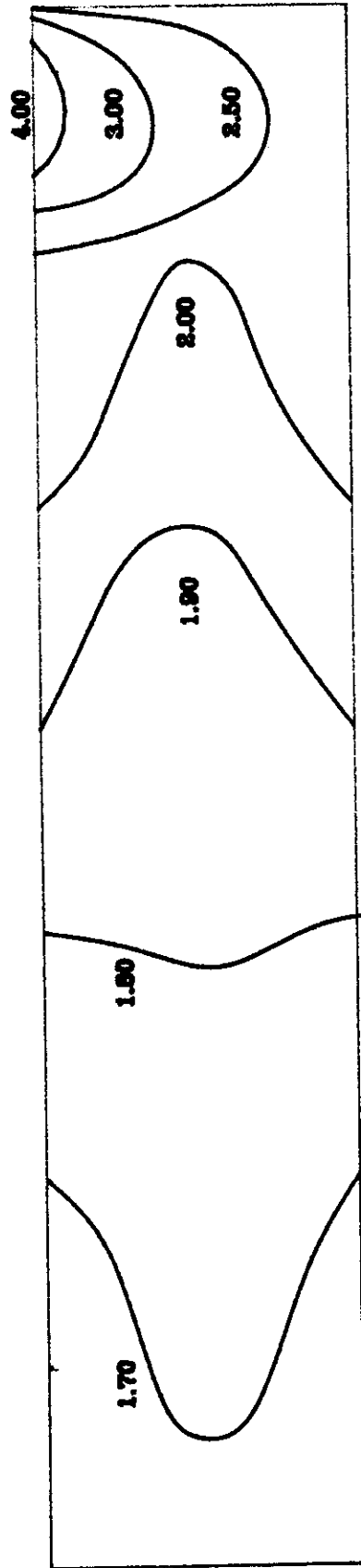


FIG. 34(b) ARIAL VARIATION OF CONCENTRATION IN MASS FRACTION
FOR CASE 4 TIME STEP 61

CHAPTER V

5.0 Recommendations

Sutra the saturated unsaturated transport algorithm for simulating fluid movement and transport of either thermal energy or dissolved substances in a subsurface environment generated by USGS has been redeveloped as a software compatible to personnel computers and fortran version 5.1. Results of the test runs for the example available in the documentation report published by USGS have been compared therein and also with some analytical solutions. Output from the package is quite encouraging one.

Apart from the objectives stipulated in chapter I, it was initially opted to implement it for the Upper Palar zone of Palar river basin in Tamilnadu, but subsequently subject to the limitations of storage available on RAM and hard disk (RAM-2MB and Hard disk-234MB) and restriction of mesh peclet number for stability of the results, only an alluvium river stretch between Vaniyambadi to Minnur has been dealt as an hypothetical case based on the available field data of the region. This pilot run outputs though look like satisfactory results, but no definite conclusions in regard of pollution management could be drawn as large amount of assumptions were enforced to mitigate meagre data availability for the simulation. These assumptions are stated below.

- (1) The aquifer is homogeneous and isotropic.
- (2) Alluvium is in fully saturated condition
- (3) Darcy's law is applicable
- (4) Aquifer is independent and unaffected from any activity in the nearby domain.
- (5) In absence of enough observation points available for dictating initial and boundary conditions, it has been assumed that the pressure and concentration variations are only along the river bed and values remain constant across the river bed. Hence spatial interpolation of the respective value has been carried out at the required nodes based upon the available values at two observation points, i.e. Vaniyambadi and Minnur.
- (6) Recharge has been considered only through rainfall. While steady state simulation it was found that there is some additional indirect recharge available, may be through disposal of effluents from tanneries and other small scale industries. Rate of discharge of this effluent disposal is not known therefore could not be introduced.
- (7) Total withdrawal rates are not known. Therefore no discharge rates could be simulated.

(8) There is no pump test data available inside the study area. Table 1 shows results of some of the pump tests carried out on bore wells of nearby locations. The storativity parameter has been evaluated by Theis method of solution, i.e.

$$S = \frac{4TU}{r^2/t} \quad \text{-----}$$

A convenient match point is assumed with well function $W(u) = 1.00$, $u = 1 \times 10^{-2}$ and $r^2/t = 216,000$ sq.mt./day for an observation well 60 mt away from the testing well.

(9) There is no river gauging stations available near by the study plot. Nearest gauging stations are at Avarankuppam and Ponnayanicut which are quite away from the location. Therefore interaction between river and ground water has been neglected.

(10) A recharge rate of 20% of the monthly rainfall has been considered.

(11) Contaminants are assumed to be of non-reactive nature.

(12) There is no decay process in the subsurface.

(13) Density and compressibility of the fluid remain unchanged

(14) Ratio of longitudinal to transverse dispersivity is 10:1.

(15) Diffusivity is constant.

(16) Monthly Concentration variation is linear between post and pre monsoon values.

In the present circumstances following recommendations are inevitable for the goal oriented future simulation of flow and transport in Palar river basin.

(i) The pilot mesh adopted hardly can resemble the extent of actual polluted aquifer system, because it is comparatively quite small to project the complete system response. In the subsequent future simulations it should include hard rock formations also to produce global scenario. Mesh should be defined through hydrogeological boundaries as far as possible. Pattern of fractures in hard rock formations has to be dealt with special attention.

(ii) Additional data collection for defining initial and boundary conditions can not be overlooked. Figure 35 suggests a proposed observation network which may be considered as a basis for expanding the scope of the future data monitoring and collection. It would be appropriate if fluid head and concentration can be monitored on each nodal point of this network. This network ultimately may be refined according to the mesh peclet number to use it as finite element discretized set up for future simulations.

(iii) At present quality data is being monitored on pre and post monsoon basis, which has to be modified to atleast monthly basis to use convenient time step for stability of the results.

(iv) Long term pump tests should be carried out both in dugwells and borewells and as well in all types of formation inside the mesh. One pump test per element of fig 35 is recommended for hard rock formations. This will lead towards local aquifer parameter estimation.

(v) Permeability being the most sensitive parameter, it should be measured in longitudinal, transverse and vertical direction.

(vi) River gauging and stream gauging is recommended in few locations between vaniyambadi and Gudiyattam.

(vii) Spatial and temporal variation in rate of abstraction from the aquifer should be known.

(viii) Field estimation of dispersivity values are essential.

(ix) Surface water quality details should be monitored.

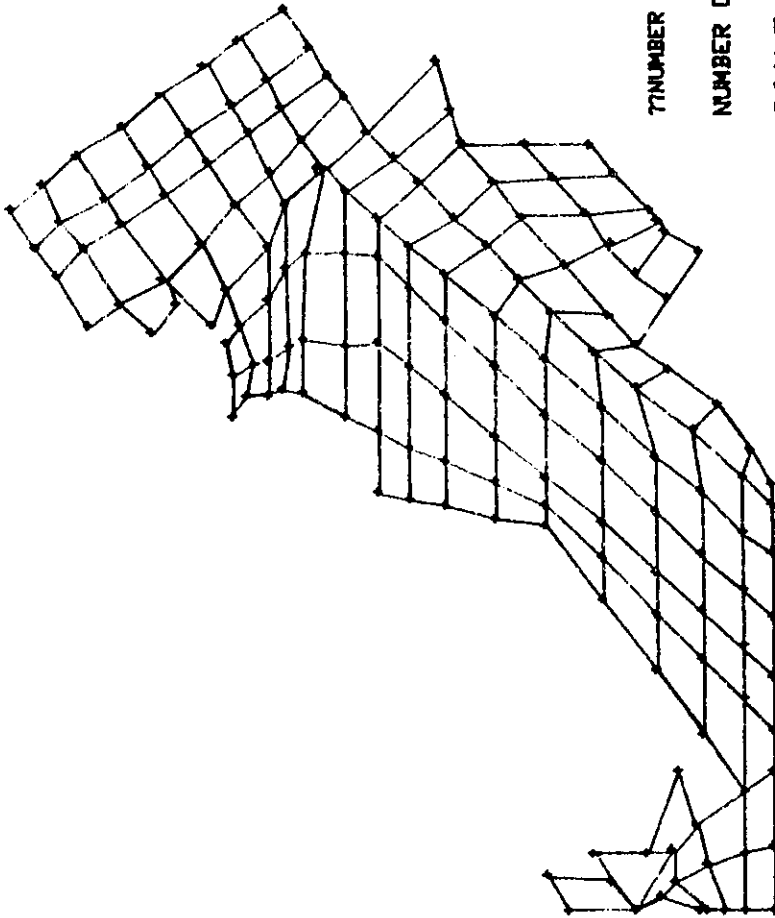
(x) Quantity and quality wise details are required for the effluent disposal to the river from the tanneries and other industries.

(xi) Quality and quantity of irrigation return flows has to be assessed.

5.1 Conclusion

Present study intends towards the introduction of SUTRA, a saturated-unsaturated transport algorithm developed by USGS, for Groundwater quality modeling in Palar River Basin. Package has been redeveloped to suit our practical environment. It has been tried to simulate a trial portion of the river basin with available hydrogeological data and the results are encouraging. Through these test runs it can be argued that applicability of the model has tremendous prospects.

Parameter identification for future simulation is carried out. The same is recommended instead of concluding the study. It is essential that field work and model work should interface each other. With all the recommended implications it would be necessary to transfer the model to bigger system with minor modifications.



NUMBER OF ELEMENT = 122

NUMBER OF NODES = 163

SCALE: 1 CM = 2.5 KM

FIG.35 OBSERVATION NETWORK FOR FUTURE SIMULATION IN PALAR RIVER BASIN

Bibliography

Azimi-Zonooz Ali and Duffy C.J., 1993, Modelling Transport of Subsurface Salinity from a Mancos Shale Hillslope. Vol 31, No.6- Ground Water.

Bear Jacob 1979, Hydraulics of Groundwater, McGraw Hill, New York.

Bear Jacob & Verruijt Arnold, 1987, Modelling groundwater flow and pollution, D. Peidel Publishing Company, Holland.

Javandel I., Doughty C. and Tsang C.F., 1984, Groundwater Transport: Handbook of mathematical models, American Geophysical Union, Washington, D.C.

Majumdar P.K., 1993, Groundwater quality modelling study in upper palar zone of Palar river basin in Tamilnadu. NIH report CS-110.

Majumdar P.K., 1993, Groundwater quality modelling, NIH report SR-33

Miller D.W., Chemical Contamination of Ground water.

Thangarajan M., 1985, Report on Numerical Simulation of Flow & Mass Transport and Geostatistical Estimate of Water levels in Vaippar River Basin, South India.

Todd David Keith, 1980, Groundwater Hydrology, John Wiley & Sons, New York.

Voss, Clifford I., 1984, SUTRA, U.S. Geological Survey water Resources Investigation Report B4-4369.

Wang H.F., Anderson M.P., 1982, Introduction of Groundwater modelling, W.H. Freeman and Company USA.

ACKNOWLEDGEMENT

Authors are extremely grateful to Dr.S.M.Seth,Director,NIH , Roorkee and Dr.G.C.Mishra,Coordinator,RCNIH,Belgaum for their keen interest and permission to carry out this work.

The study group is sincerely thankful to Dr.P.V.Seethapathi,Scientist 'F',NIH,Roorkee for his perfect guidance,keen interest,inspiration and constructive suggestions.

Deepest gratitude are due to Prof.Ed.A.Macbean, Professor,University of Waterloo,Ontario,Canada and Mr.A.G. Bobba, National Water Research Institute , Ontario,Canada for their fruitful suggestion.

Authors are grateful to Institute of Water Studies for extending their cooperation regarding data collection.

Thanks are also due to Mr.A.V.Shetty and Mr.Venkatesh B.,both Scientist 'B' of RCNIH,Belgaum for their keen interest during program compilation.

At last but not least the authors take this opportunity to express deep sense of gratitude to Mr.G.Babu,Draftsman III,RCNIH,Belgaum for his continuous support in terms of ACAD-Graphics ,without which this report would have not come out so soon as it would have been without the assistance from Mr.S.R.Majalatti,LDC,RCNIH,Belgaum.

DIRECTOR : S M SETH

COORDINATOR : G C MISHRA

STUDY GROUP

P K MAJUMDAR

RAMA MEHTA

B K PURANDARA